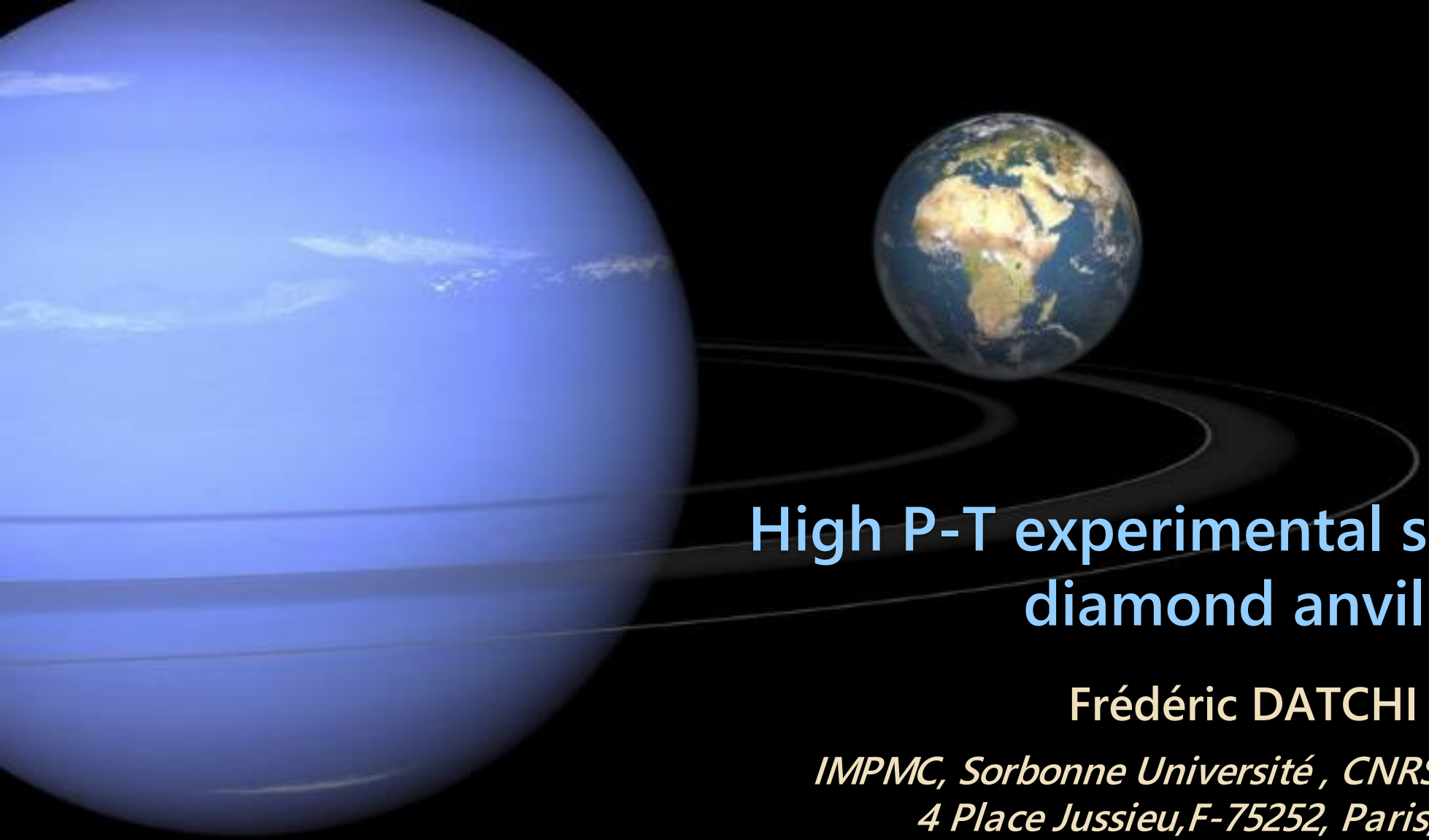

High P-T experimental studies in the diamond anvil cell

Frédéric DATCHI

IMPMC, Sorbonne Université , CNRS, MNHN, IRD,
4 Place Jussieu,F-75252, Paris, France.

Summary

- Overview of DAC techniques based on resistive heating
- P-T metrology in the RH-DAC
- Going beyond the temperature limit of the RH-DAC: induction heating
- Examples of applications and perspectives with EBS

Overview of DAC techniques based on resistive heating

Pioneer experiments: (1) External resistive heater

Invention of the DAC : late 1950's. First high temperature (RH) experiments: late ~60's

1969

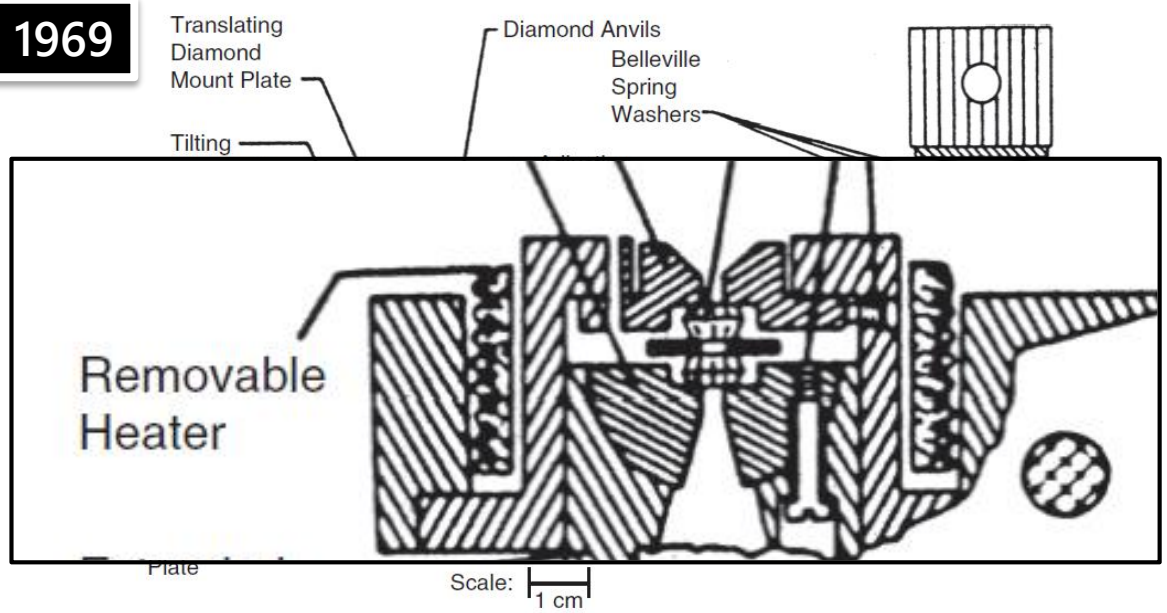

Fig. 1.36 The NIST diamond anvil cell with temperature capability [47]. This cut-away cross section shows the essential components of the NIST DAC including the anvil support alignment design, lever-arm assembly and spring washer loading system. For high-temperature experiments the entire cell, except for the spring washers, is fabricated from Inconel 718, a high-temperature high-strength superalloy which permits sample temperatures as high as 1,073 K to be maintained routinely [58]

G. J. Piermarini, J. Res. Nat. Inst. Stand. Technol. 106, 889-920 (2001); http://nvl.nist.gov/pub/nistpubs/jres/106/6/j66pie.pdf

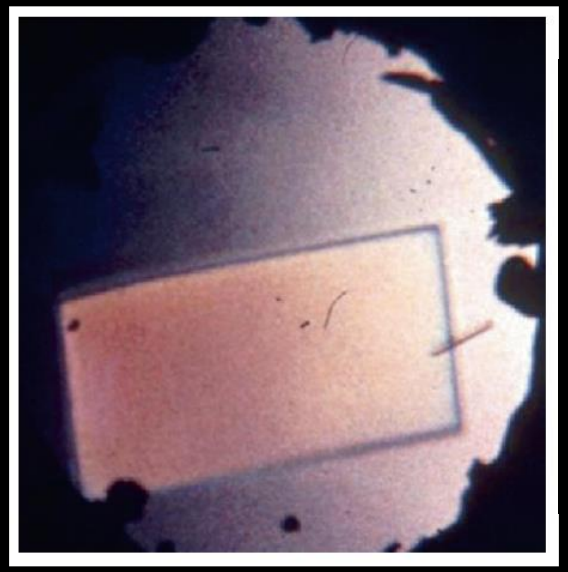

Fig. 1.22 A single crystal of benzene II in equilibrium with liquid at about 310°C and 3 GPa, showing well-defined crystal morphology. This crystal was slowly grown to fill the gasket cavity by gradually reducing the temperature to RT. A crystal such as this one was used to study the structure of benzene II [36]

Benzene II

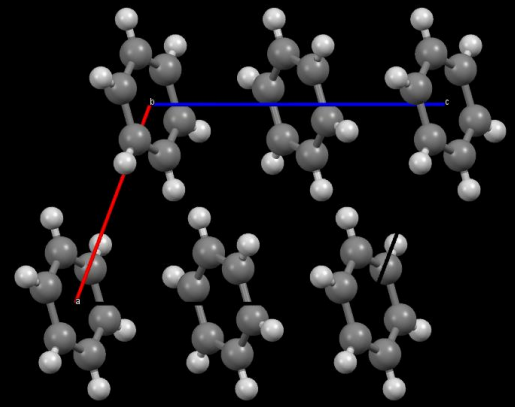

Piermarini et al, Science 1969

Pioneer experiments: (2) internal (direct) heating

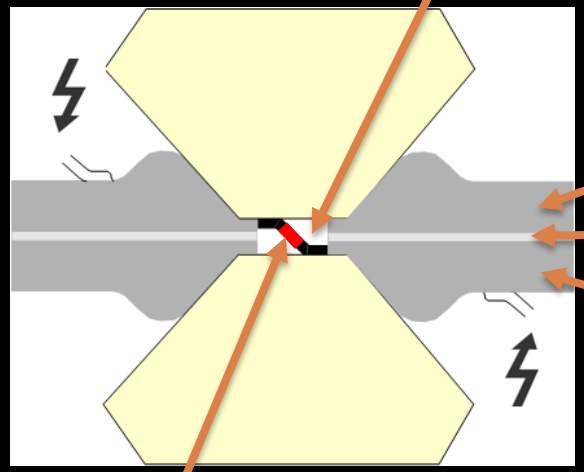

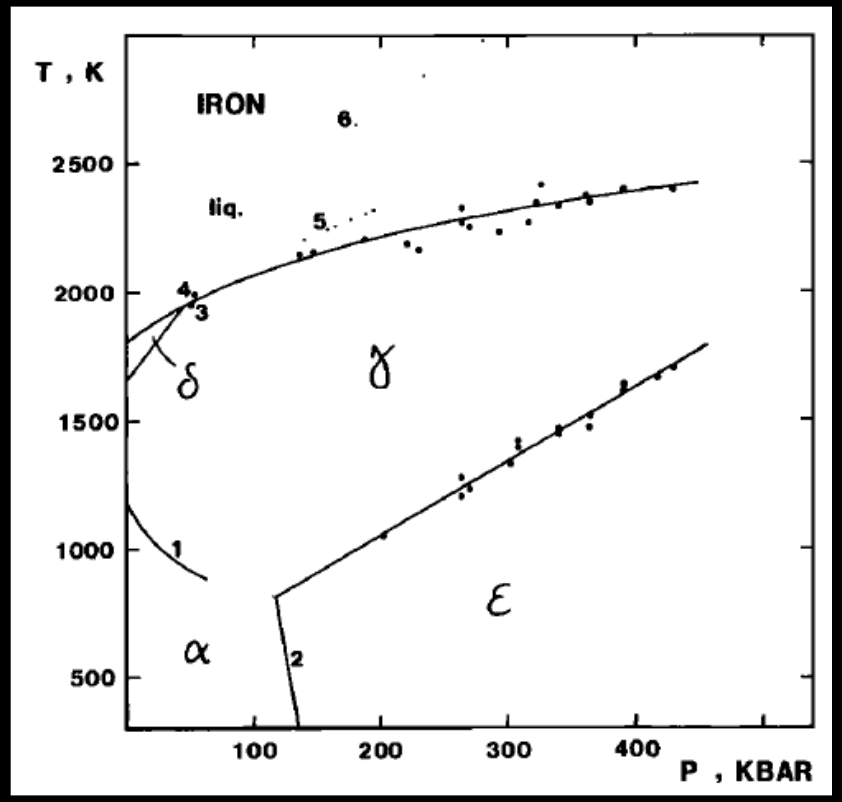

- The metallic sample is directly heated by the electric current
- Sample is a thin wire (∅ 0.02 mm, 0.2 mm long)
- Phase transitions are detected by changes in sample resistance

Liu & Basset, J. Geophys. Res. 1975
R. Boehler, Geophys. Res. Lett. 1986

Internal heating: Refinements

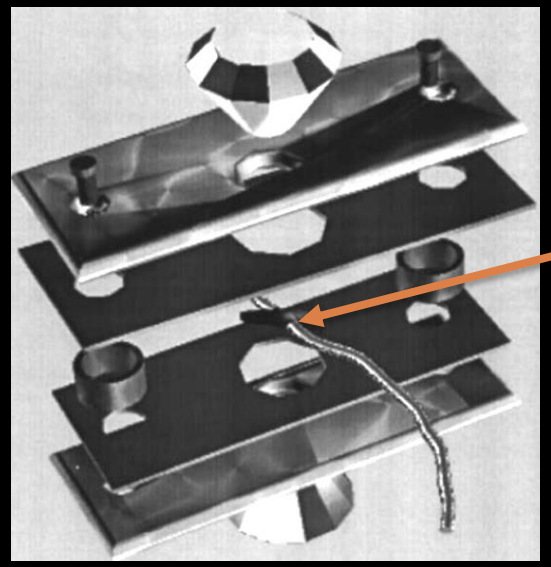

Dubrovinsky et al, PCM 1998

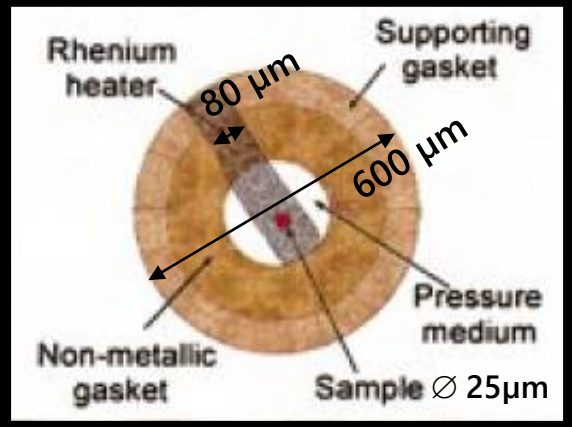

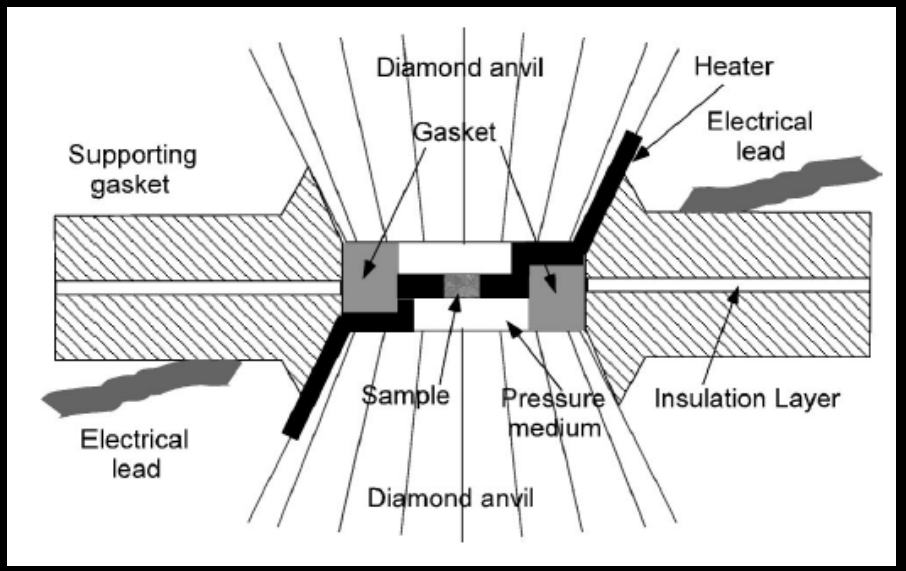

Zha & Basset, RSI 2003

- Direct heating of a thin metallic foil (or flatened wire)
- The sample is placed in a hole (∅25-100 µm) drilled in the foil
- T up to 2000 K

- Complex assemblage, non reusable
- Several thermal cycle needed to relax deviatoric stresses

Various designs of resistive heating

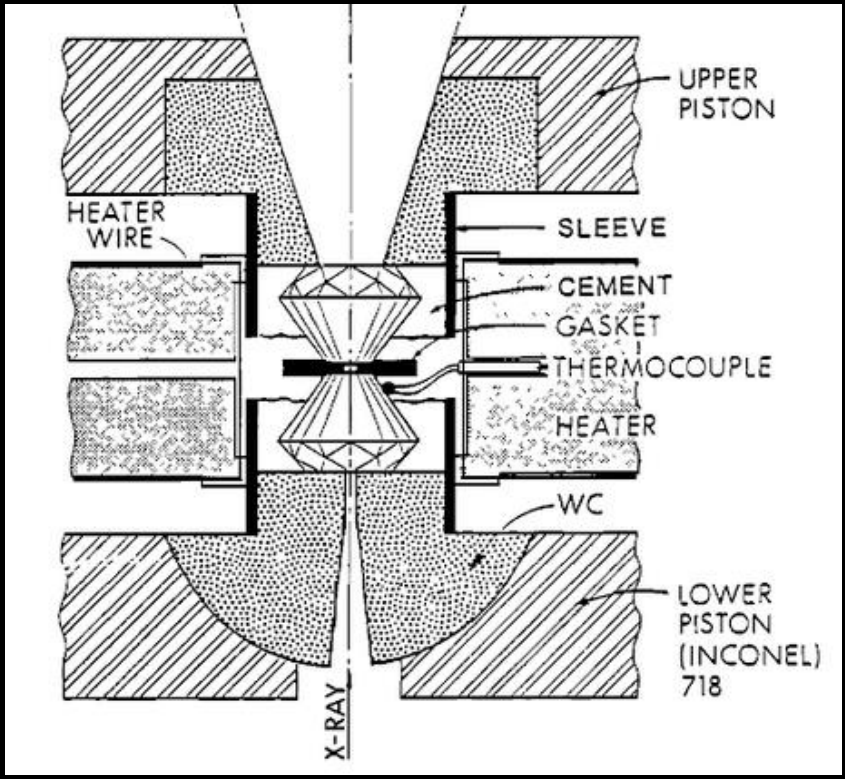

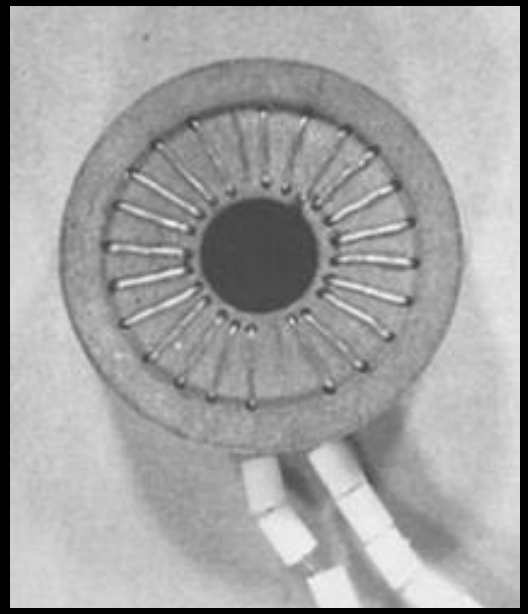

L.C. Ming et al, High P Res. Min. Phys. 1987

- Most designs include:
  - An external heater T<~700 K
  - An internal heater T<~1000-1200 K
- The body of the cell must be constructed out of high temperature materials:
  - Refractory metals (Mo, Re, Inconel 718, Udimet 700…)
  - Ceramics (Alumina, Zirconia,…)

Various designs of resistive heating

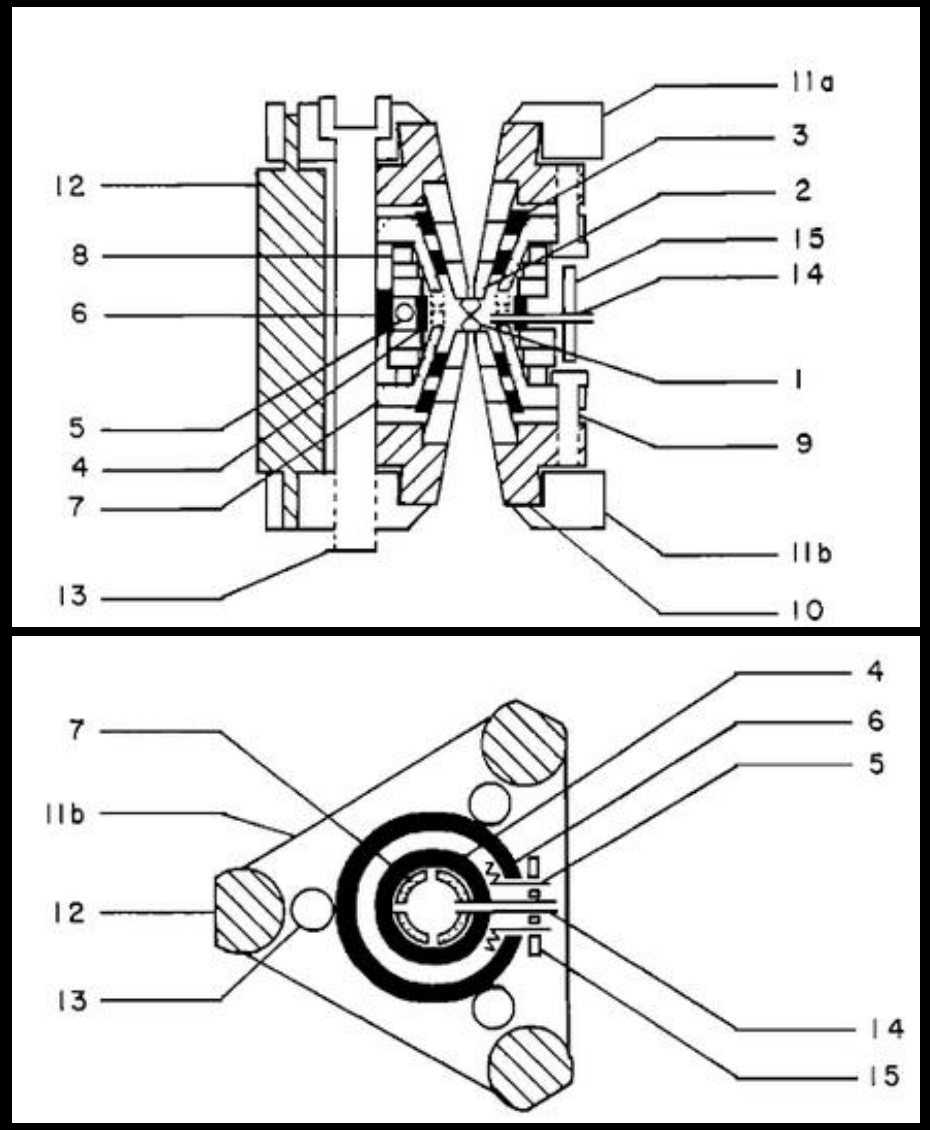

Schiferl et al, High P Res. Min. Phys. 1987

- Most designs include:
  - An external heater T<~700 K
  - An internal heater T<~1000-1200 K
- The body of the cell must be constructed out of high temperature materials:
  - Refractory metals (Mo, Re, Inconel 718, Udimet 700…)
  - Ceramics (Alumina, Zirconia,…)

Various designs of resistive heating

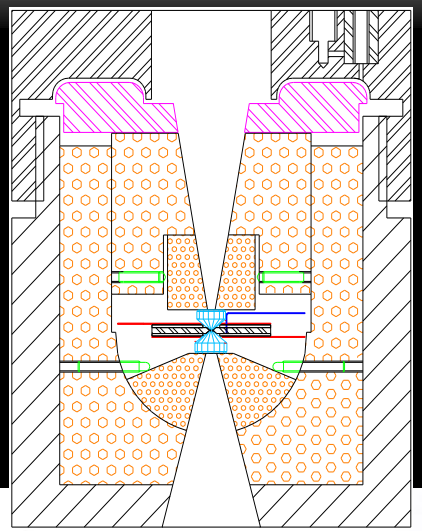

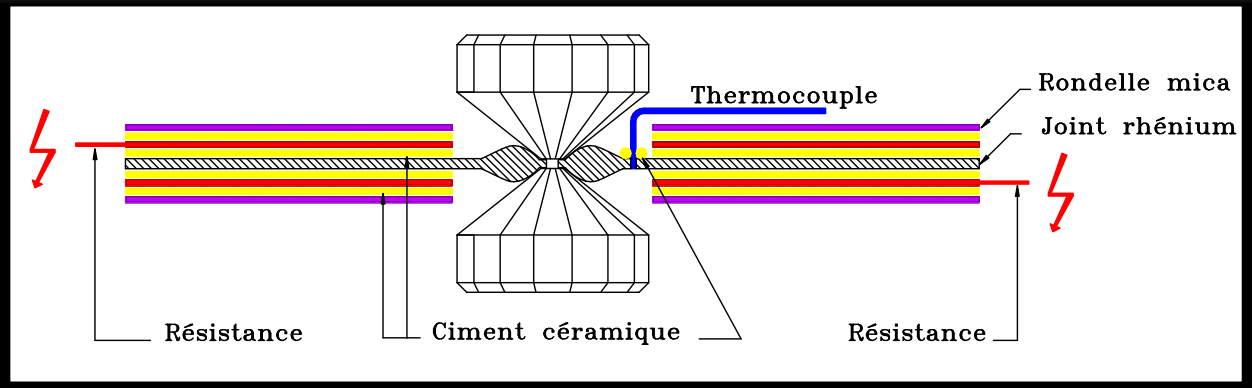

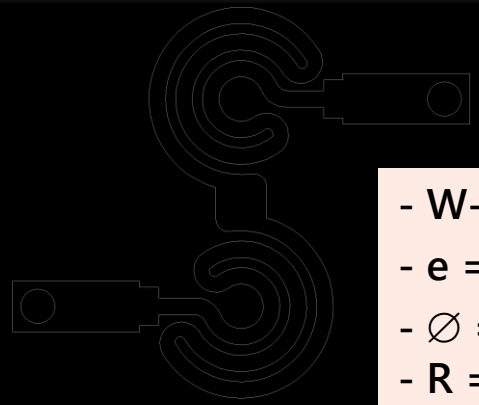

- W-Re alloy
- e = 0.1 mm
- ∅ = 12.7mm.
- R = 0.7 Ω

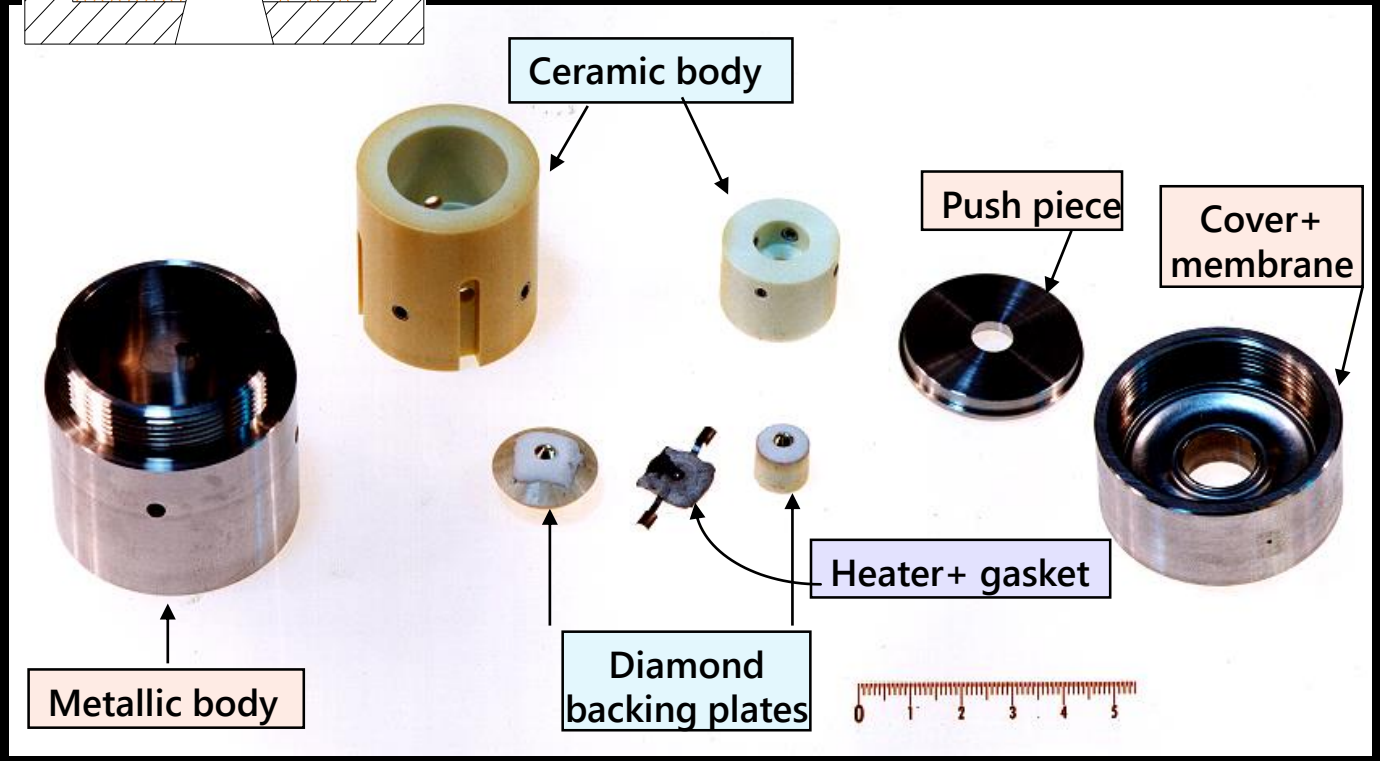

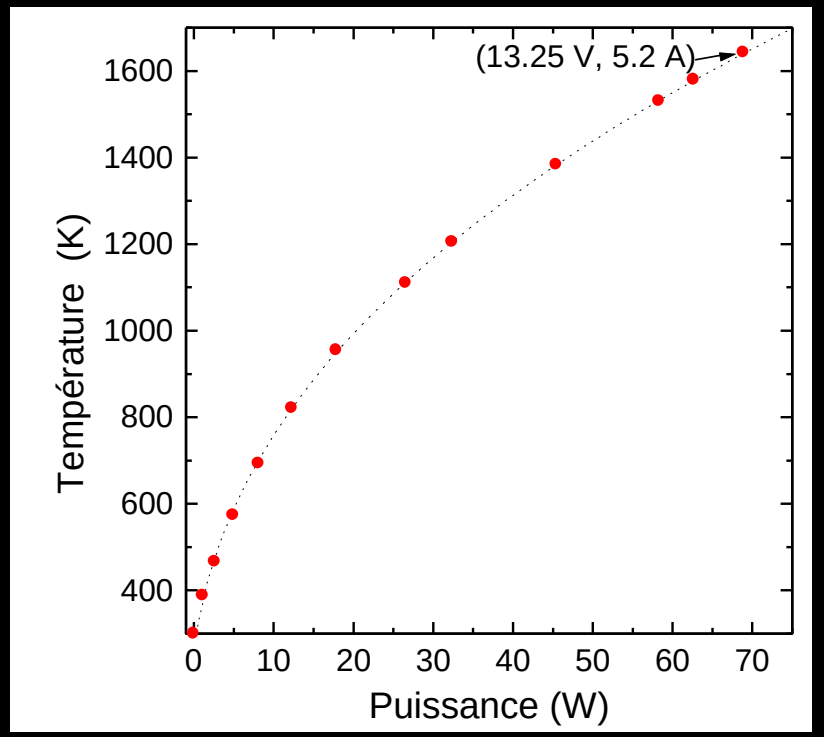

Le Toullec et al, High P Sci. Technol. 1996

Various designs of resistive heating

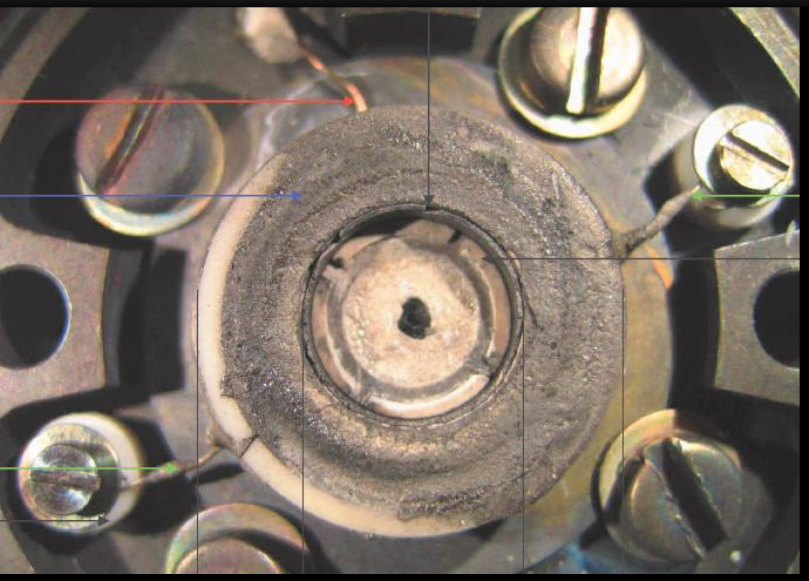

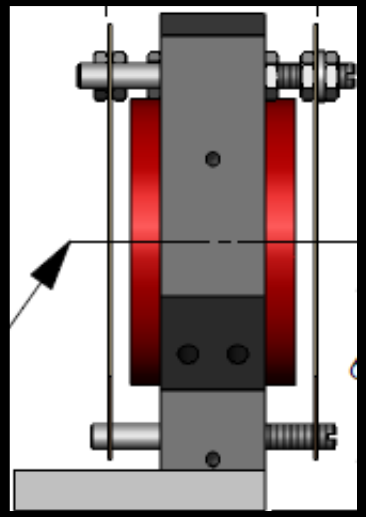

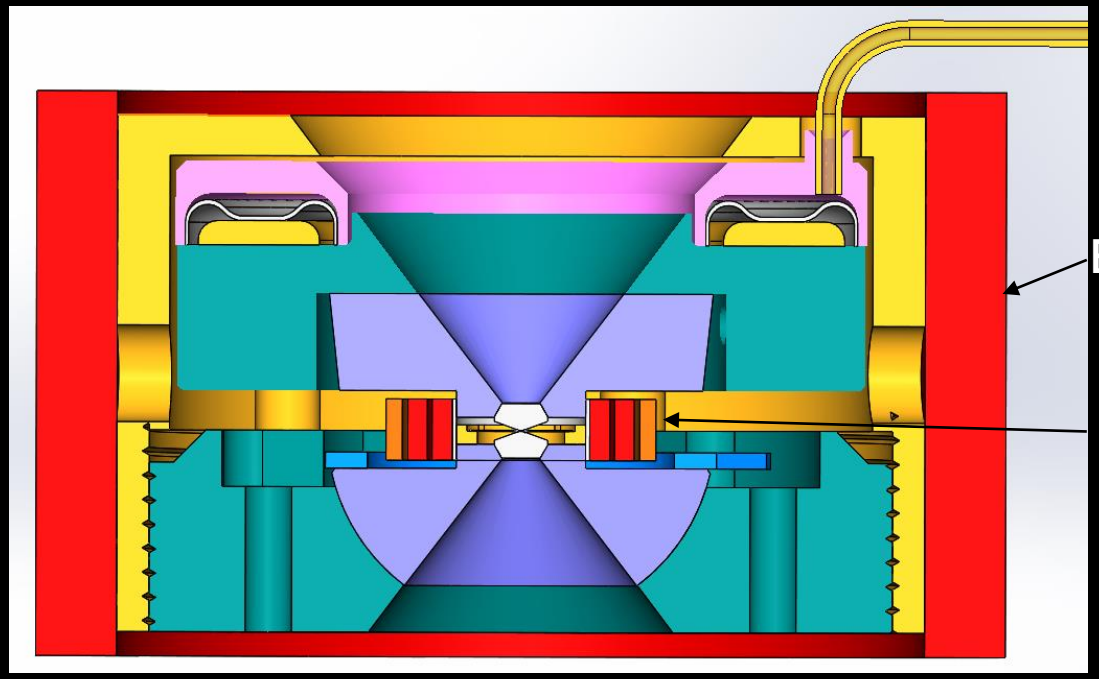

- External heater:
  - Ring-shaped, enclosing the full DAC
  - T<750 K
- Internal heater
  - Single unit made of a double coil of Re-W wire
  - T<~1000 K
  - Thermal contact through a thin graphite ring

- Small footprint
- Easy to set-up
- Reusable

F. Datchi & B. Canny, 2002

Various designs of resistive heating

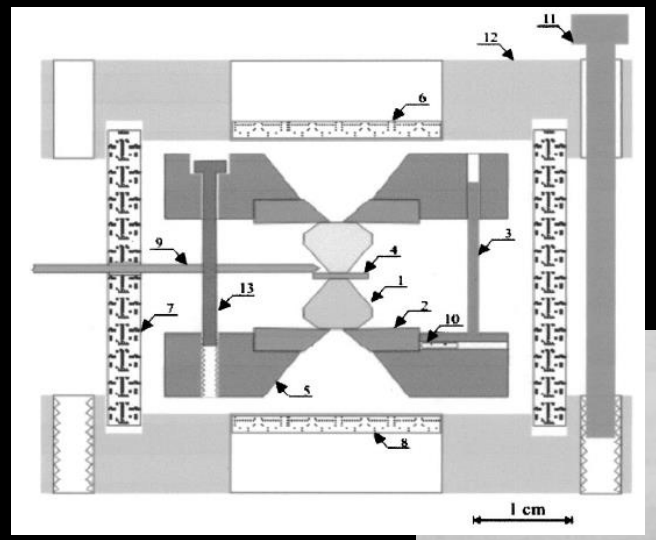

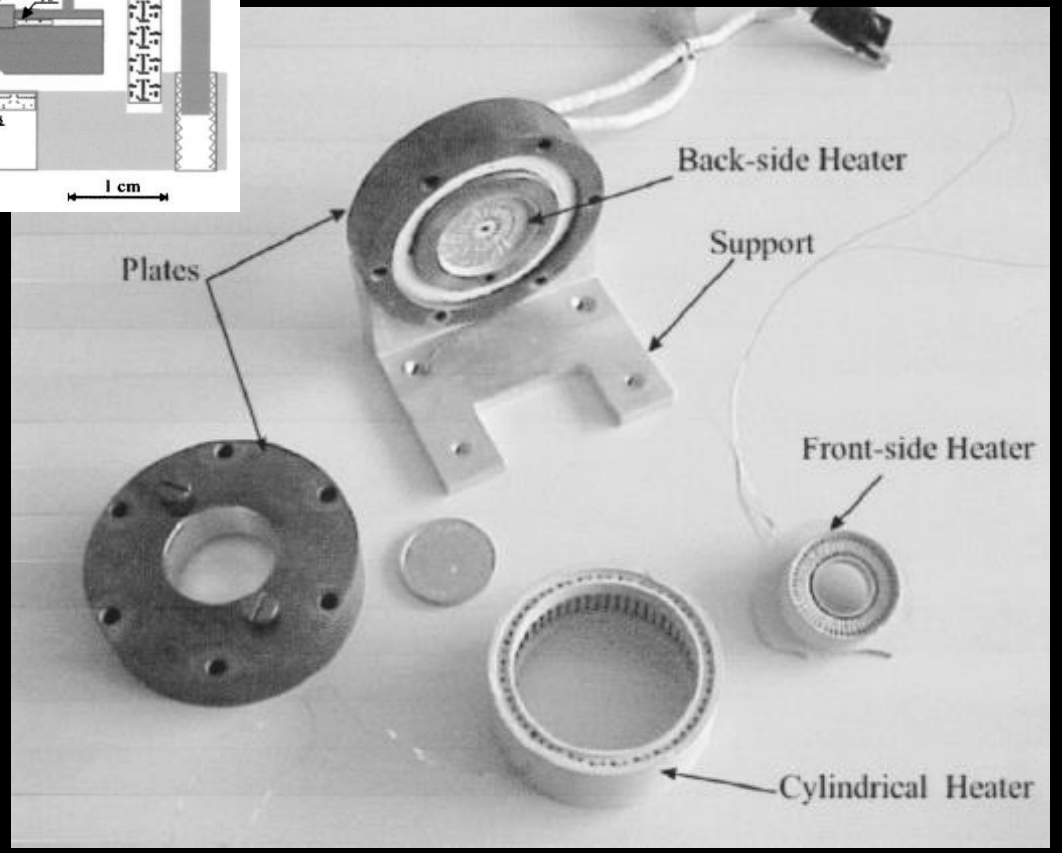

- 3 heaters around the body and at the back and front of the DAC
- Tmax~1200 K
- Enables isobaric heating (according to authors)

Dubrovinskaia et al, RSI 2003

Various designs of resistive heating

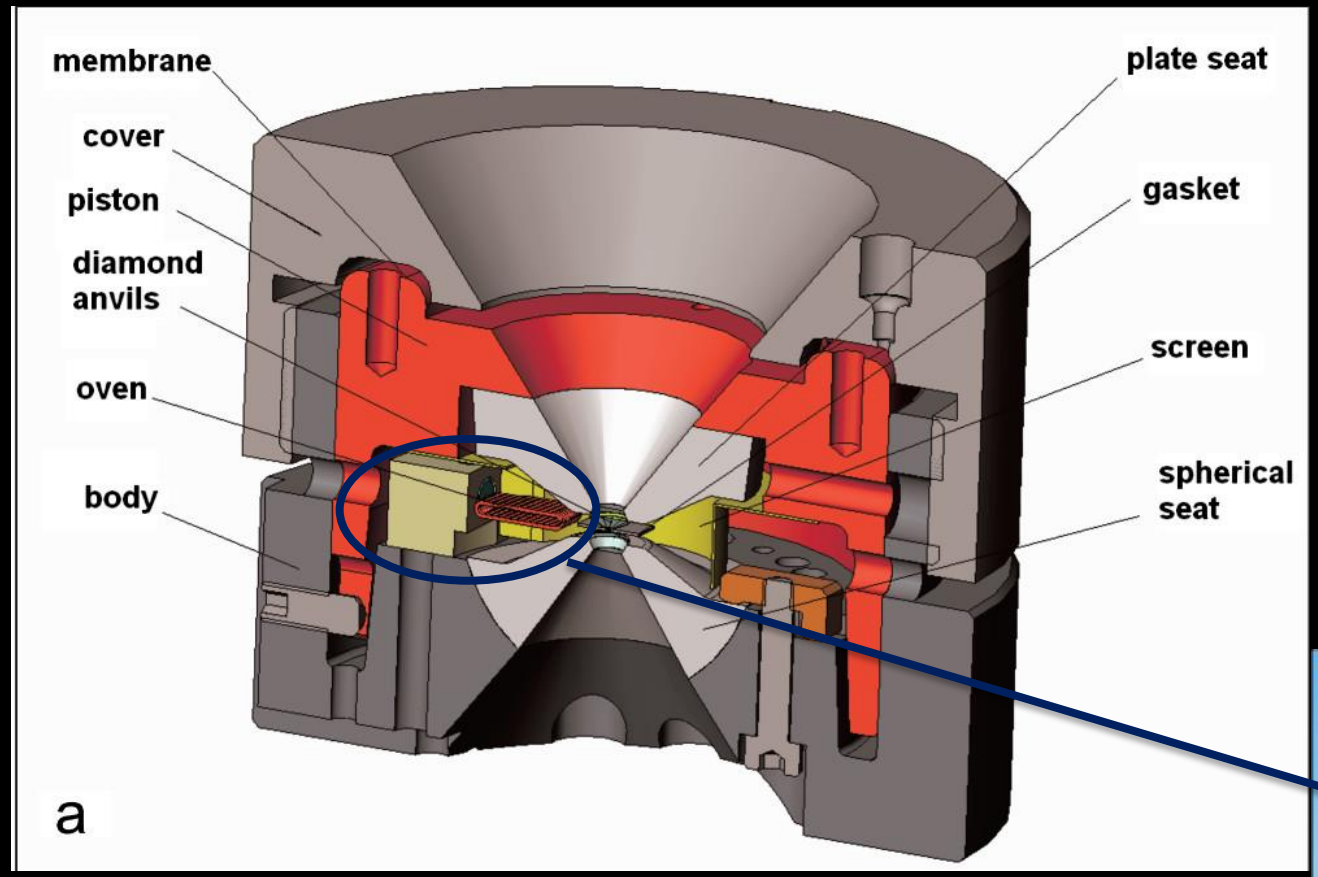

Pasternak et al, RSI 2008

- Radiative heating via a resistively heated tungsten coil of halogen lamp
- Tmax~1200 K

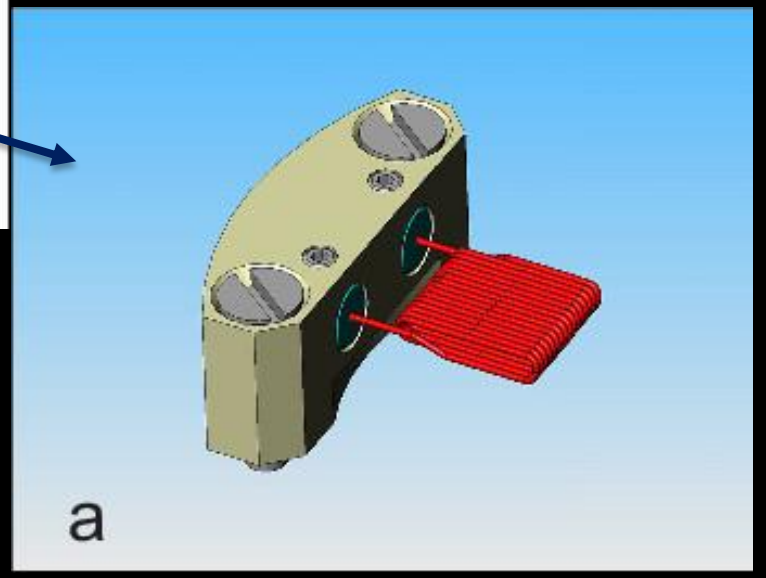

Graphite internal heater

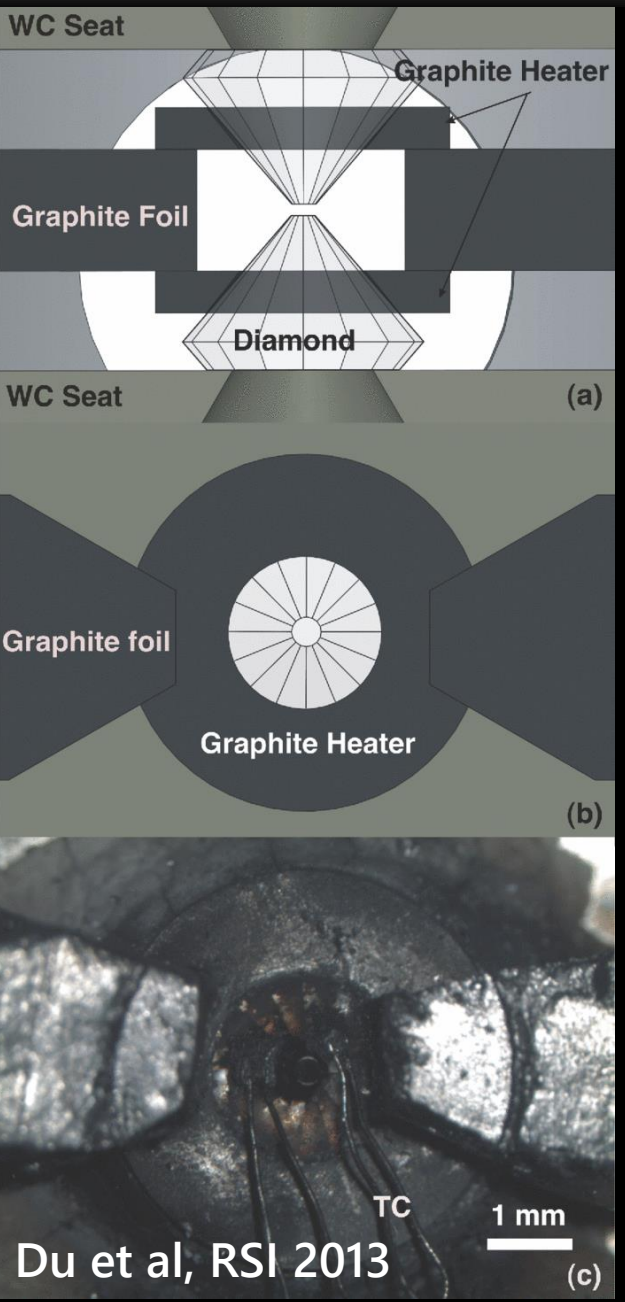

Du et al, RSI 2013

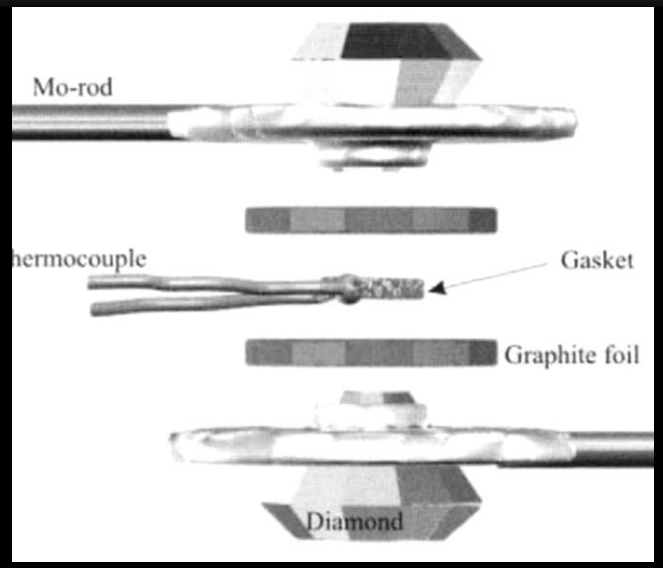

Dubrovinsky et al, 1999

ESRF DAC (Garbarino/Jacobs)

- Internal heater made of ring-shaped graphite
- Graphite is a good electric and thermal conductor and is easly machined
- T up to ~1300 K

- Requires large current (>100 A)
- Complex assemblage and non reusable
- Large variation of P during heating

Gaskets in the RH-DAC

- Re gaskets perform well up to T~1150-1200K [1,2]
- For T>~1200 K, composite gaskets have been developped, consisting of amorphous B, BN or C mixed with epoxy

Pros:

- Higher mechanical strength at high T
- Higher thickness at high P
- Quasi-transparent for hard x-rays

Cons:

- Longer preparation
- May react with sample. Other fillers than epoxy has been proposed (MgO)
- Insert is porous and may mix with sample=>not suited for fluid/gas loading

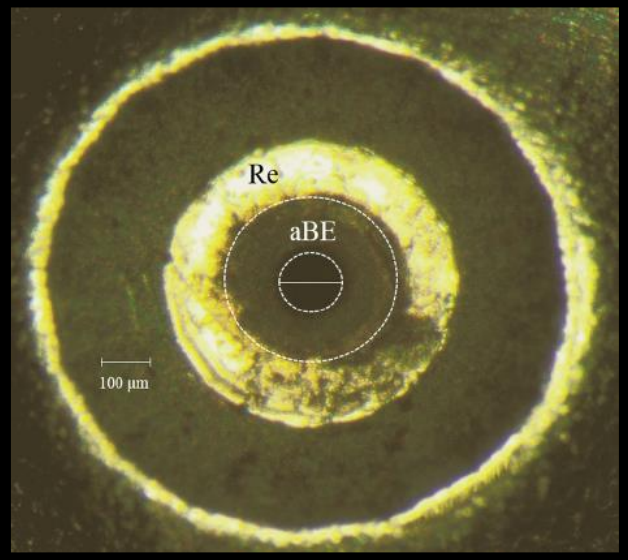

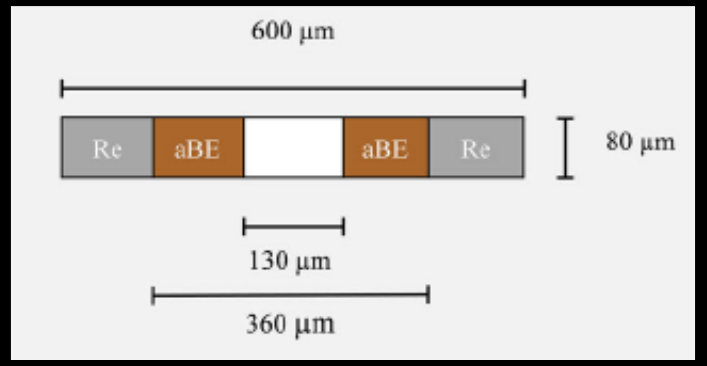

a-B + epoxy gasket [Rosa et al, 2016]

[1] Dubrovinskaia et al, 2005; [2] Rosa et al, 2016

Stability of diamond at high T

Diamond is a metastable form of carbon at room pressure, so what is the temperature limit for using diamond anvils ?

- Oxygen chemically attack diamond surfaces. Oxydation is enhanced by T
  - Need to work in a reducing atmosphere (Ar/H2(1%)) or vaccum (10^{-5} mbar)

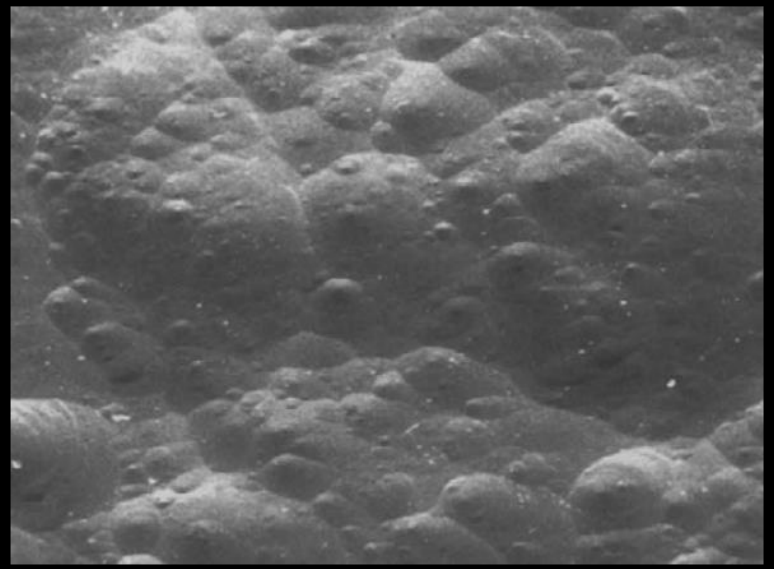

[110] face after 10% weight loss under O_2 flow

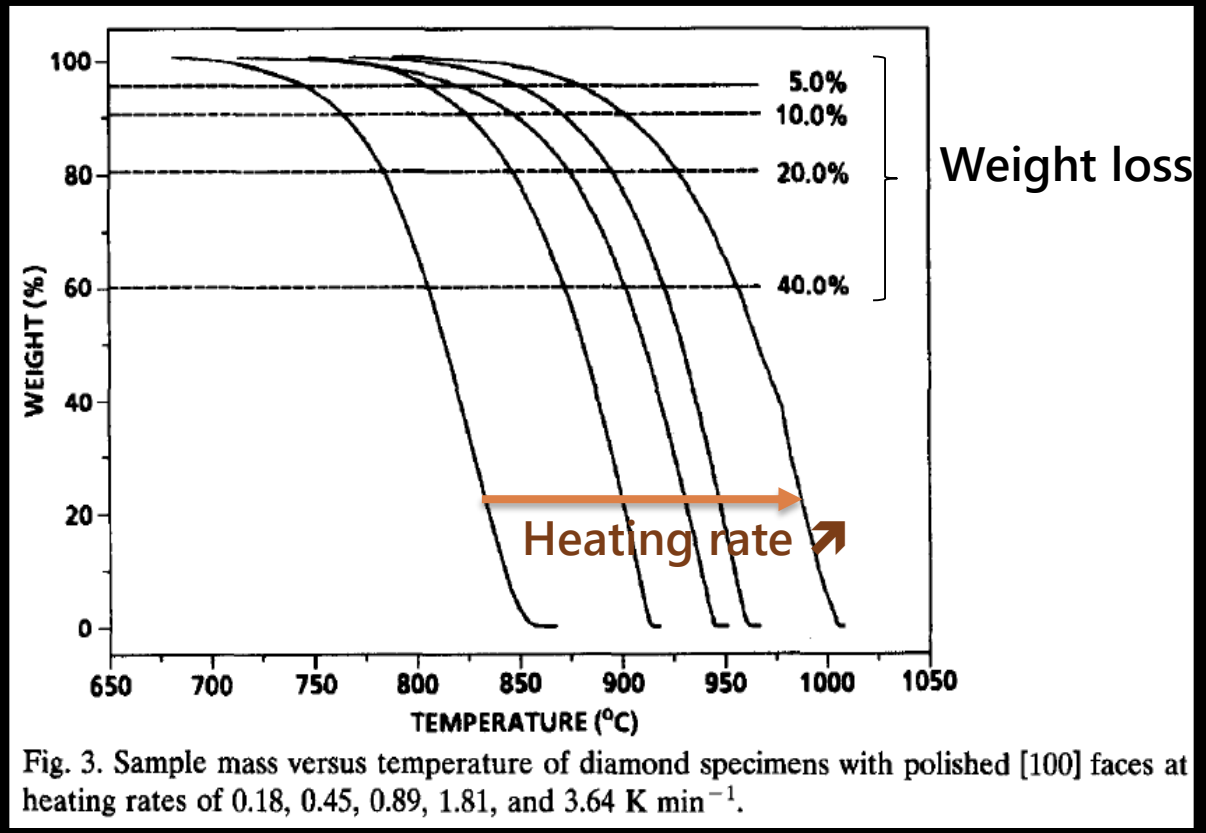

Fig. 3. Sample mass versus temperature of diamond specimens with polished [100] faces at heating rates of 0.18, 0.45, 0.89, 1.81, and 3.64 K min^{-1}.

Dallek et al , Thermochimica acta 1991

Stability of diamond anvils at high T

- Graphitization of anvil surfaces start at ~1600°C in vaccum (<6x 10^{-5} mbar) and progress rapidly above
- Threshold T and rate depend on crystal faces. The more resistant is (100).

➢ Heating to ~1600 °C is safe under vaccum of a few 10^{-5} mbar

➢ Higher T's may be achieved for a short time.

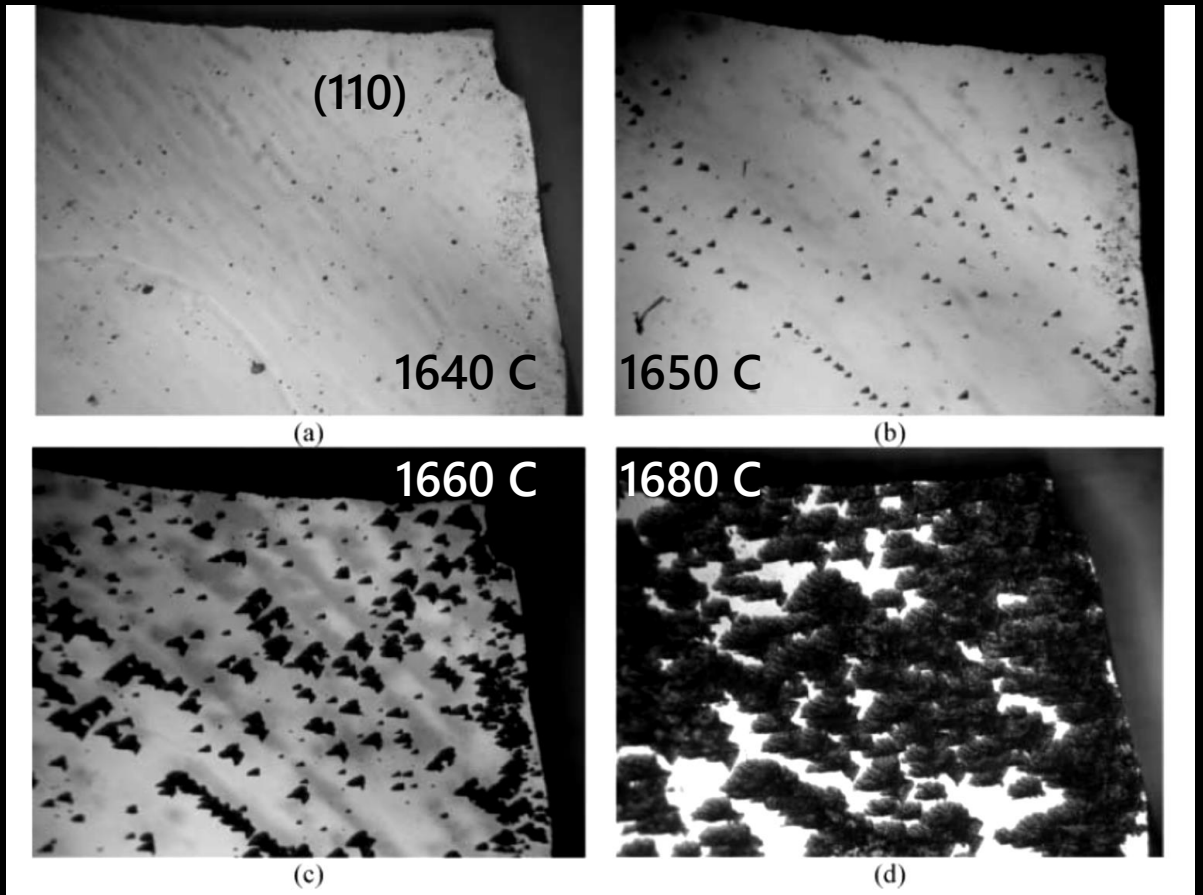

Figure 1. Successive stages of graphitization of diamond. Polished plate (110) from a natural crystal. Annealing at temperatures: (a) 1640 °C, (b) 1650 °C, (c) 1660 °C, and (d) 1680 °C. No removal of graphite material by chemical etching in intervals between annealing stages was done. Graphitization figures are shaped as butterflies. The micrographs were taken in transmitted light. Frame size, 2.67 × 2 mm.

Khmelnitsky & Gippius, Phase trans. 2014

P-T metrology in the RH-DAC

Measuring P-T with x-rays

- Various calibrants may be used with an x-ray source: Au, Pt, MgO, NaCl,…
- Crossing EOS of two calibrants allow simultaneous measurements of P and T [Crichton & Mezouar, 2012]

- But… you are not always at a synchrotron !

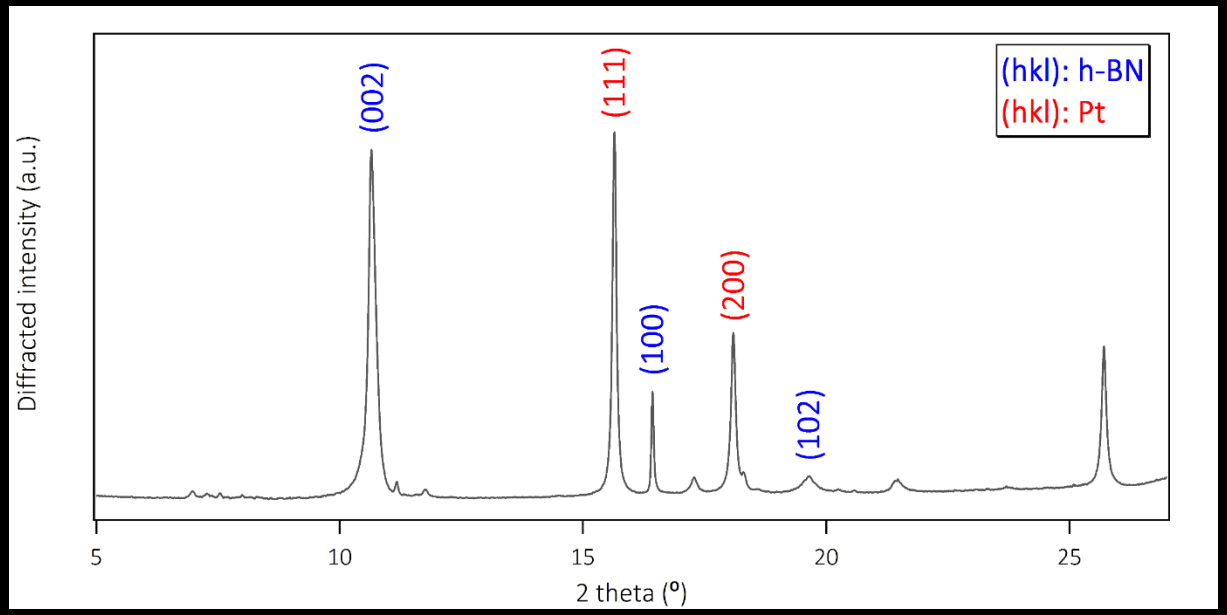

Diffraction pattern of the couple h-BN-Pt

Measuring pressure at high T in the lab

How to precisely measure the sample pressure at high T in the DAC (in the lab)?

- Pressure measurement with the standard ruby sensor gets less and less accurate with T
  - Broadening of the R lines, complex background
  - Sensitivity of R lines to errors in T

- Selected alternatives:
  - Fluorescence sensor : $SrB_4O_7:Sm^{2+}$
  - Raman sensor : c-BN

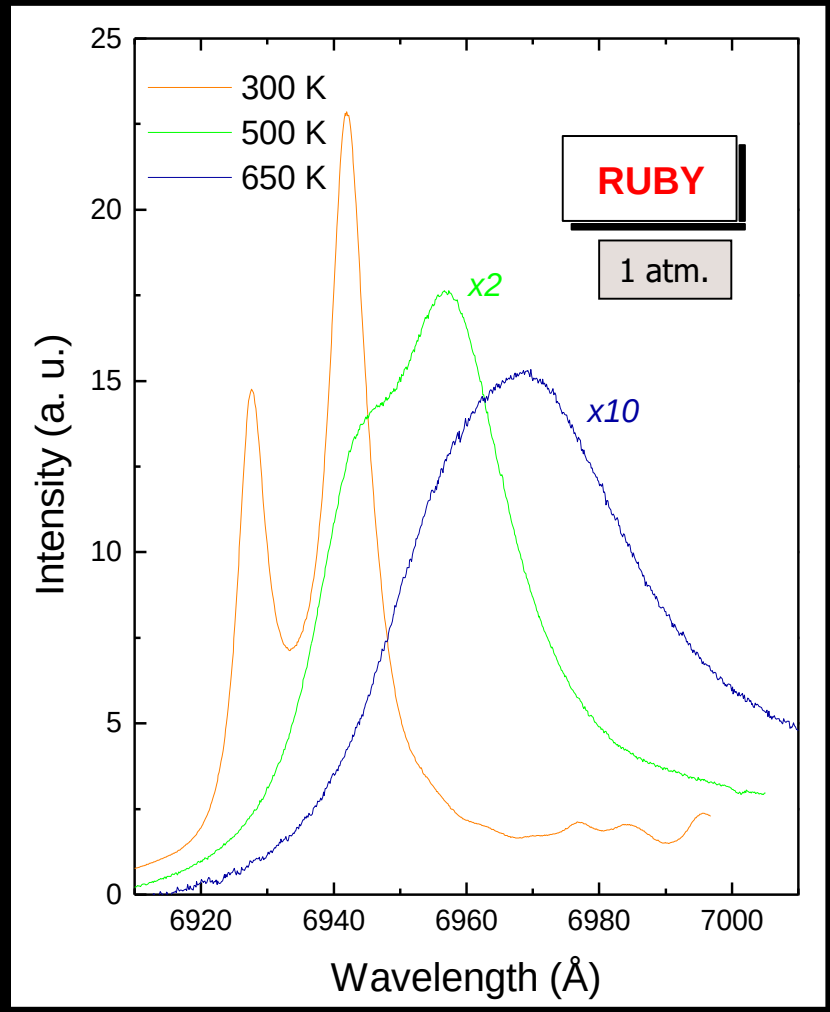

$SrB_4O_7:Sm^{2+}$: The best fluorescence sensor ?

- **Pros:**
  - Strong, isolated line ($^5D_0$-$^7F_0$) at 685.41 nm at ambient.
  - Small bandwidth: $\delta\lambda_{FWHM}$ ≈0.1 nm at ambient conditions
  - lower $(d\lambda/dP)_{P=0}$: 0.253(5) nm/GPa vs. 0.365 nm/GPa for ruby *but improving* with P
  - P calibration weekly dependent on PTM
  - Very small wavelength shift with temperature ($d\lambda/dT$)
  - Small broadening with temperature $d(\delta\lambda_{FWHM})/dT$
  - Easy to synthesize

- **Cons:**
  - Prone to chemical attack (dissolved by water and acids at HP-HT, but so is ruby)
  - Rapid decrease of intensity with T: limits to ~1000 K

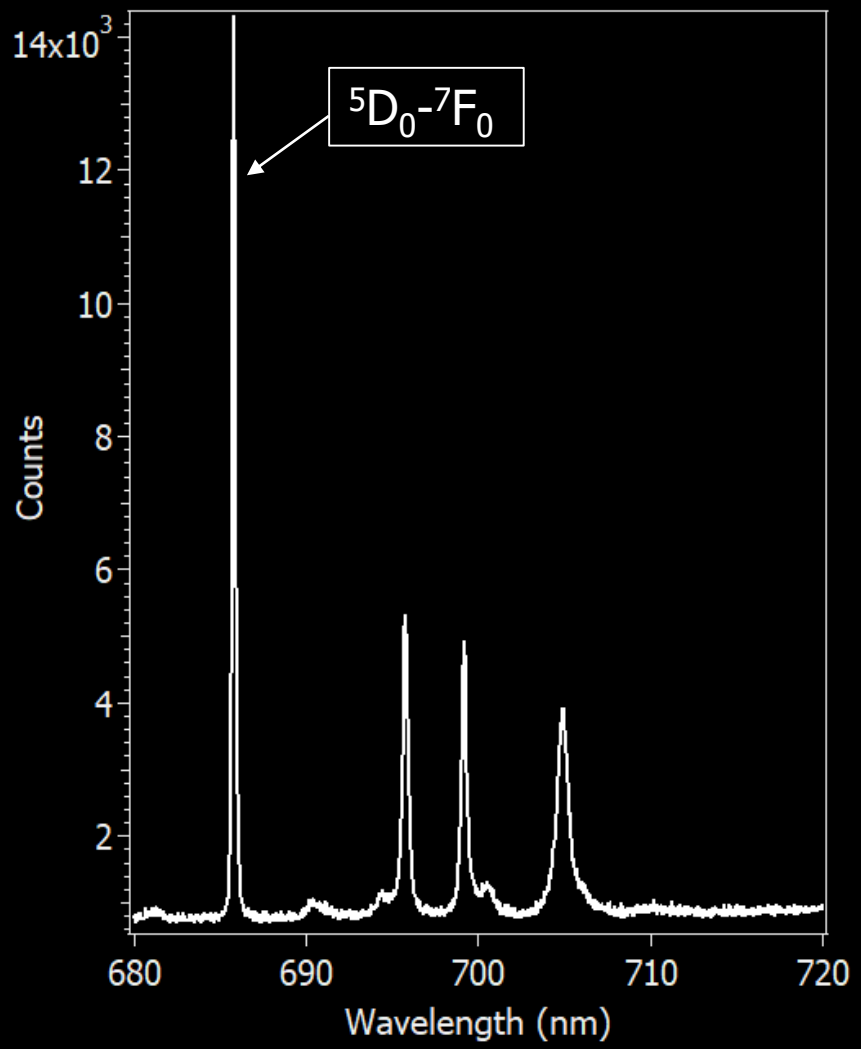

Lacam and Château, J. Appl. Phys. 66,366 (1989)

$SrB_4O_7:Sm^{2+}$: High temperature measurements

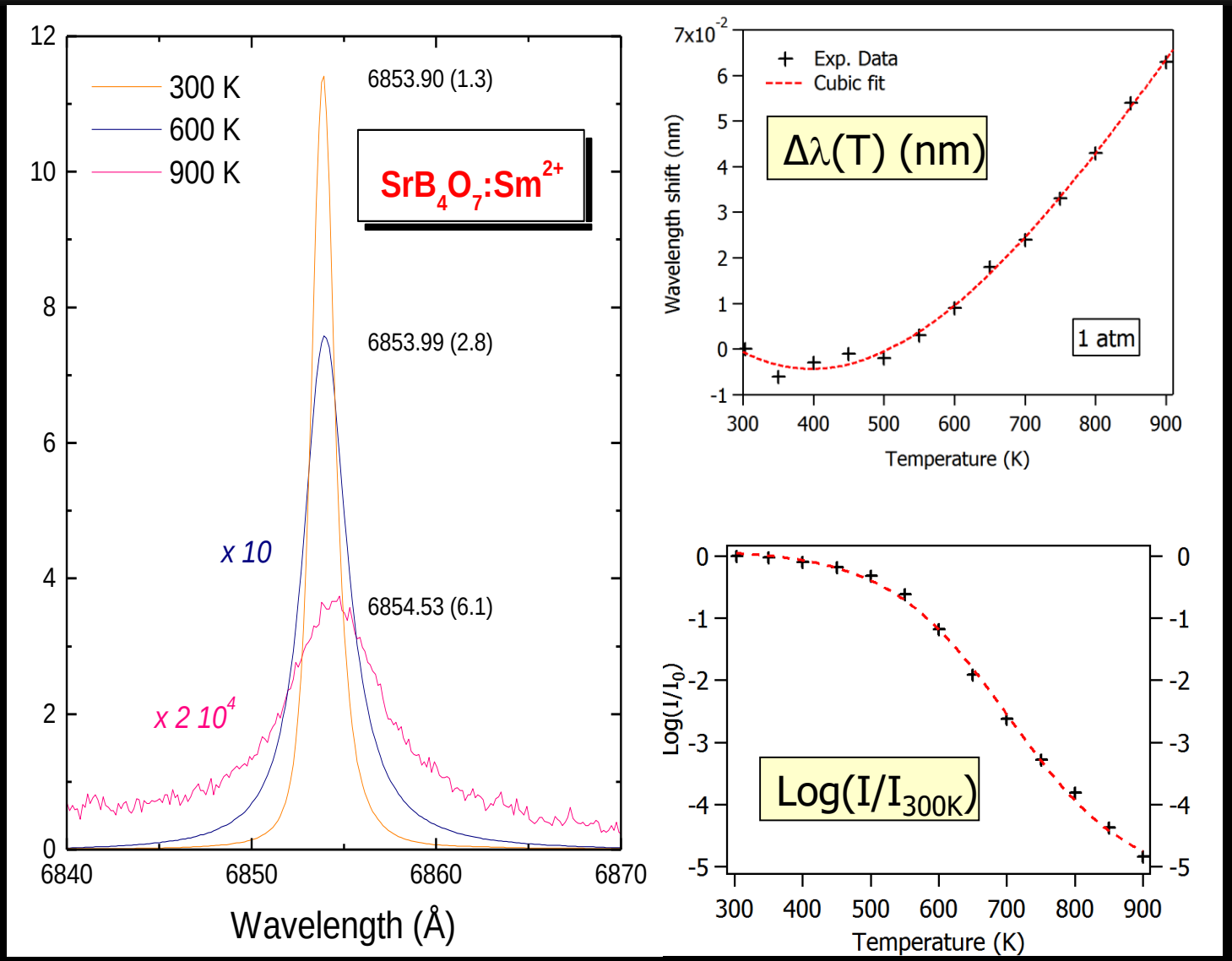

0-0 line at 1 atm and high T

- Wavelength shift 2 orders of magnitude smaller than ruby at 900 K
- No overlap with other bands
- Rapid decrease of intensity above 500 K, but measurable to ~900 K

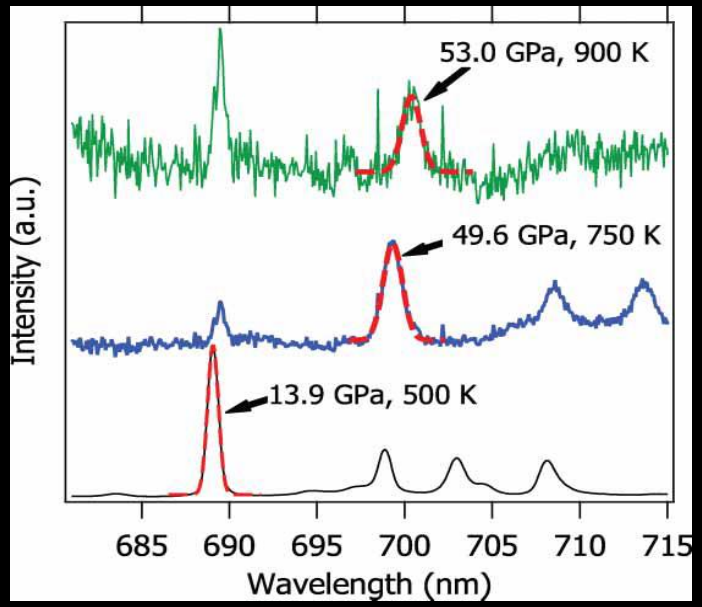

Fluorescence spectra at high P-T

F. Datchi, R. LeToullec and P. Loubeyre, J. Appl. Phys. 81, 3333 (1997); F. Datchi et al, High Pres. Res. 27, 447 (2007)

$SrB_4O_7:Sm^{2+}$:Pressure calibration in He

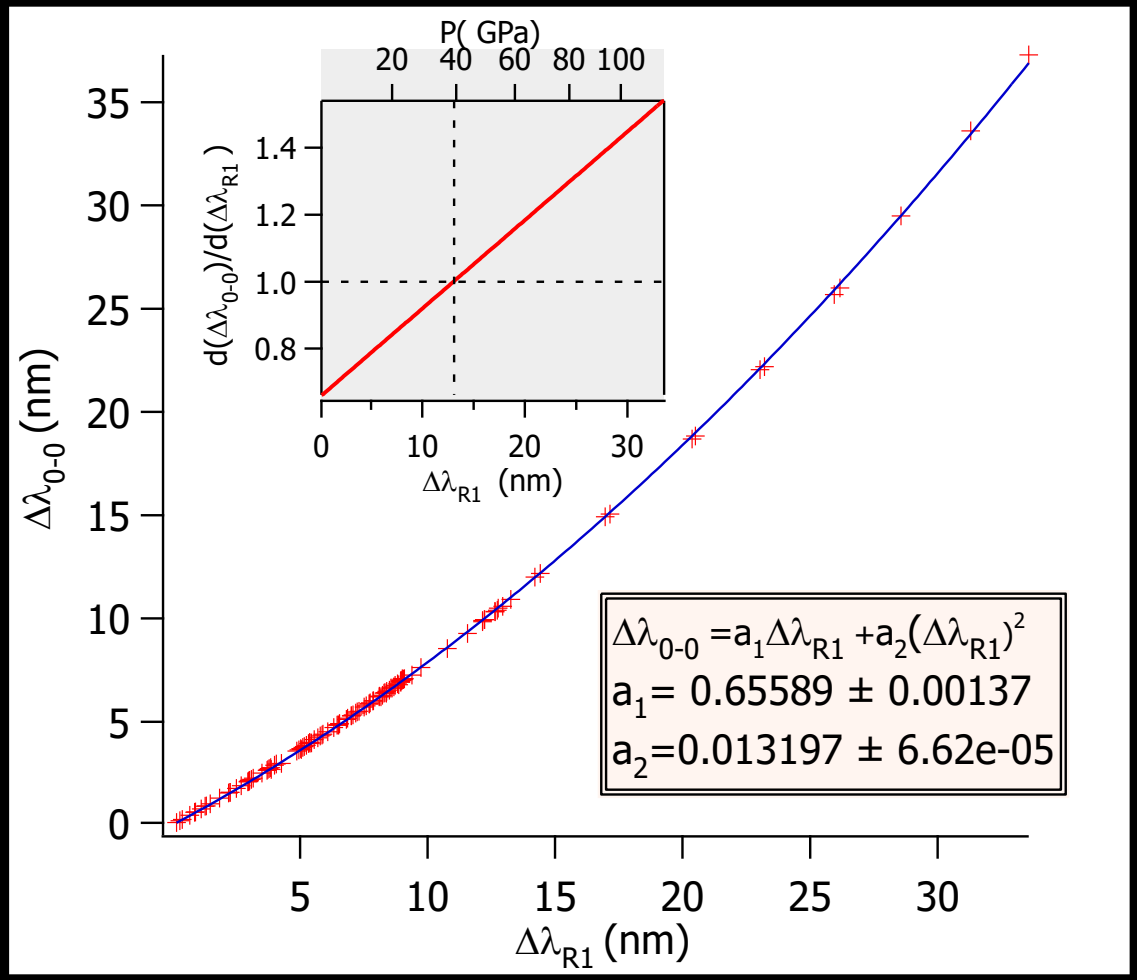

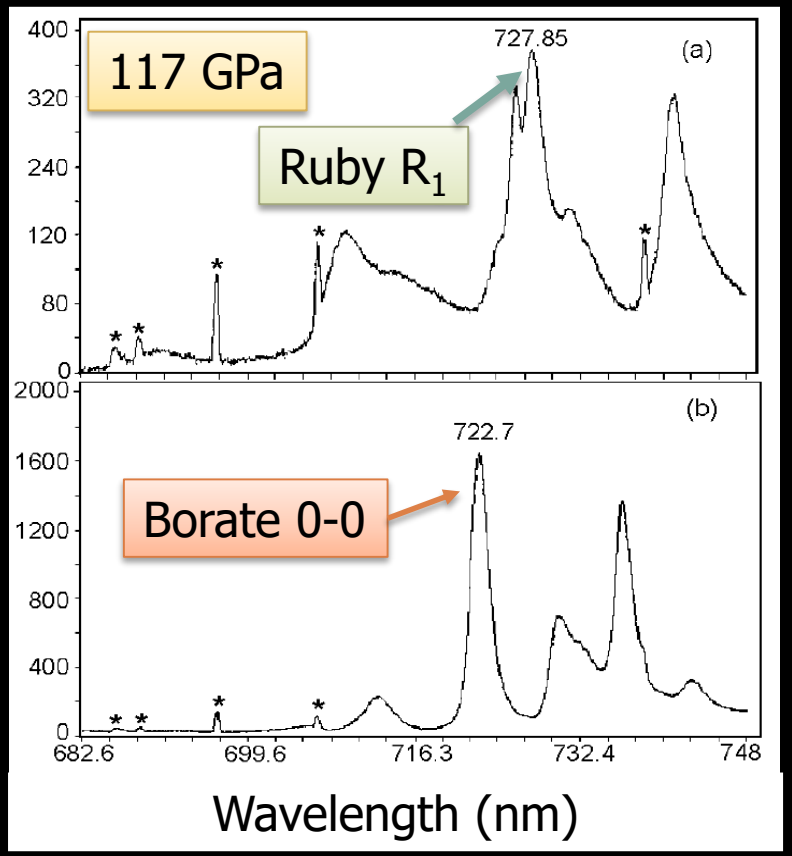

$\Longrightarrow \partial\lambda_{0-0}/\partial P > \partial\lambda_{R_1}/\partial P$ **for** $P >\sim 40$ **GPa**

F. Datchi, R. LeToullec and P. Loubeyre, J. Appl. Phys. 81, 3333 (1997); F. Datchi et al, High Pres. Res. 27, 447 (2007)

c-BN - Advantages as a pressure sensor

- Intense Raman TO mode (1054 cm^{-1} at ambient), well separated from the anvil signal (1332.5 cm^{-1})
- Small linewidth (~3.5 cm^{-1} at ambient) which increases slowly with T
- Chemically inert: suitable for corrosive media
- Structurally stable in a wide P-T domain
- Easily available in sizes suitable for DAC
- Measurable at T>1000 K (provided you have a good Raman setup)

HP-HT Raman and EOS data of c-BN

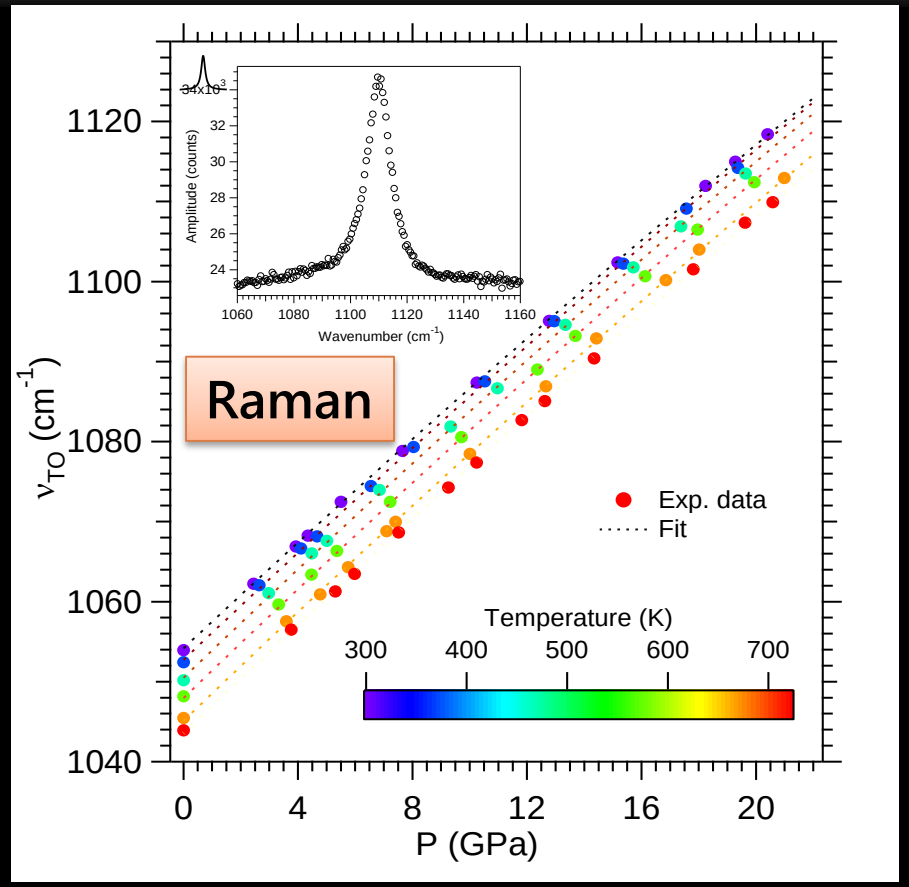

- TO mode
- Ne PTM
- 373 K < T < 723 K
  0 < P < 21 GPa

F. Datchi & B. Canny, PRB, 69,144106 (2004)

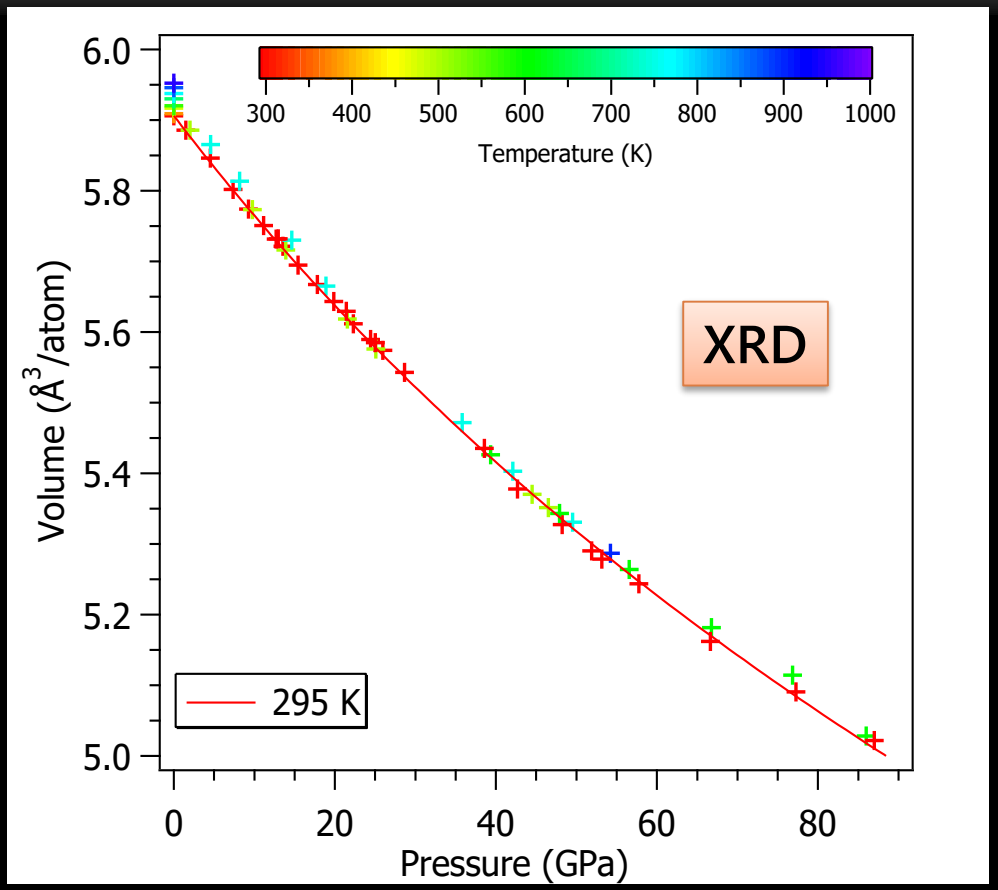

- Single-crystal sample
- Ne (HT) or He (295 K) PTM
- P<160 GPa at 295 K
  P<80 GPa, 500<T<900 K

F. Datchi et al, PRB, 75, 214104 (2007).

Mie-Grüneisen EOS for c-BN

Pressure is expressed as the sum of a cold (T=0 K) part and a thermal part due to vibrational energy:

$$P(V) = P_{0K}(V) + P_{th}(V)$$

$$P_{OK}(V) = 3B_0[(1-x)/x^2]\exp[1.5(B_0' - 1)(1-x)]\,,$$

$$x = (V/V_0)^{1/3}$$

$$P_{th}(V) = 3RT\left(\frac{\gamma_{th}}{V}\right)\mathcal{D}(\Theta_D/T)$$

Where γ_{th} is the Grüneisen parameter and $\mathcal{D}(\Theta_D/T)$is the Debye function.

γ_{th} is allowed to vary with volume according to:

$$\gamma_{th} = \gamma_{th0}(V/V_0)^q$$

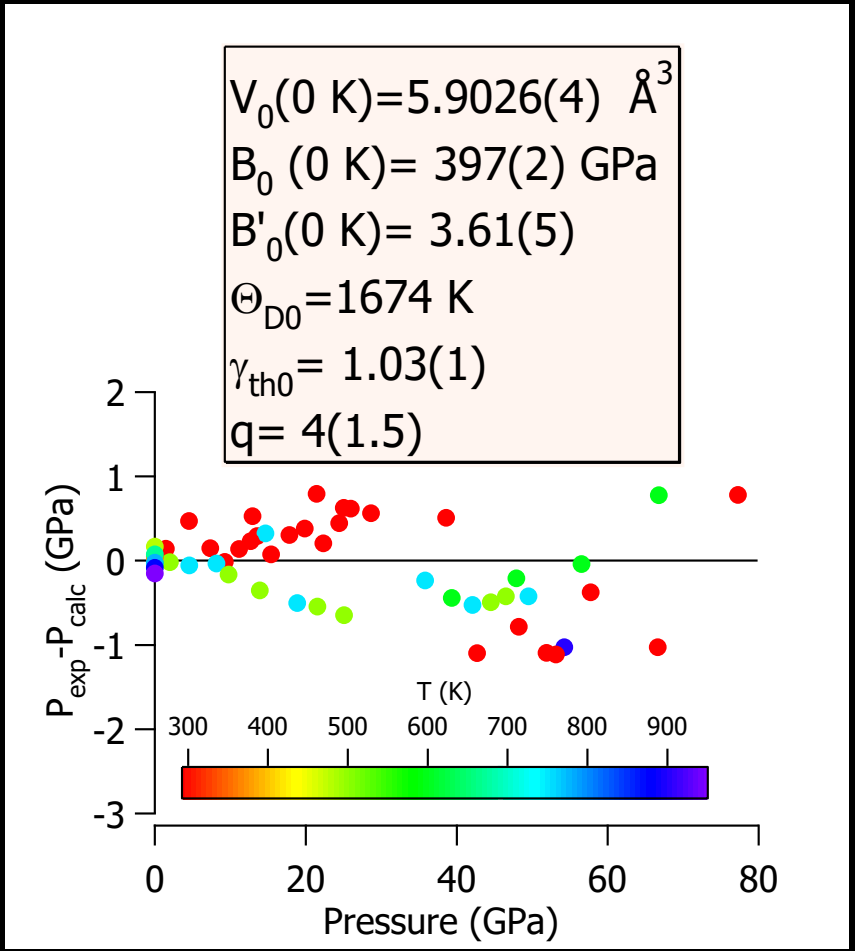

F. Datchi et al, PRB, 75, 214104 (2007).

The constrained Raman pressure scale

- Using the first-order Murnaghan EOS, the variation of $\nu_{TO}(P,T)$ may be expressed as:

$$\nu_{TO}(P,T) = \nu_{TO}(0,T)[1 + [B_0'/B_0(T)]P]^{\gamma_{TO}/B_0'}$$

- $B_0(T)$ and B'_0 are given by the Mie-Gruneisen EOS
- $\upsilon_{TO}(0,T)$ is given by Herchen and Capelli, PRB,47,14193
- γ_{TO} is taken T-independent (1.257).
- We obtain the following pressure scale:

$$P = [B_0(T)/3.62]\{[\nu_{TO}(P,T)/\nu_{TO}(0,T)]^{2.876} - 1\}$$

with: $\upsilon_{TO}(0,T) = 1058.4(6) - 9.1(20)\times10^{-3}\ T - 1.54(22)\times10^{-5}\ T^2$

$B_0(T>300\ K) = 396.5 - 0.0288(14)(T-300) - 6.8(8)E\text{-}6(T-300)^2$

F. Datchi et al, PRB, 75, 214104 (2007); High Pres. Res. 27, 447 (2007).

Accuracy and useful range

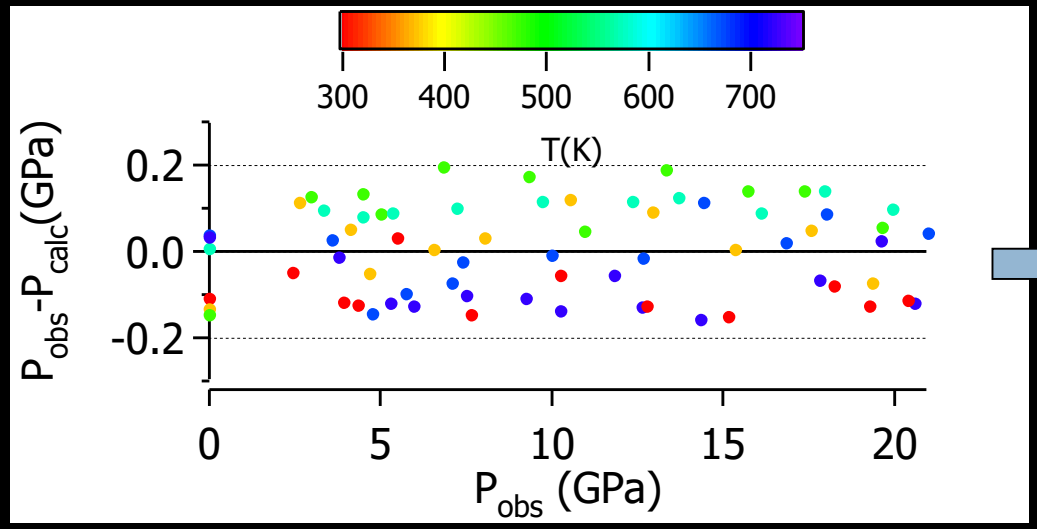

The calculated pressure is within ±0.2 GPa of the observed one

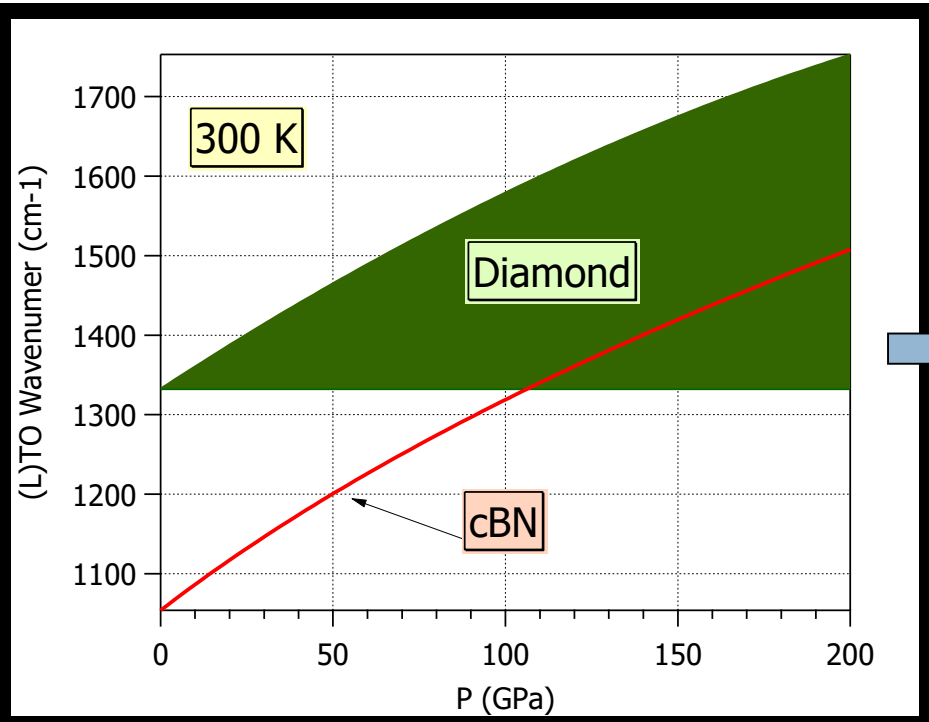

Above ~100 GPa, the TO mode is masked by the anvil signal.

Comparison with Ono et al, 2015

- Raman in DAC with resistive heating
- NaCl PTM
- P<87 GPa, T<800 K
- P measured with Au EOS from Doogokupets & Dewaele, HPR 2007
- Polynomial fit of $\nu_{TO}(P,T)$

S. Ono et al, J. Phys. Chem. Sol. 76,120 (2015).

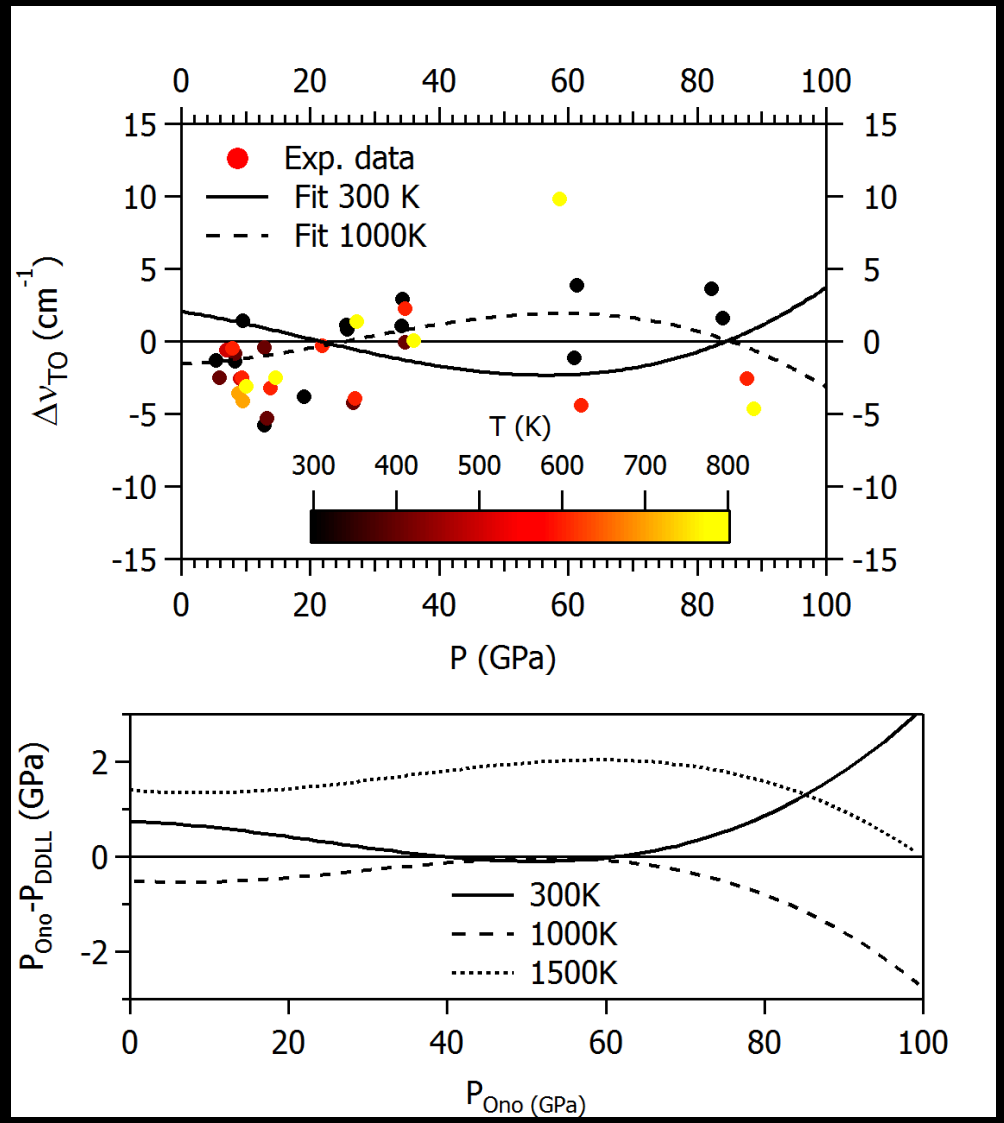

Comparison between Datchi et al c-BN scale and Ono et al's data

Conclusions/recommendations

- For T<900 K, $SrB_4O_7:Sm^{2+}$ is probably the best choice, except for corrosive media.
- For higher T, or corrosive media, c-BN and/or diamond may be used in the P ranges:
  - c-BN: P<~100 GPa
  - ^{12}C: P>15 GPa
  - ^{13}C: P<14 GPa
- It's always better to cross-check using several sensors !

Temperature measurement

- Thermocouples give an easy, rapid and accurate (within a few K) temperature measurement in the RH-DAC
- Extreme care must be taken where the thermocouple is attached ! The closer to the sample the better (especially when using internal heater)
- K- (or N-) type range is usually enough but R and S types can be used for higher T
  - K/N: T<1300 K in continuous use
  - R/S: T<1850 K in continuous use
- Optical pyrometry (as in laser heating) is also used for T> 1500 K in direct internal heating – more difficult and less accurate

Temperature gradient for the « heating gasket »

Temperature gradient measured in a HP experiment using the heating gasket. The thermocouple is cemented to a hole drilled 1 mm away. The sample temperature is meausred using the Ruby-SrBO:Sm metrology.

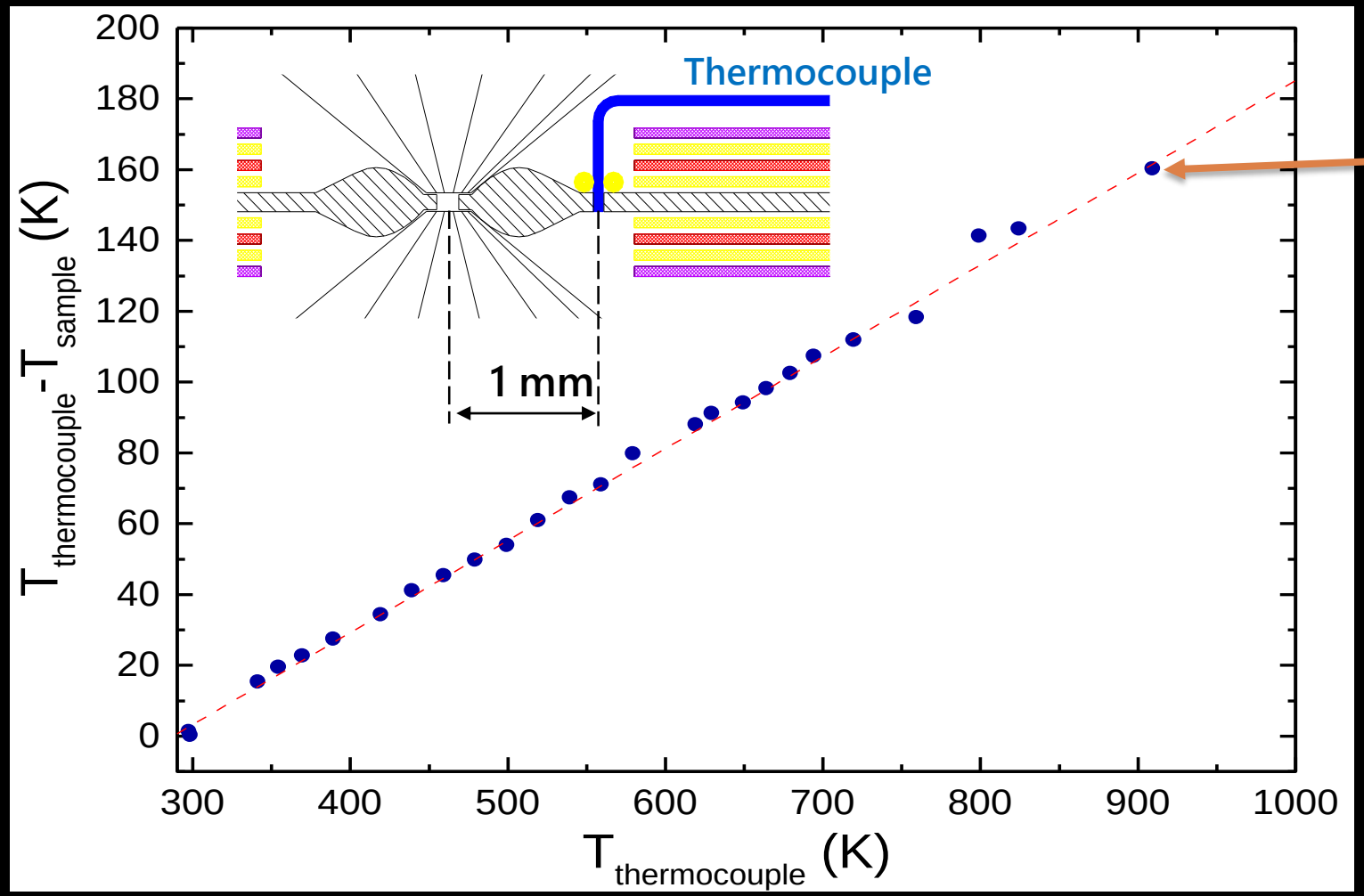

150 K difference at 900 K !

Ruby- $SrB_4O_7:Sm^{2+}$ crossed P-T metrology

The simultaneous measurement of ruby R_1 line and of $SrB_4O_7:Sm^{2+}$ $^5D_0$-$^7F_0$ line enables an *in-situ* determination of pressure and temperature

- Ruby:

$$\Delta\lambda_{R_1}(P,T) = \Delta\lambda_{R_1}(P,T_0) + \Delta\lambda_{R_1}(P_0,T)$$

- $SrB_4O_7:Sm^{2+}$:

$$\Delta\lambda_{0-0}(P,T) \cong \Delta\lambda_{0-0}(P)$$

Thus:

$$\Delta\lambda_{0-0}(P) \Longrightarrow P$$

$$P \Longrightarrow \Delta\lambda_{R_1}(P) \Longrightarrow \Delta\lambda_{R_1}(T) \Longrightarrow T$$

- The two calibrants must be placed close to each other to minimze effect of P gradients
- Accuracy of about $\pm$ 3 K below 600 K, decreasing at higher T

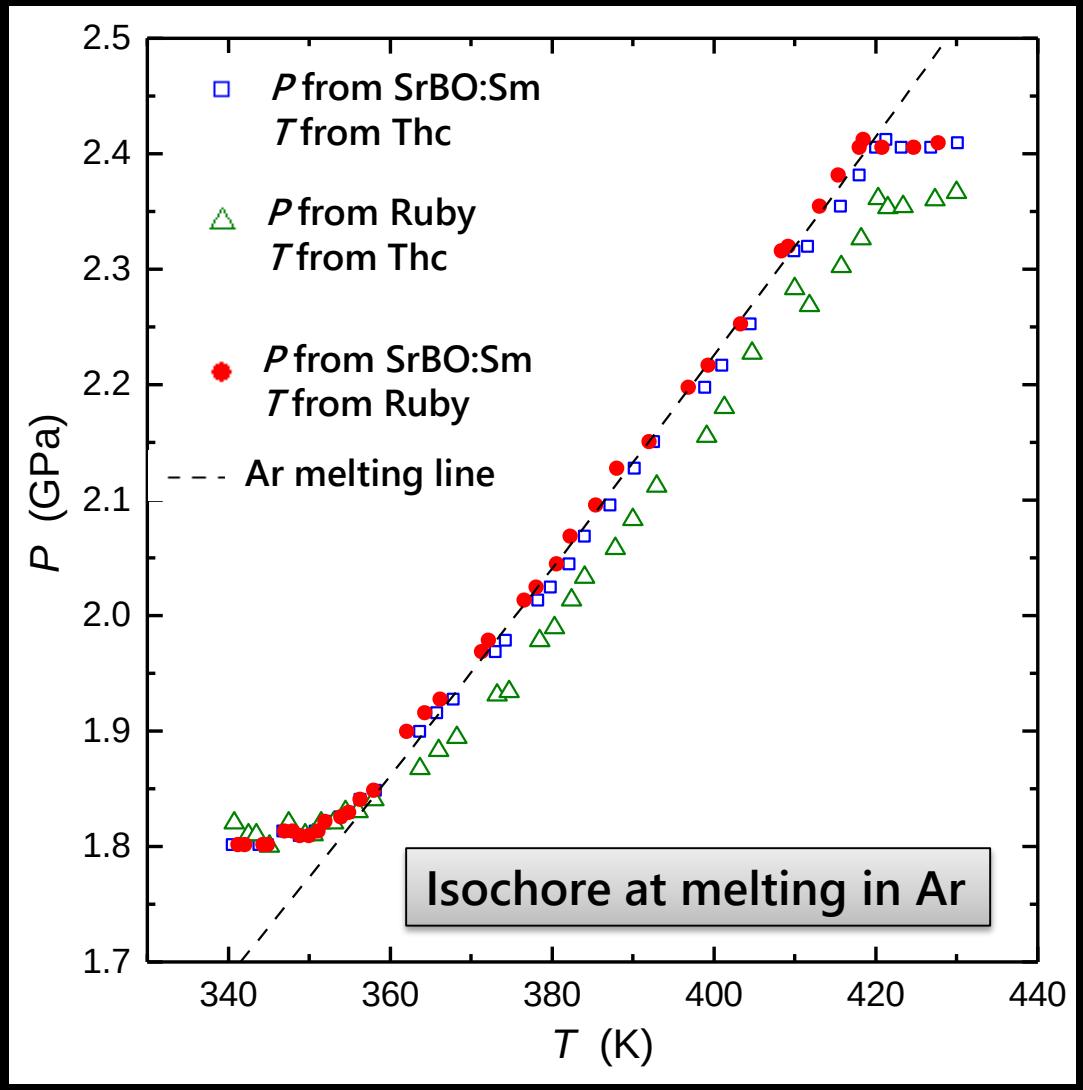

F. Datchi, R. LeToullec and P. Loubeyre, J. Appl. Phys. 81, 3333 (1997); F. Datchi et al, High Pres. Res. 27, 447 (2007)

Cross P-T dependence of ruby R_1 line

Do the T shift of ruby R_1 line depend on pressure ?

- Goncharov et al (2005):
  - Linear decrease of $\partial\lambda_{R_1}/\partial T$ with coefficient 3.5(4)x10^{-5} nm/K/GPa
    $\Longrightarrow$ 50% decrease at 100 GPa
- Rekhi et al (1999):
  $\partial\lambda_{R_1}/\partial T = 0.073(8) - 8(8) \times 10^{-5} P$
- Our data: no significant change of $\partial\lambda_{R_1}/\partial T$ from 0 to 20 GPa (300<T<600 K).

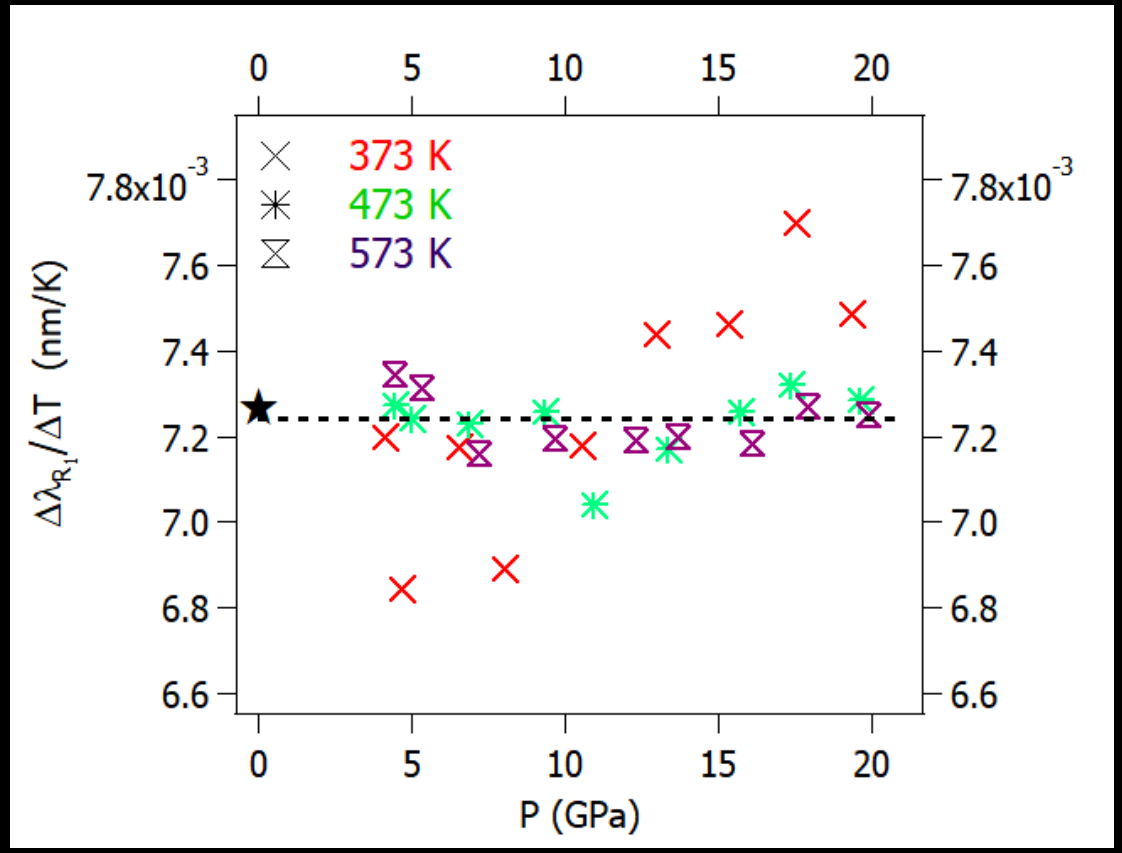

Linear T coefficient of the ruby R_1 line below 600 K, in neon PTM. P measured by SrBO:Sm.

Goncharov et al, J. Appl. Phys. 97 (2005); Rekhi et al, High Termp. High. Press 31 (1999); F. Datchi et al, High Press. Res. 27 (2007)

Going beyond resistive heating

Goal: find a way to heat at T>1000 K which is easy to set-up and operate

Going beyond RH-DAC : Induction heating

- Induction heating is based on the supply of energy by means of electromagnetic induction
- A coil is placed close to the metal parts to be heated. An alternated current in the coil induces electric (eddy) currents at the surface of the metal piece.
- Heating of the metal part is produced by Joule effect of the eddy currents and thermal transport of the heat to the bulk

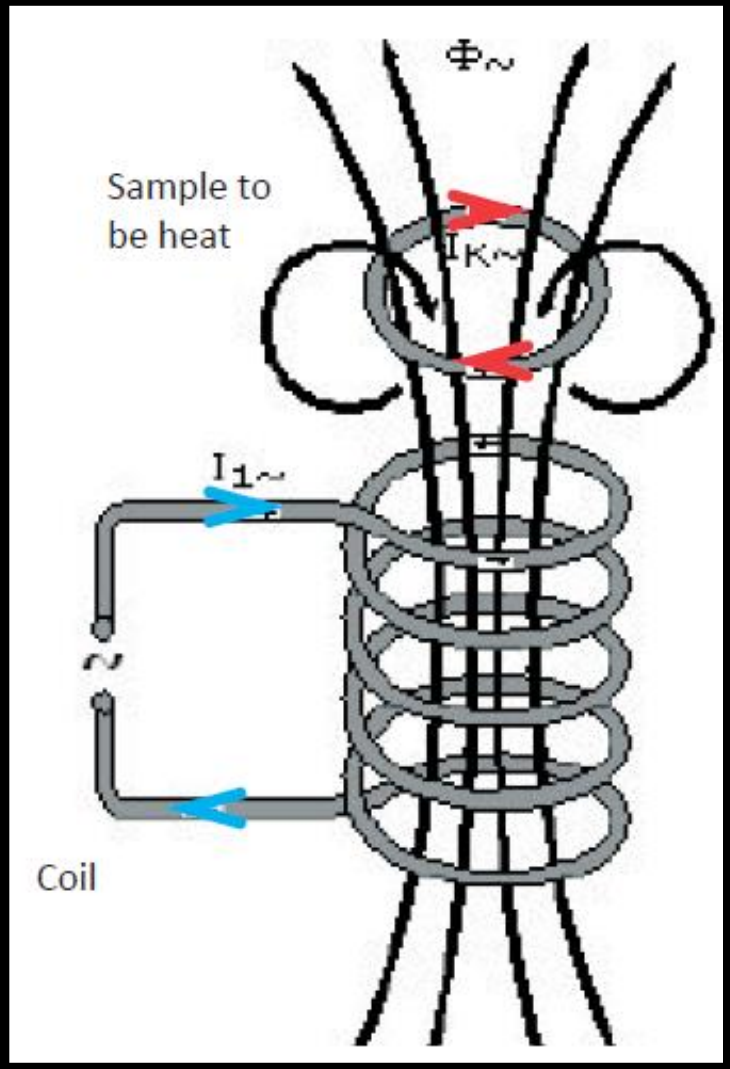

Industrial applications of induction heating

Main applications :

- Brazing/soldering
- Heat treatment (hardening, annealing, tempering,...)
- Melting
- Forging

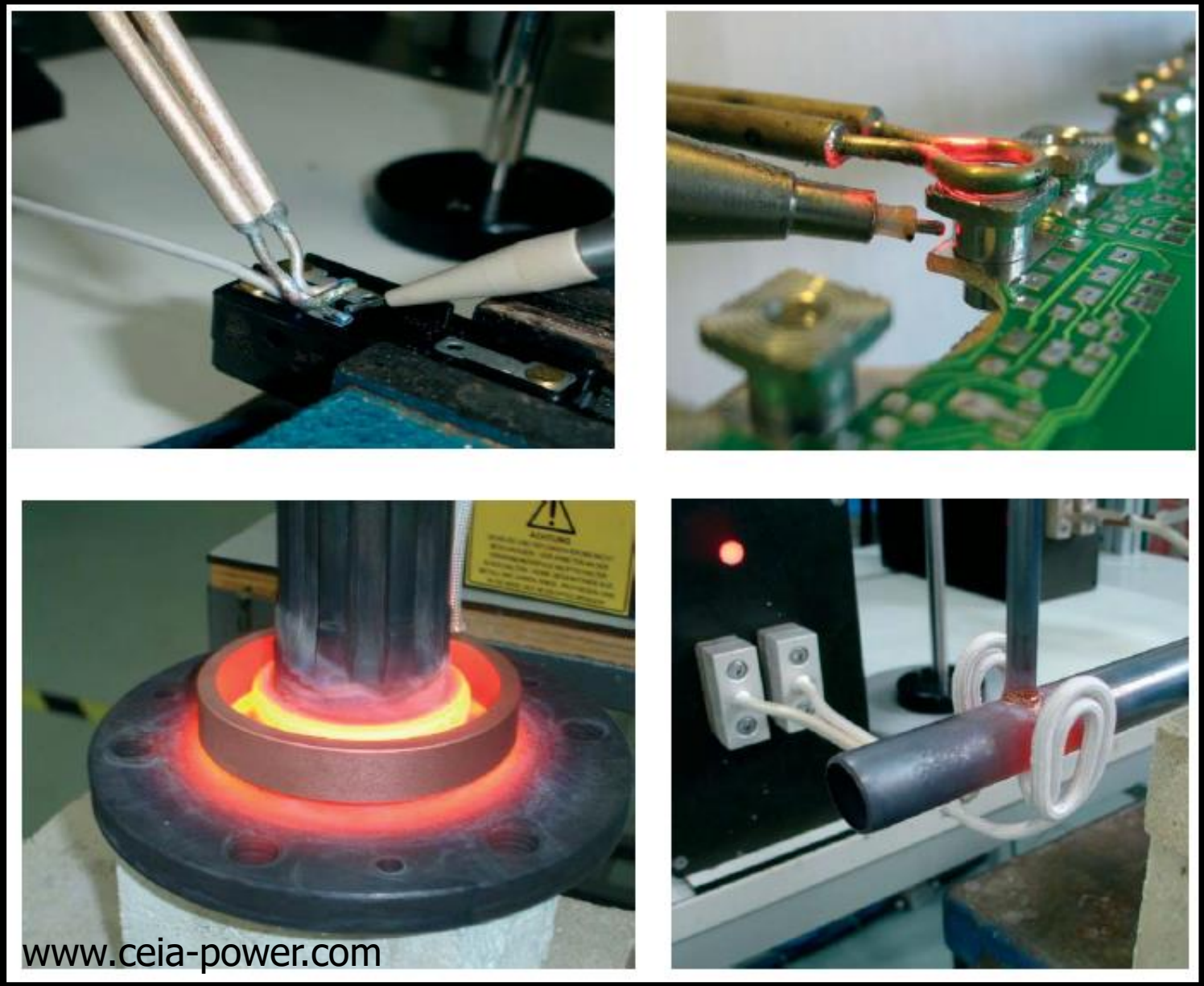

Induction heating: pros and cons for DAC use

- Pros:
  - Fast heating (seconds)
  - Localized heating
  - Controllable and reproducible

- Cons :
  - The induction zone must be free of metallic parts apart from heater
  - Thermocouples cannot be used for temperature measurement
  - DAC assembling and loading is complicated by the presence of the induction coil

Induction heating DAC by Shinoda & Noguchi (2008)

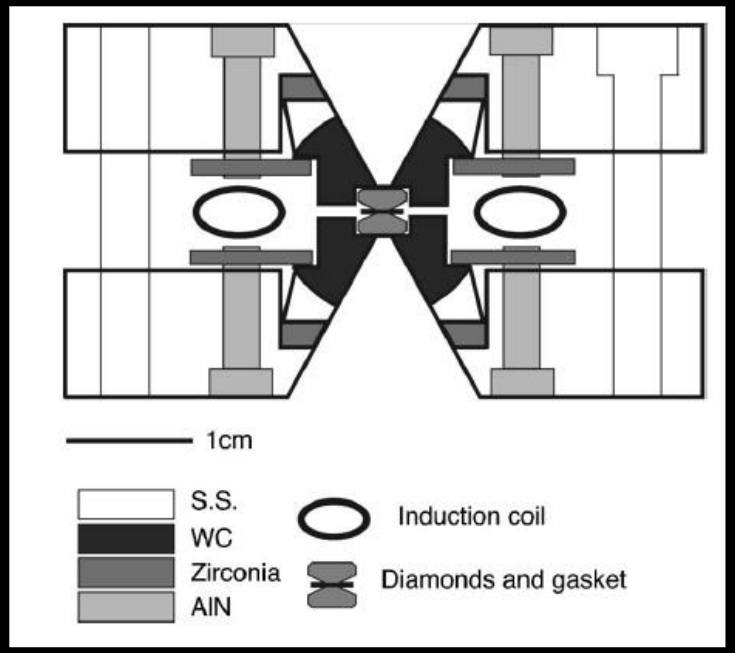

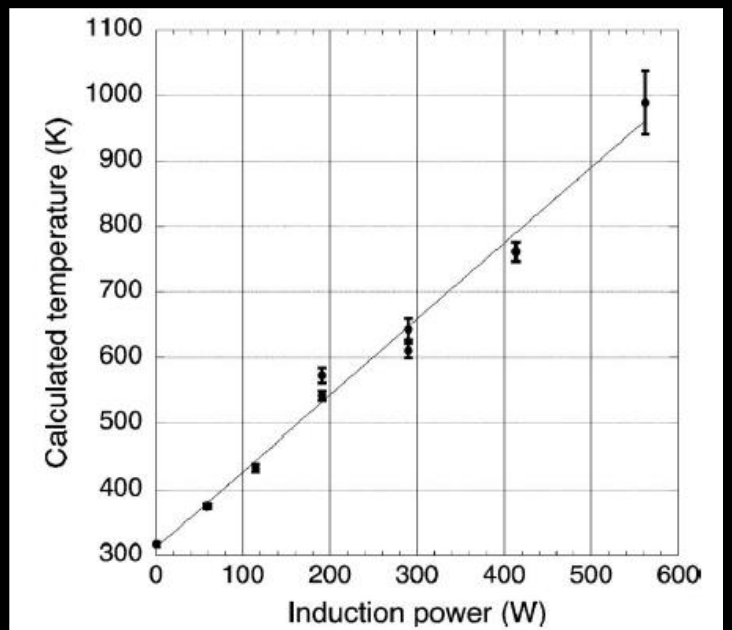

- Single turn coil made of water-cooled copper tubing
- The coil is fitted in-between the two DAC plates
- The coil heats the gasket and WC rockers. Heating the gasket alone was found unsufficient.
- Heating in air
  → limit at 1000 K
- No other publication using this DAC

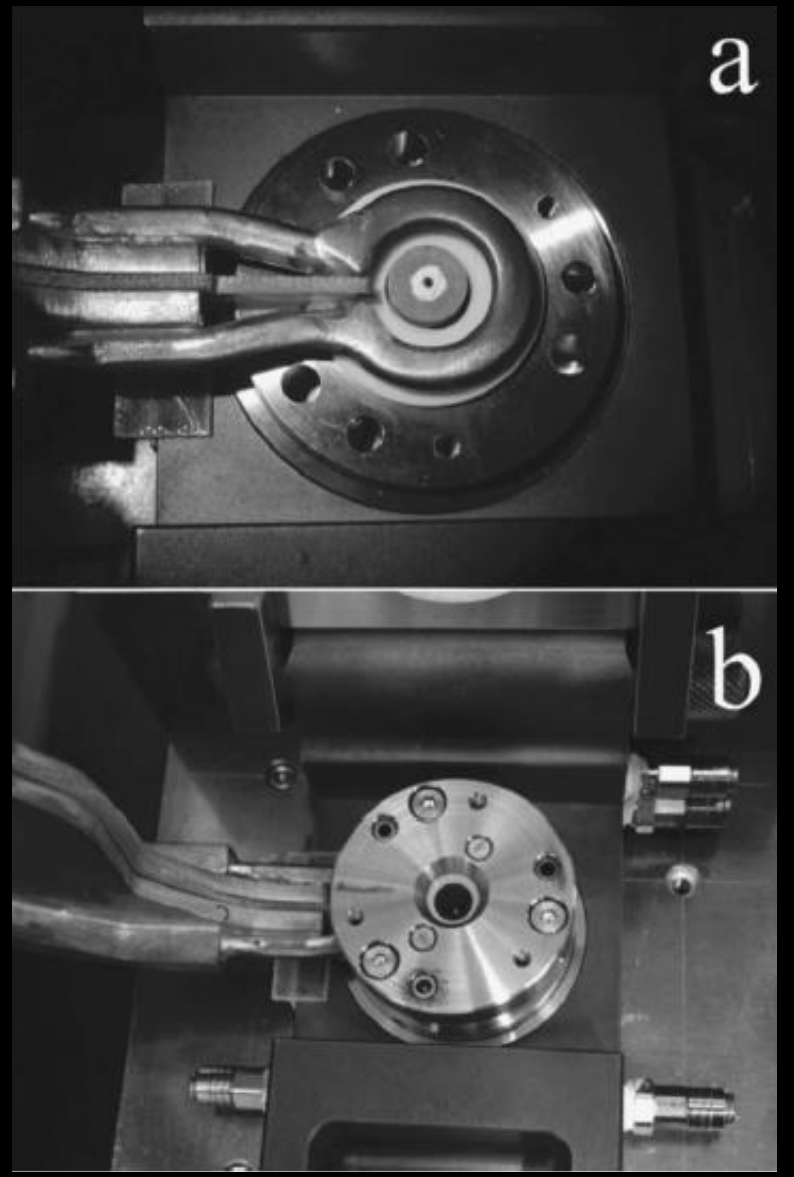

Shinoda & Noguchi, Rev. Sci. Instr. 79 (2008)

Examples of applications and perspectives

Examples of experimental setups

- RH-DAC setups are easily integrated in HP experimental measurement benches
- When using objectives (or any sensitive element), the only requirement is that working distance is long enough or the objective is well shielded from the high T zone
- Many laboratories have their own RH-DAC setups ready to be used.

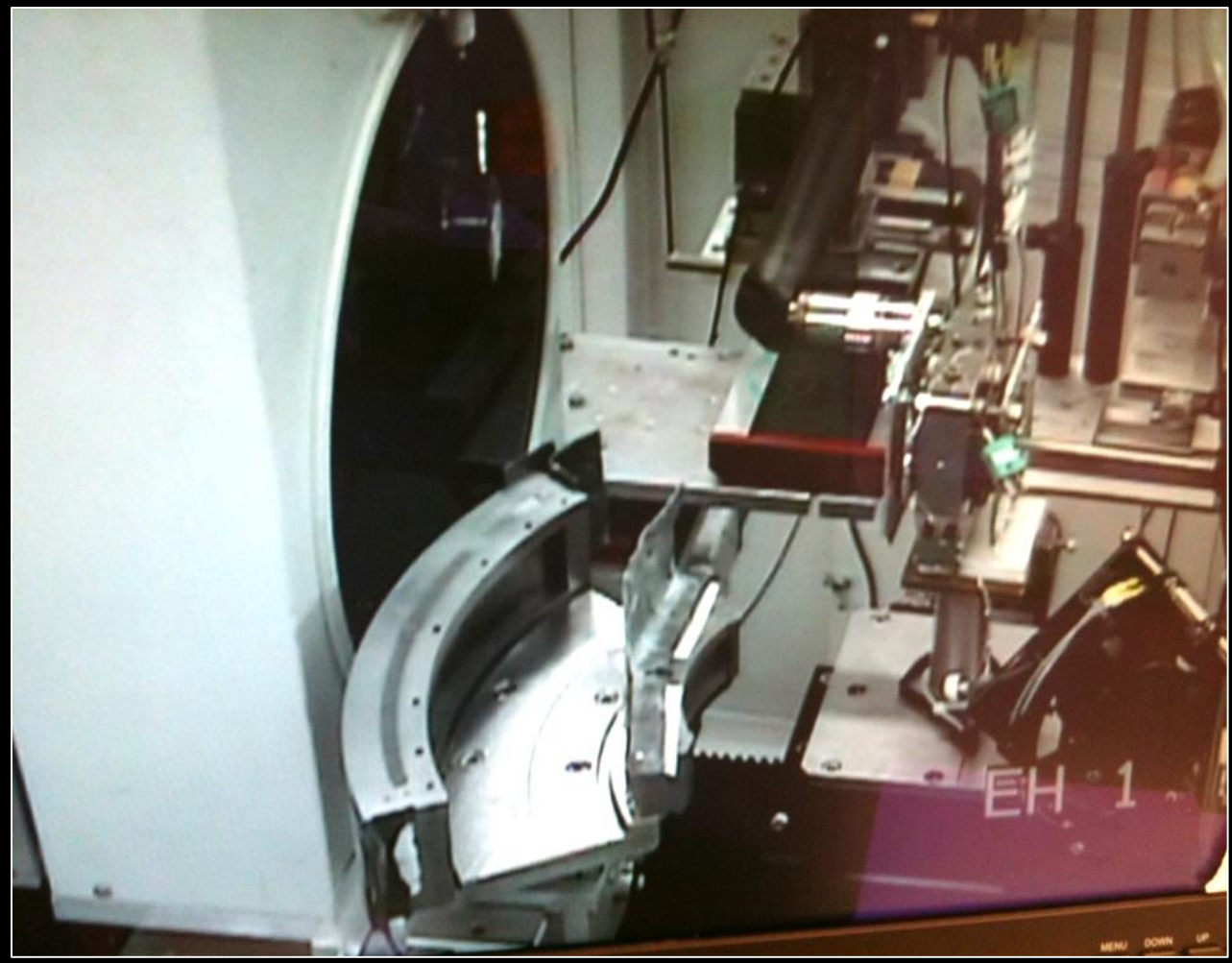

A RH-DAC installed at the ID27 EH-1 station of ESRF for X-ray diffraction experiment

Examples of experimental setups

- RH-DAC setups are easily integrated in HP experimental measurement benches
- When using objectives (or any sensitive element), the only requirement is that working distance is long enough or the objective is well shielded from the high T zone
- Many laboratories have their own RH-DAC setups ready to be used.

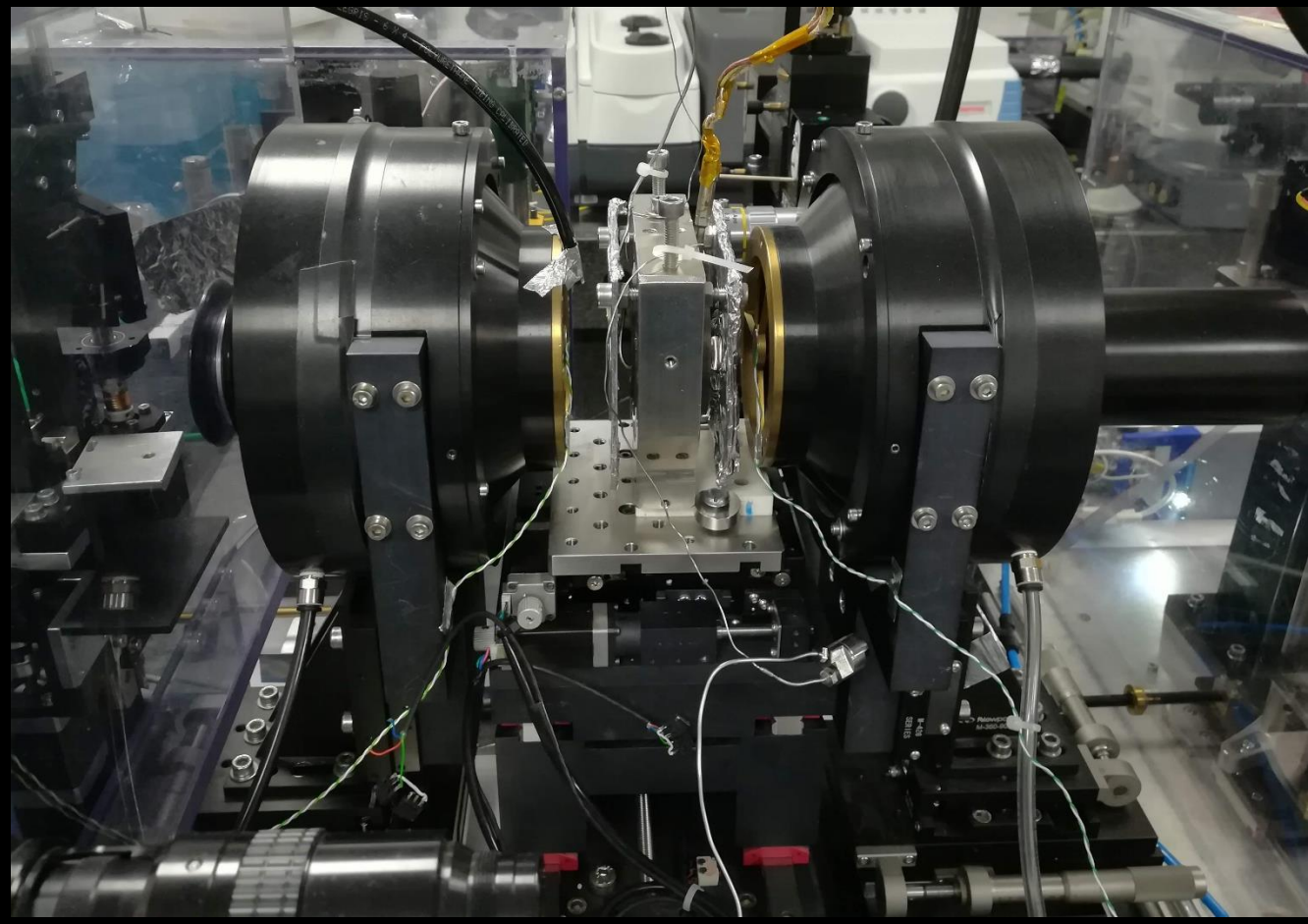

A RH-DAC installed at the SMIS station of SOLEIL
For IR spectroscopy

Examples of experimental setups

- RH-DAC setups are easily integrated in HP experimental measurement benches
- When using objectives (or any sensitive element), the only requirement is that working distance is long enough or the objective is well shielded from the high T zone
- Many laboratories have their own RH-DAC setups ready to be used.

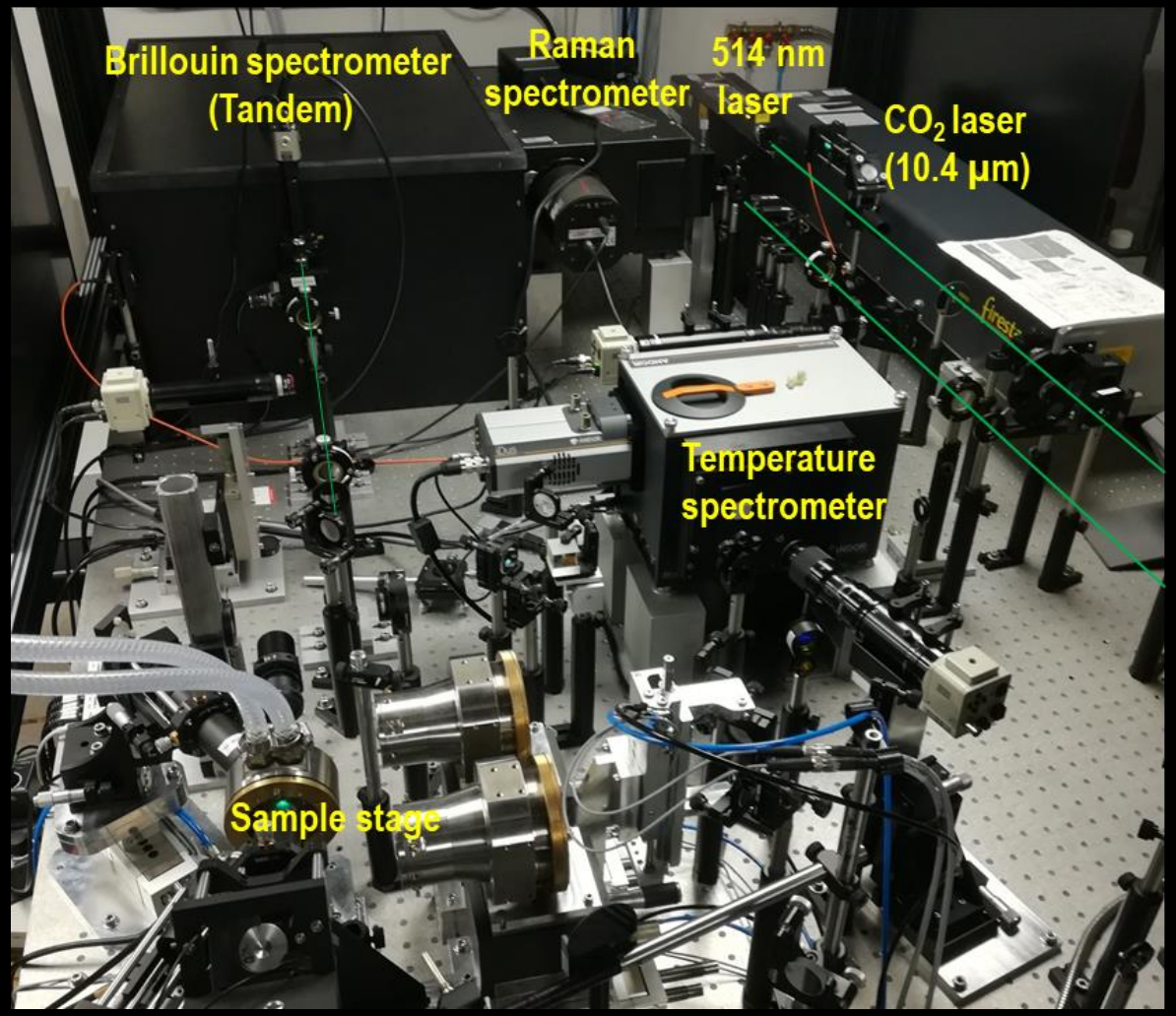

Brillouin and Raman spectroscopic bench at IMPMC compatible with LH-DAC, IH-DAC and RH-DAC

Solid CO_2 : the « intermediate bonding states »

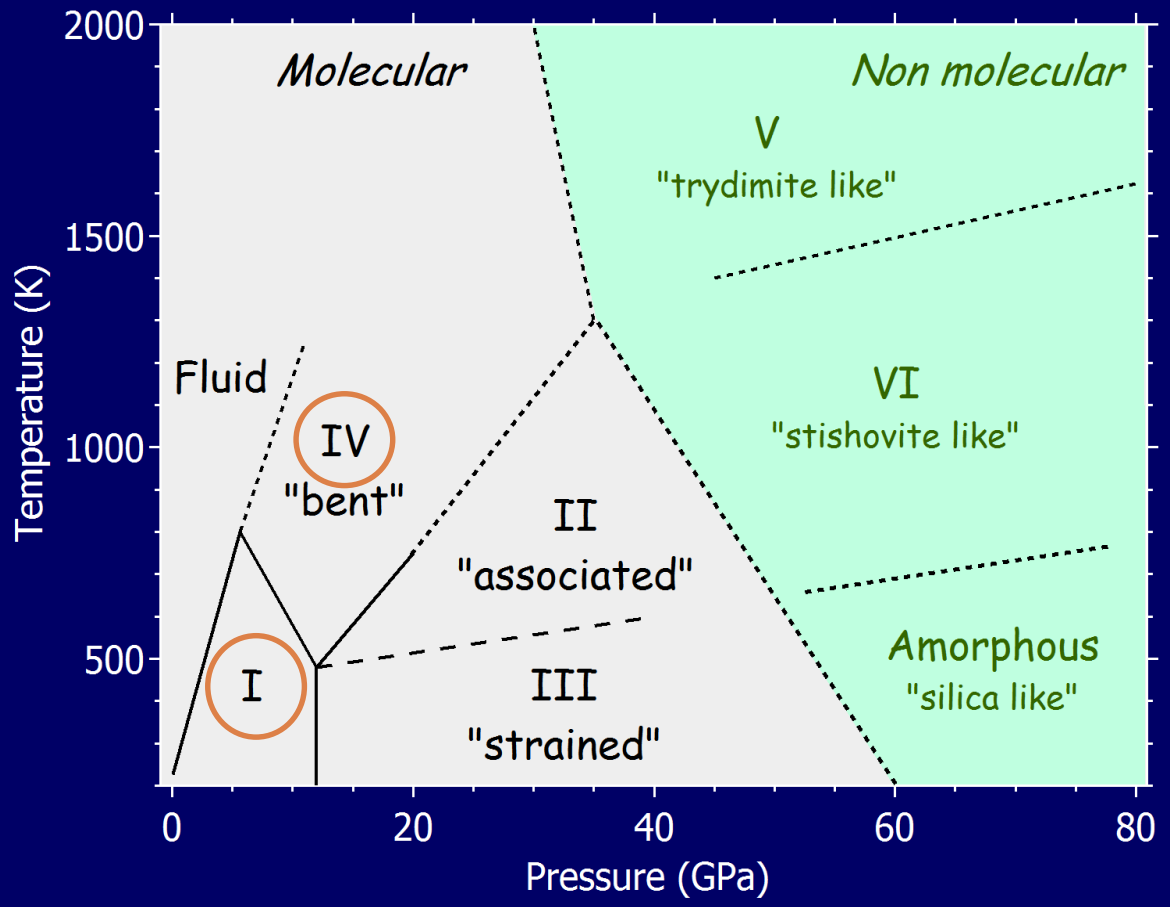

Experimental phase diagram of CO_2
[After Yoo et al, 2006]

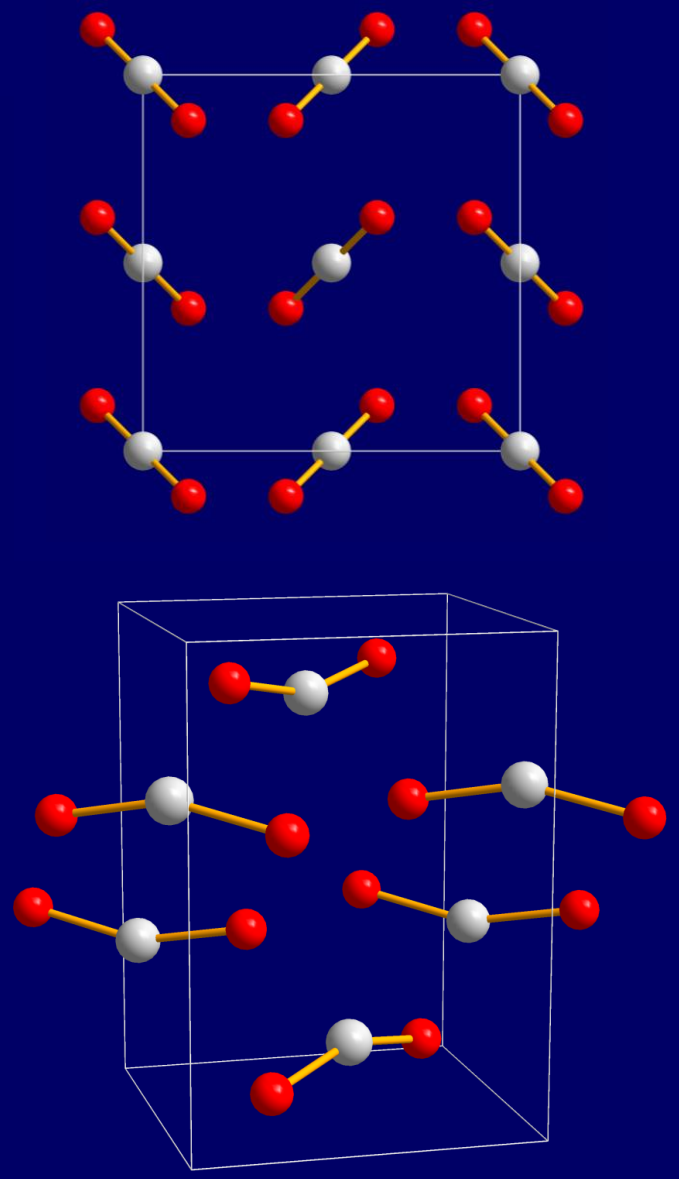

PHASE I

(dry ice)

d(C-O)=1.168 Å

at 1 GPa

PHASE IV

- d(C-O) = 1.487 Å at 15 GPa
- Bent molecules (160°)
- "Intermediate bonding state"

Is phase IV an intermediate state?

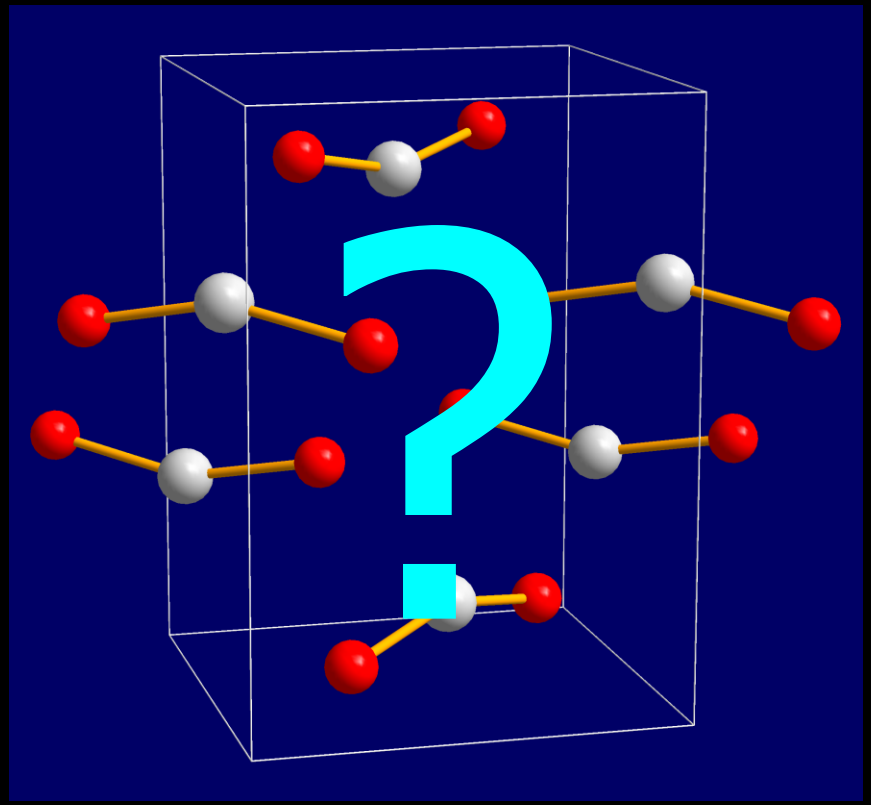

Phase IV (Pbcn)

Yoo, et al, PRL. **86** (2001).
Park *et al.*, PRB **68** (2003)

- This structure is by far unstable in theoretical (DFT) calculations [Bonev et al, PRL 2003]
- What is the true structure of phase IV ?
- Synthezing a good powder sample in the DAC is very hard. A better solution is to grow a single crystal.

Growing a single crystal of phase IV

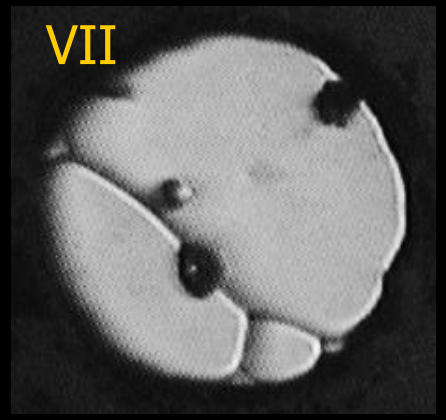

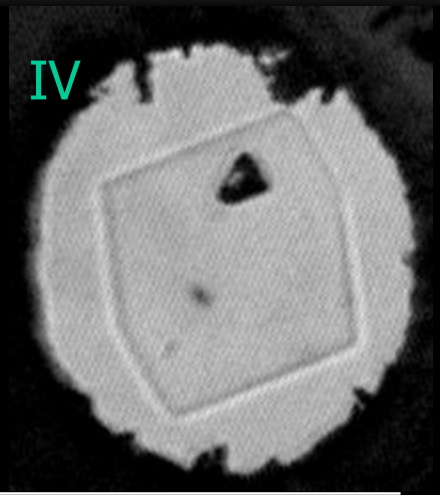

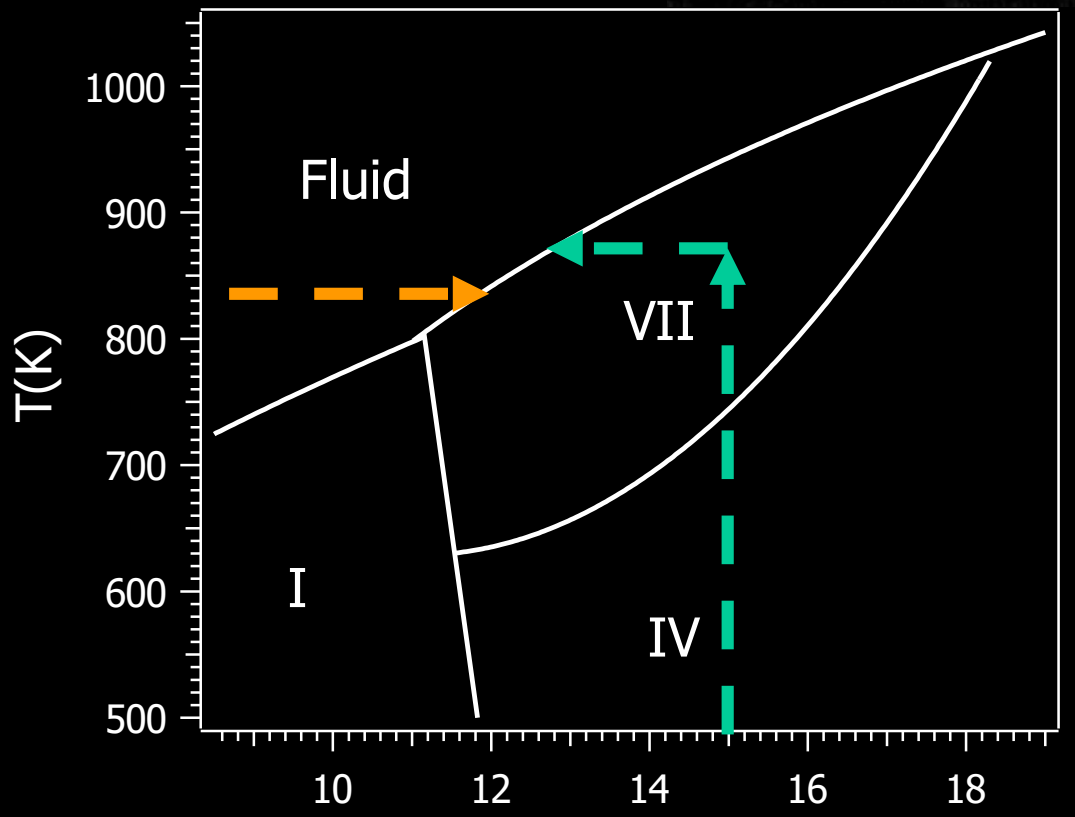

Growing a single crystal of phase IV requires:

- A very stable temperature above 800 K
- A fine control of pressure to decompress the solid down to the melting point and reach the solid/liquid equilibrium

Structure of phase IV

XRD image @ 15 GPa, 300 K (ESRF)

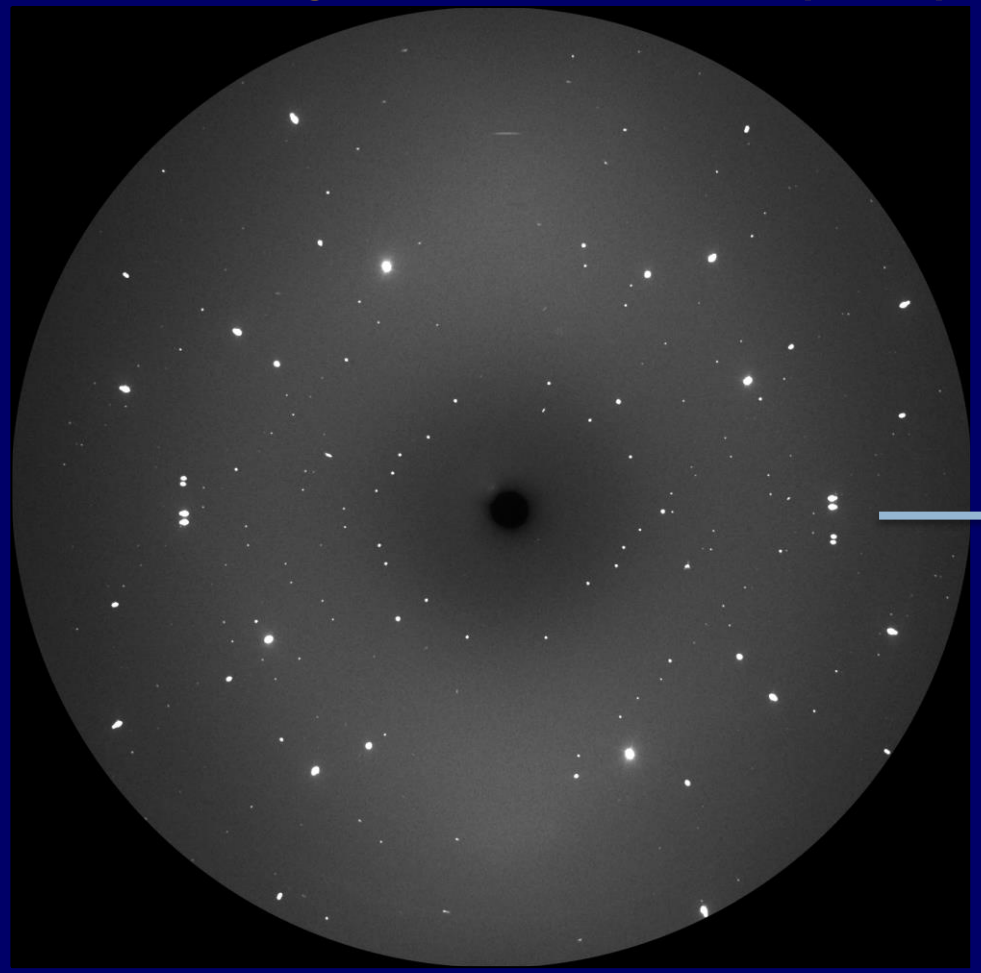

Phase IV (R-3c)

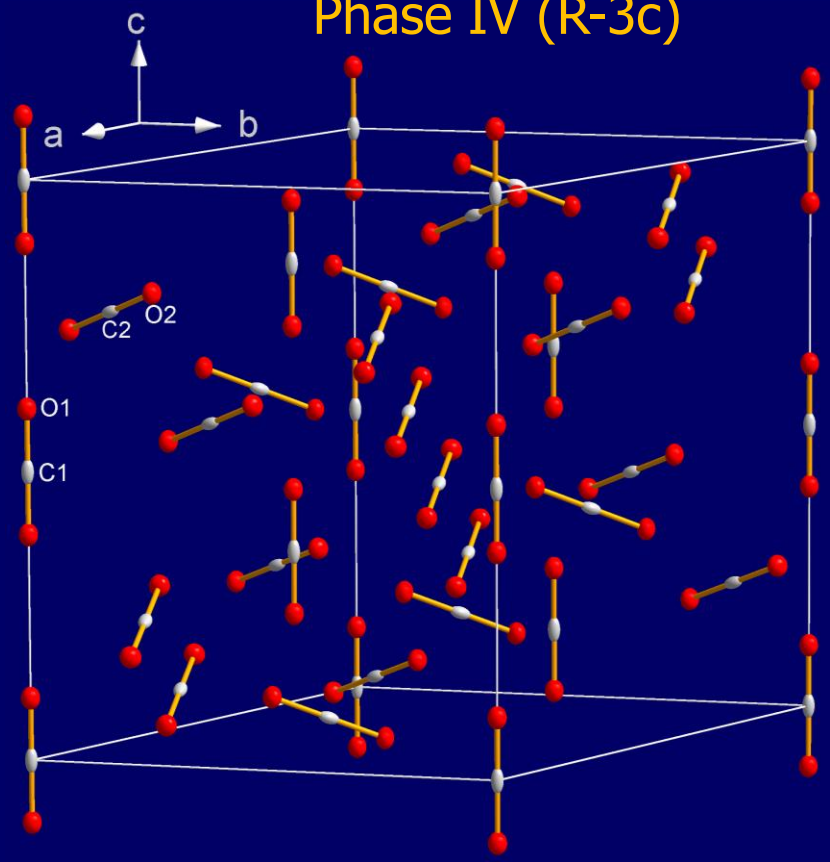

Structure of phase IV

- Molecules are *linear* (no bending)
- The bond *shortens* with pressure, in contradiction with the intermediate state scenario

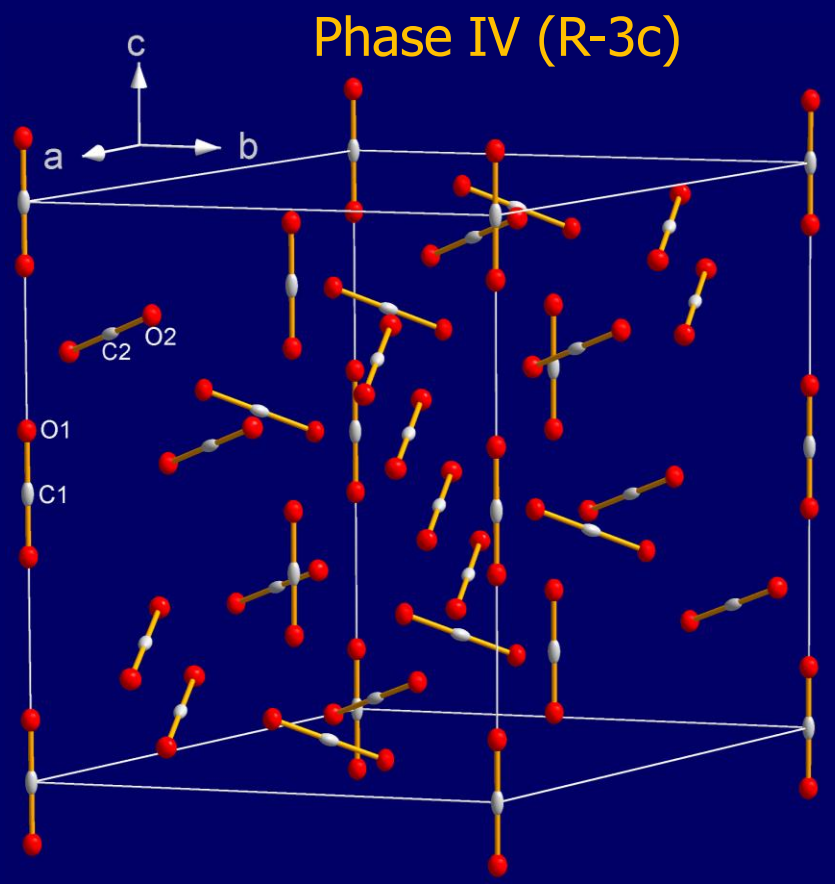

F. Datchi, V. M. Giordano, P. Munsch & A. M. Saitta, Phys. Rev. Lett. 103 (2009)

Future research on CO_2 at EBS

The structures of solid CO_2 are well established to ~1 Mbar: above 40 GPa, CO_2 is 4-fold coordinated (phase V)

DFT predicts new 4-coordinated structures at ~250 GPa and 6-fold coordination at ~1 TPa. Could be reached by new anvil designs and evidenced by XRD at EBS.

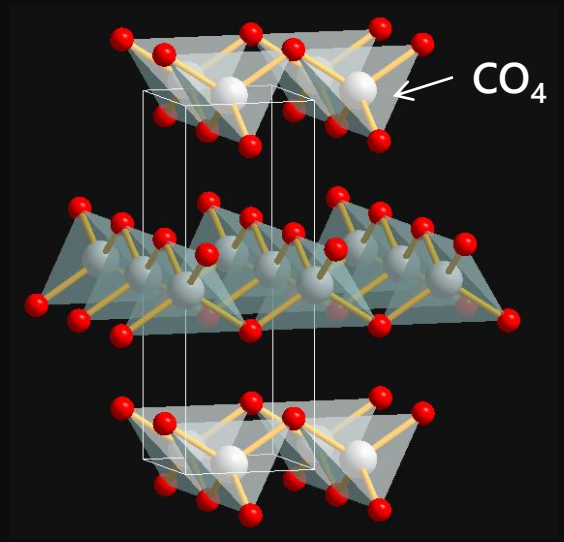

Lamellar phases P>250 GPa

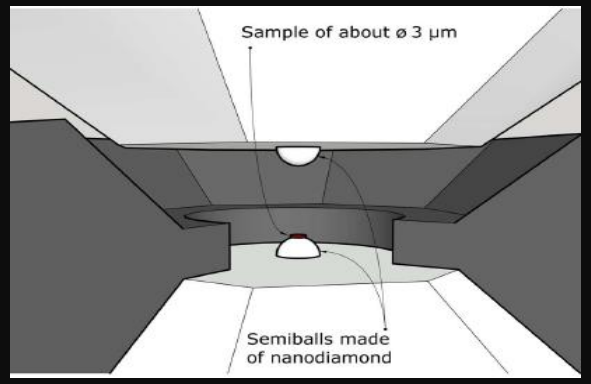

ds-DAC
Dubrovinskaia et al, 2016

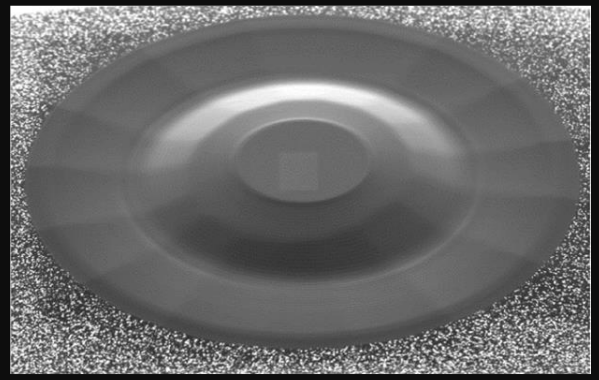

Toroidal anvils
Dewaele et al, 2018

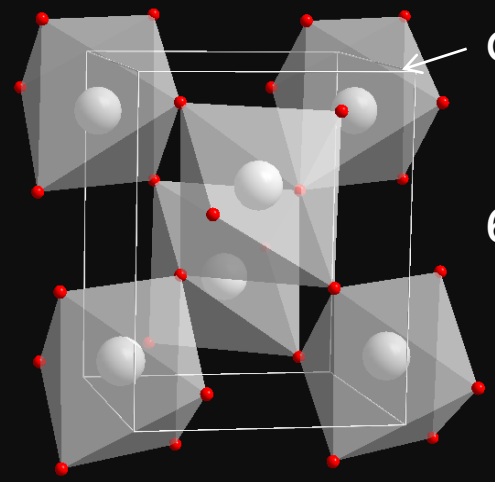

6-coordinated CO_2 , P~1 TPa

Lee et al, Phys. Rev. B 79 (2009)
Lu et al, JACS 135 (2013)

Superionic ices

Superionic and Metallic States of Water and Ammonia at Giant Planet Conditions

C. Cavazzoni, G. L. Chiarotti,* S. Scandolo, E. Tosatti, M. Bernasconi, M. Parrinello

Science , 1999

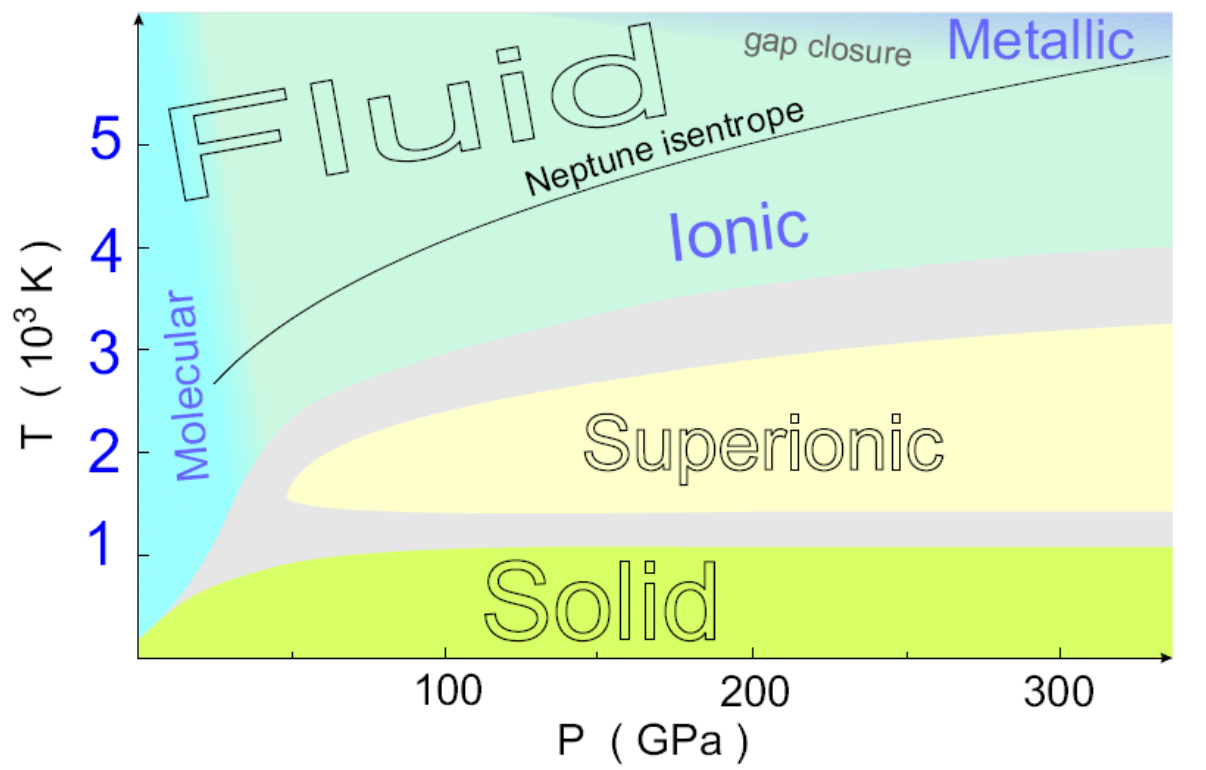

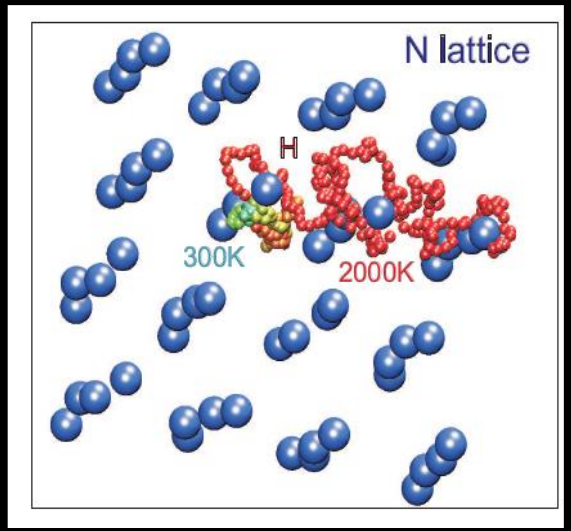

- T<1200 K: protons are strongly bonded to O/N atoms
- T>1200 K: protons become highly diffusive within fixed O/N lattice
  → Superionic solid

Superionic ices

Superionic and Metallic States of Water and Ammonia at Giant Planet Conditions

C. Cavazzoni, G. L. Chiarotti,* S. Scandolo, E. Tosatti, M. Bernasconi, M. Parrinello

Science , 1999

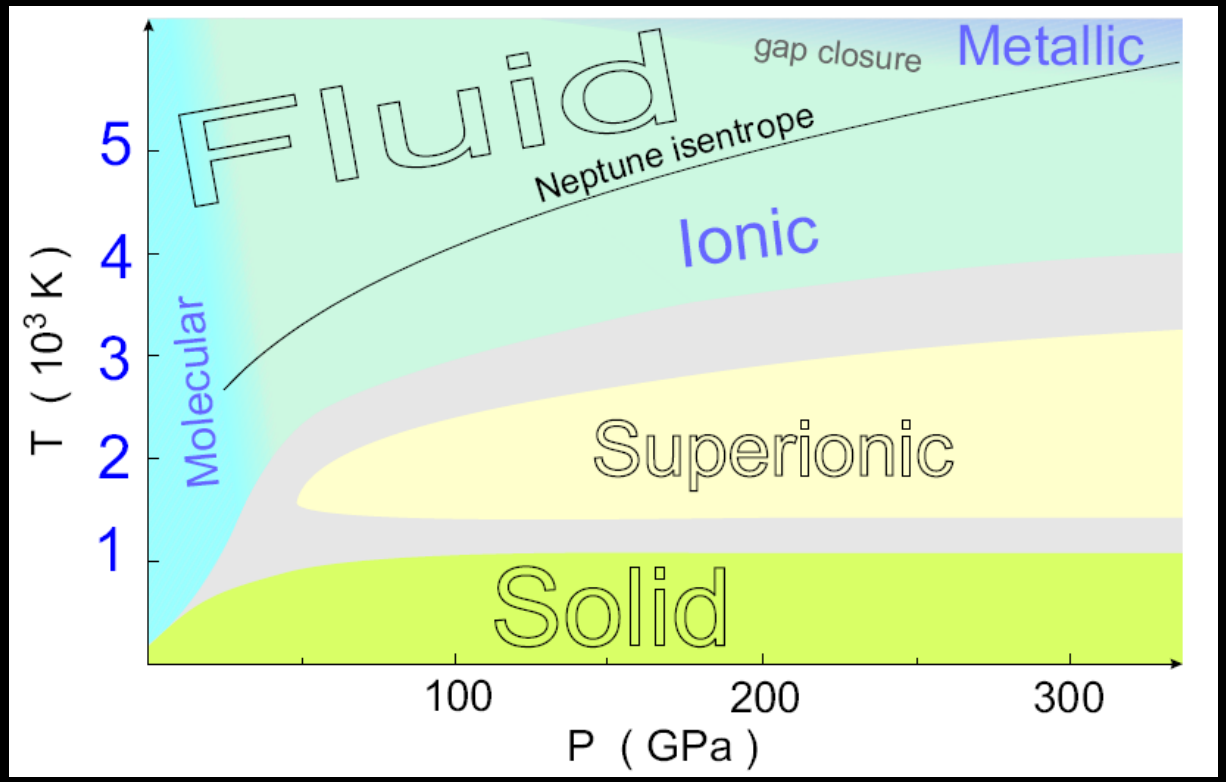

Neptune

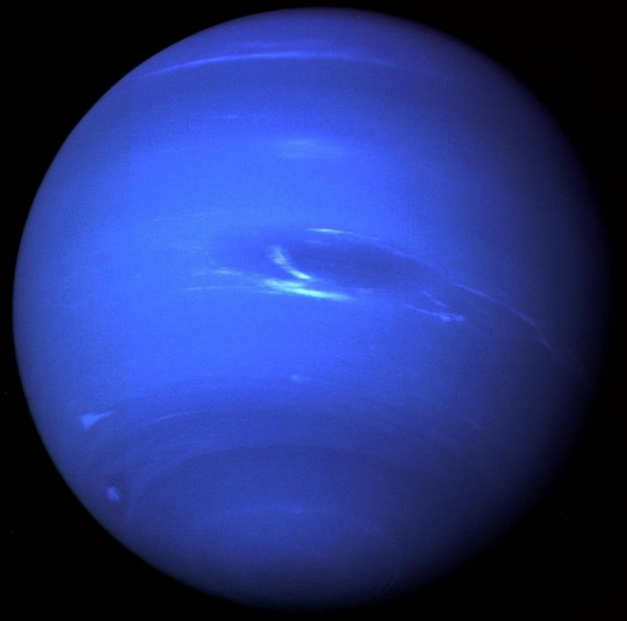

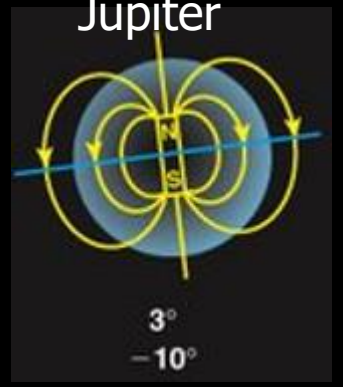

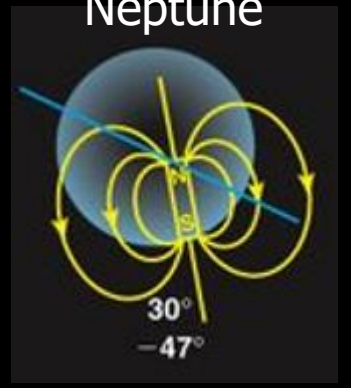

Source of non-axisymmetric magnetic fields of Neptune and Uranus ?

Order-disorder transition in solid NH_3

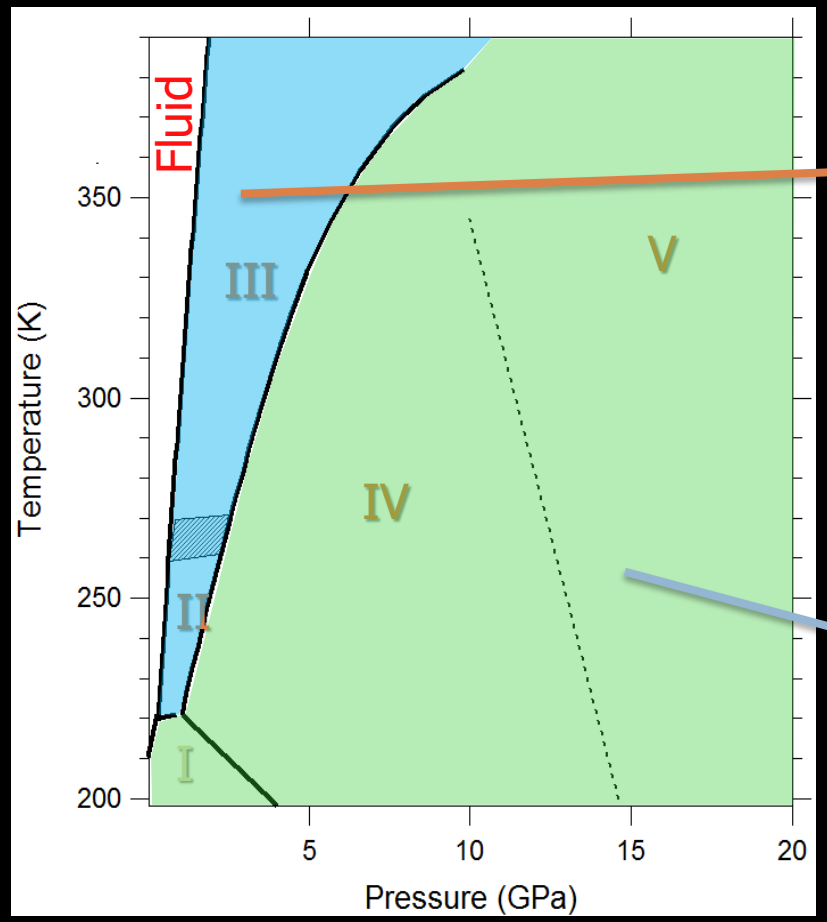

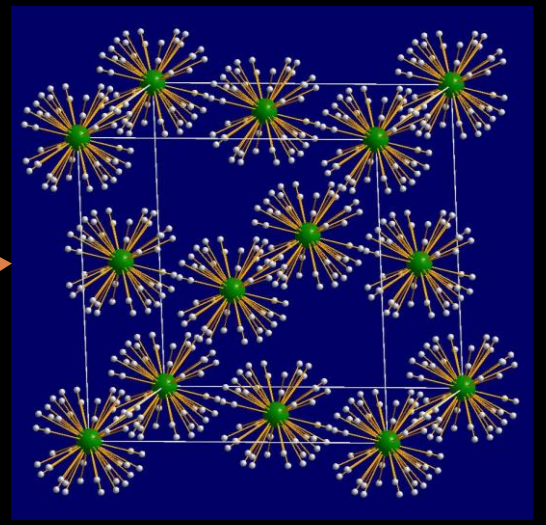

High T

III
Proton disordered
(plastic)

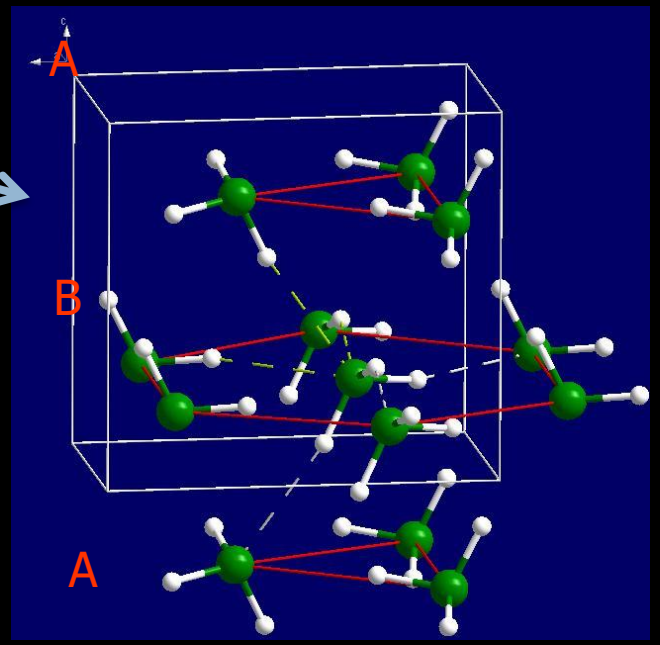

Low T

IV/V
Proton ordered

Order-disorder transition line: Raman

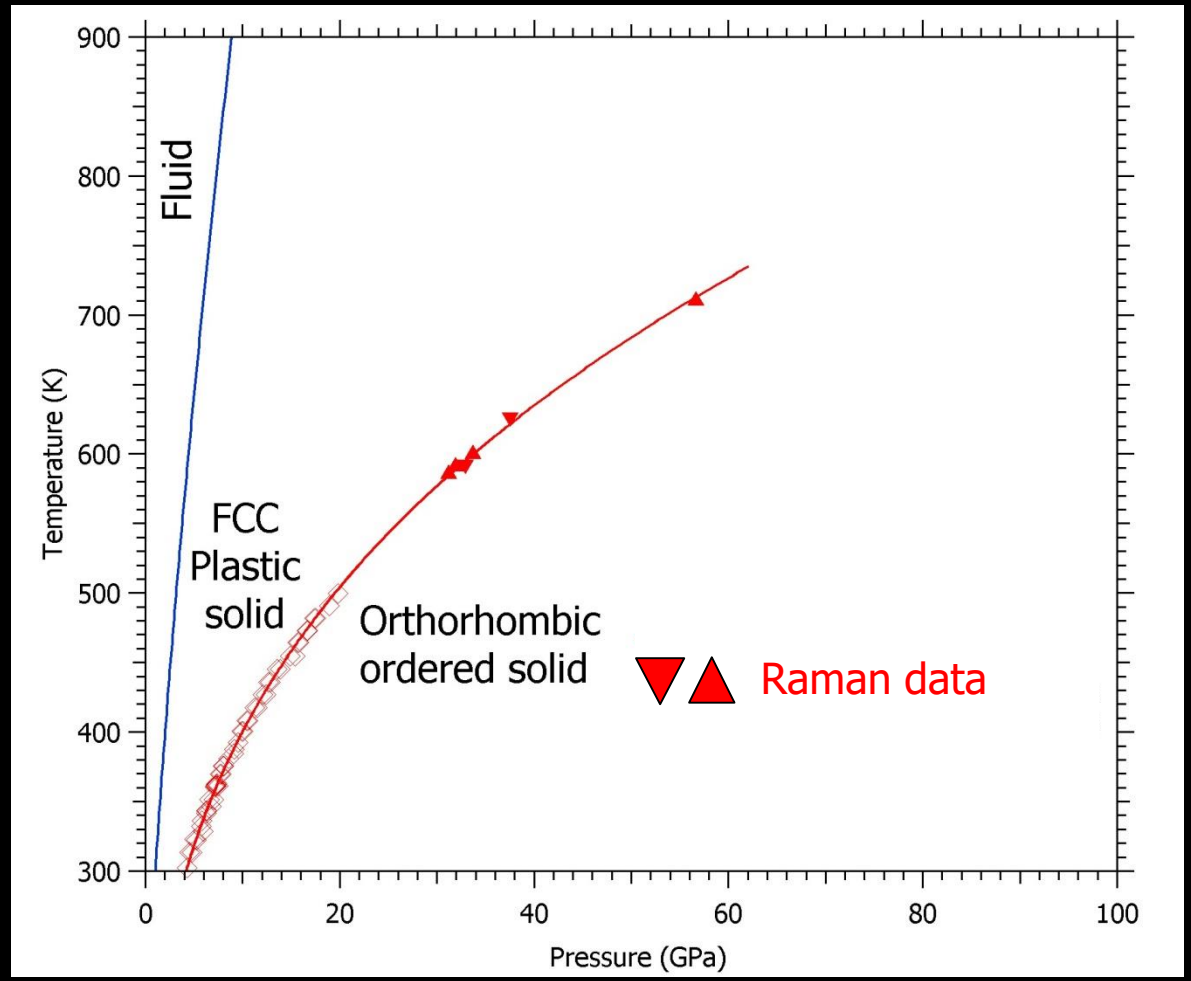

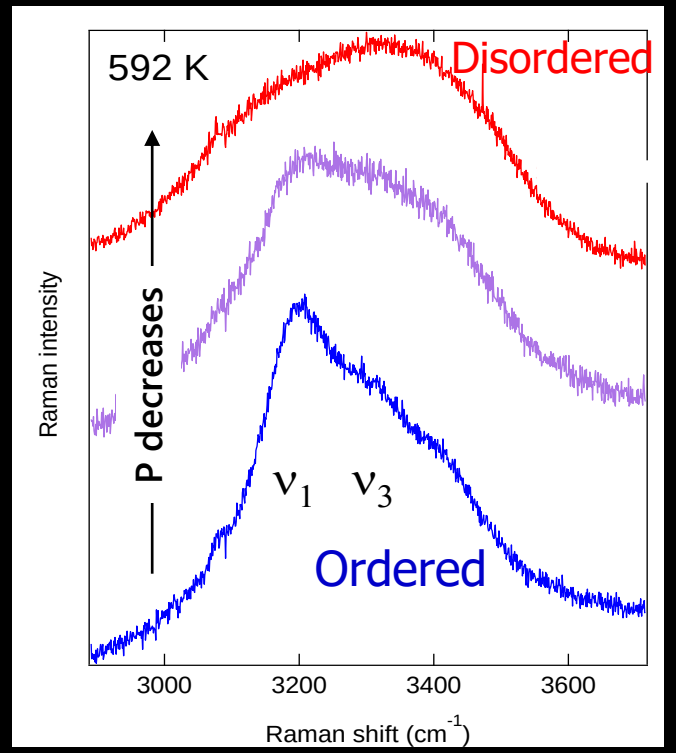

NH_3 stretching modes

The transition line follows a smooth power law up to 57 GPa and 700 K…

Order-disorder transition line: Raman

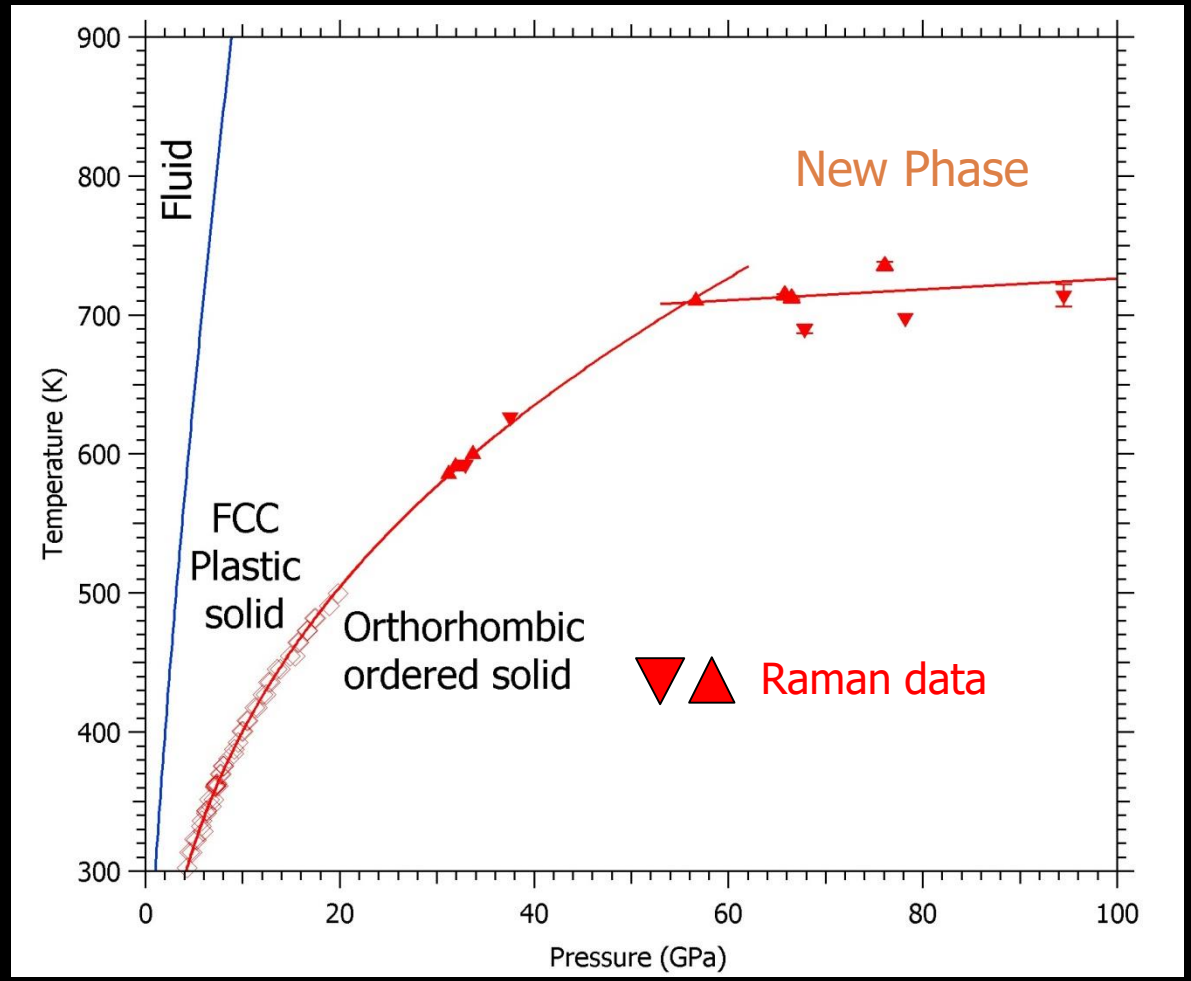

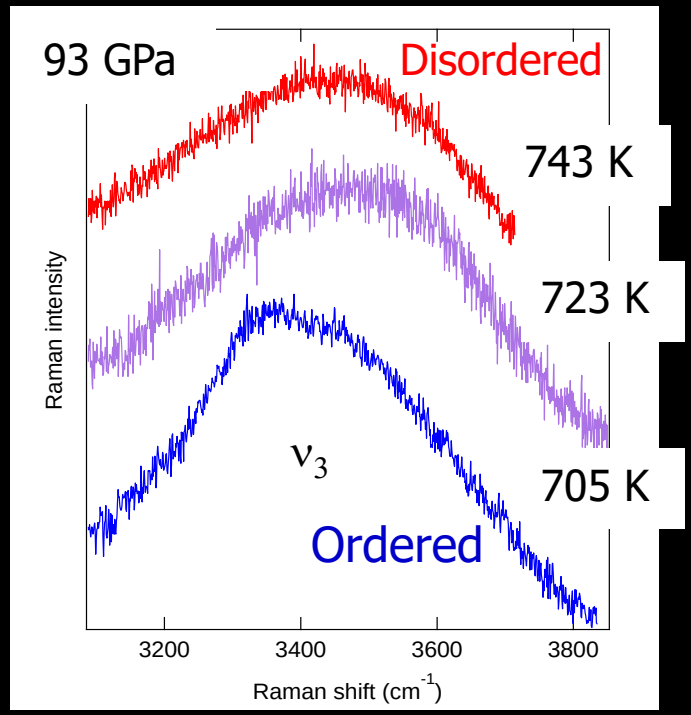

NH_3 stretching modes

- P>57 GPa: New regime – dT/dP decreases suddenly
- The HT phase is proton disordered

Order-disorder transition line: XRD

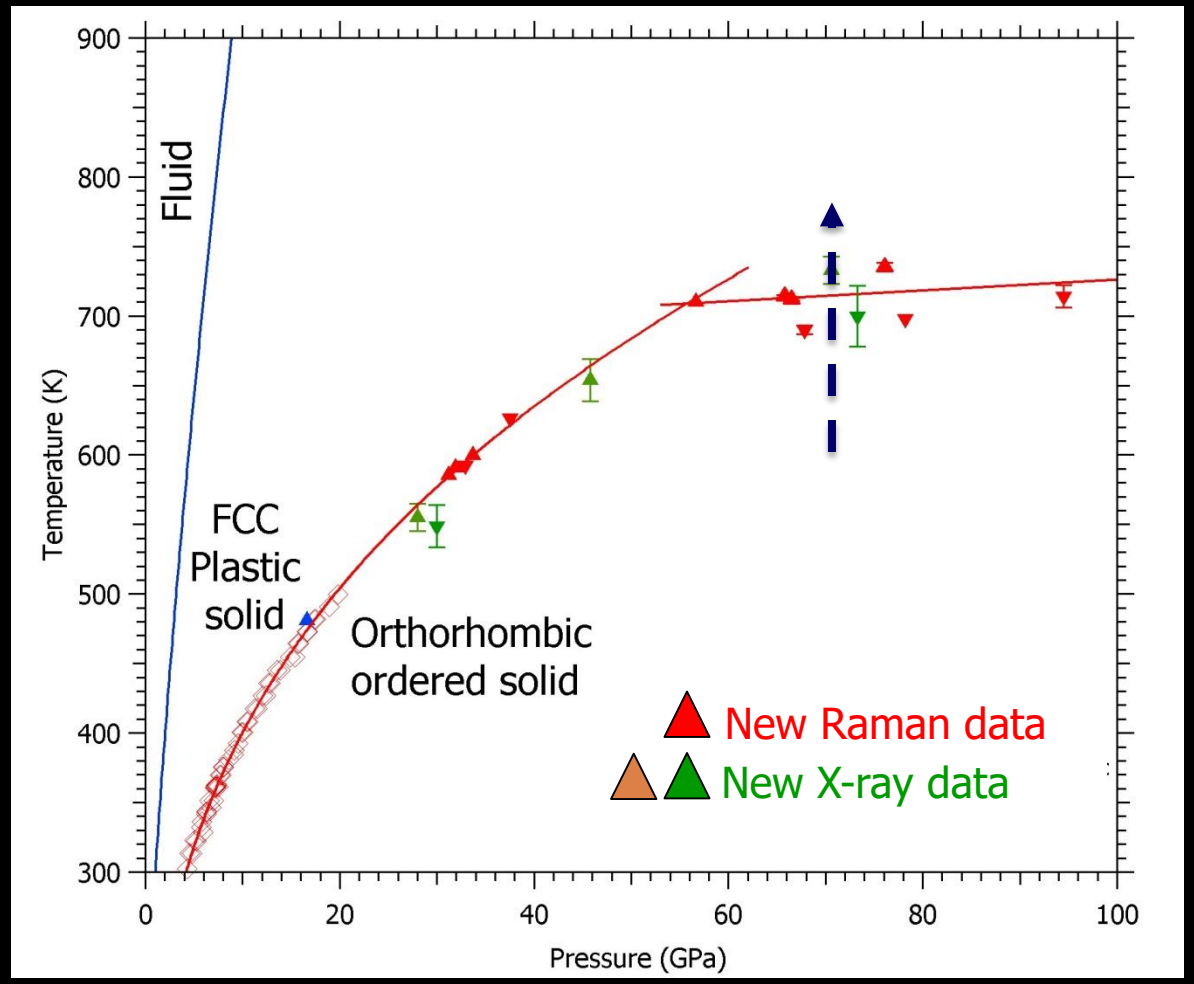

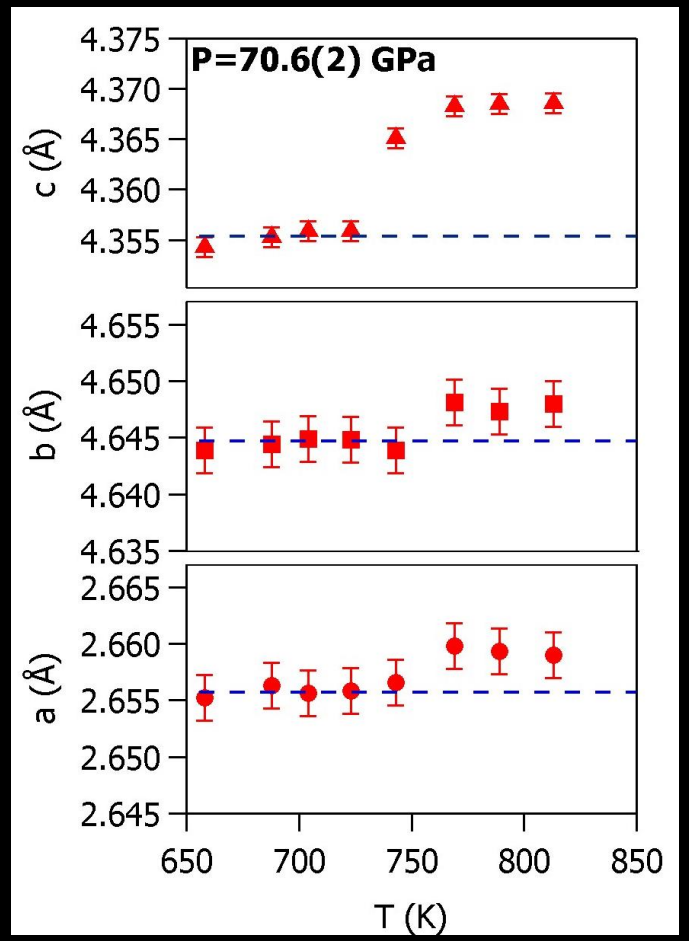

- First order transition (volume discontinuity)
- Orthorhombic lattice of N is maintained through the transition

Phase diagram of NH_3 and proton disorder

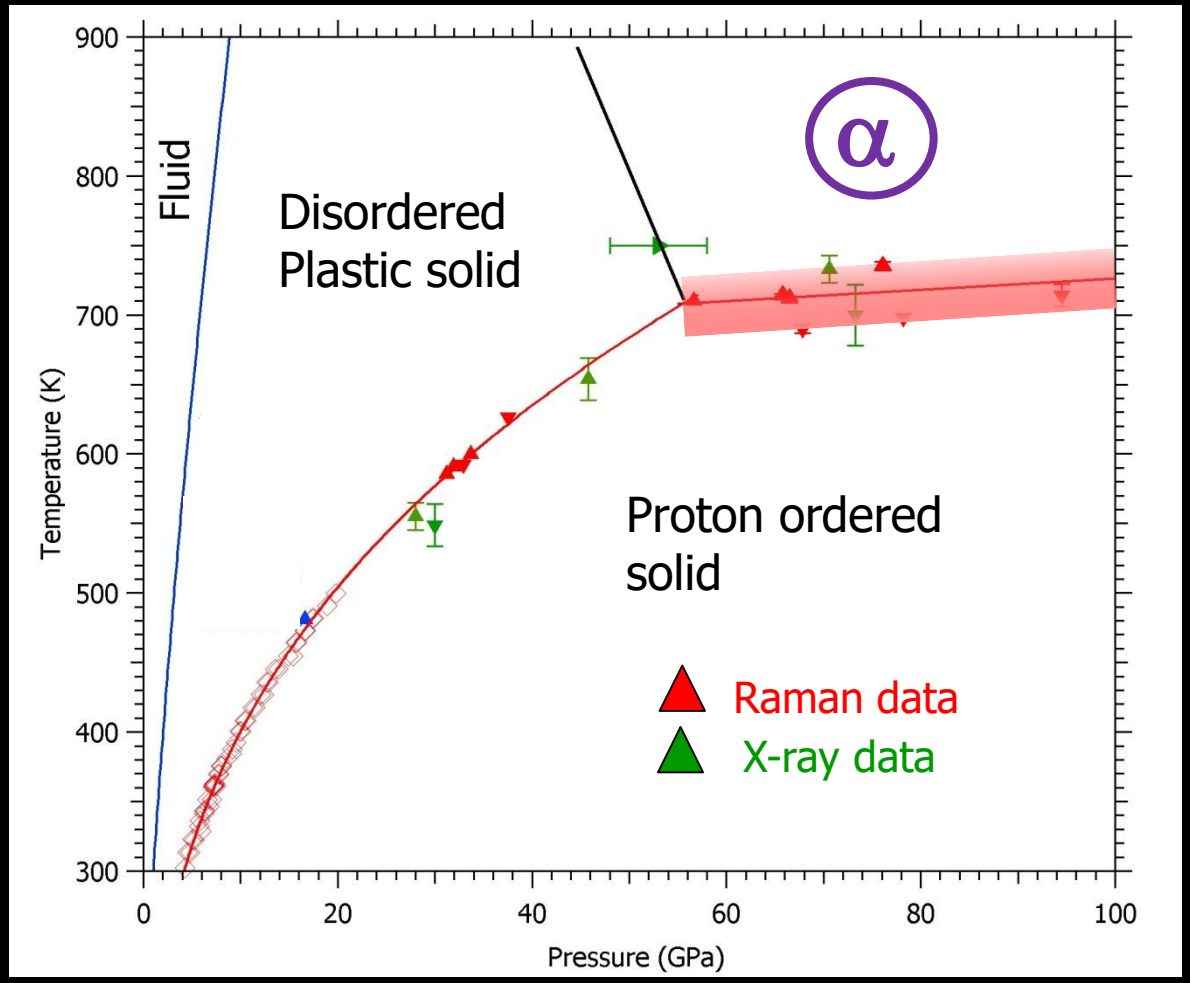

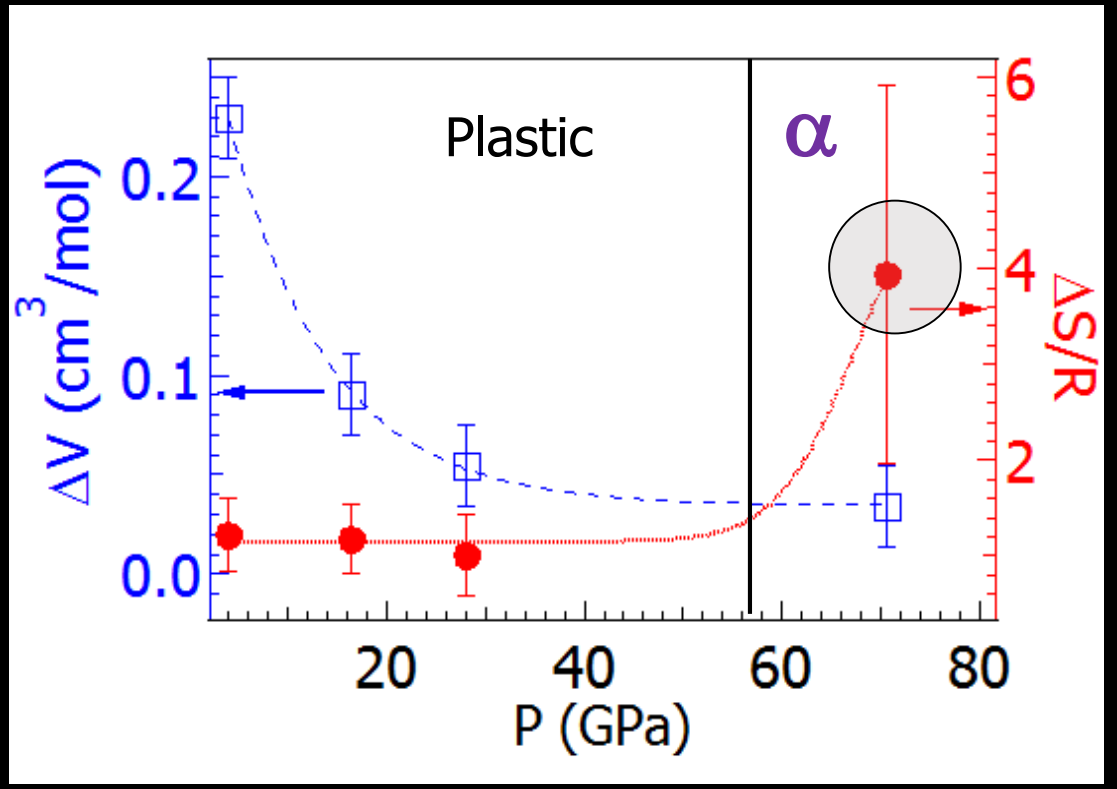

$\Delta S = \Delta V.(dP/dT)$

The number of accessible sites for the H atoms is much greater in the α phase than the plastic phase

Ab initio MD - Annealing at 40 GPa

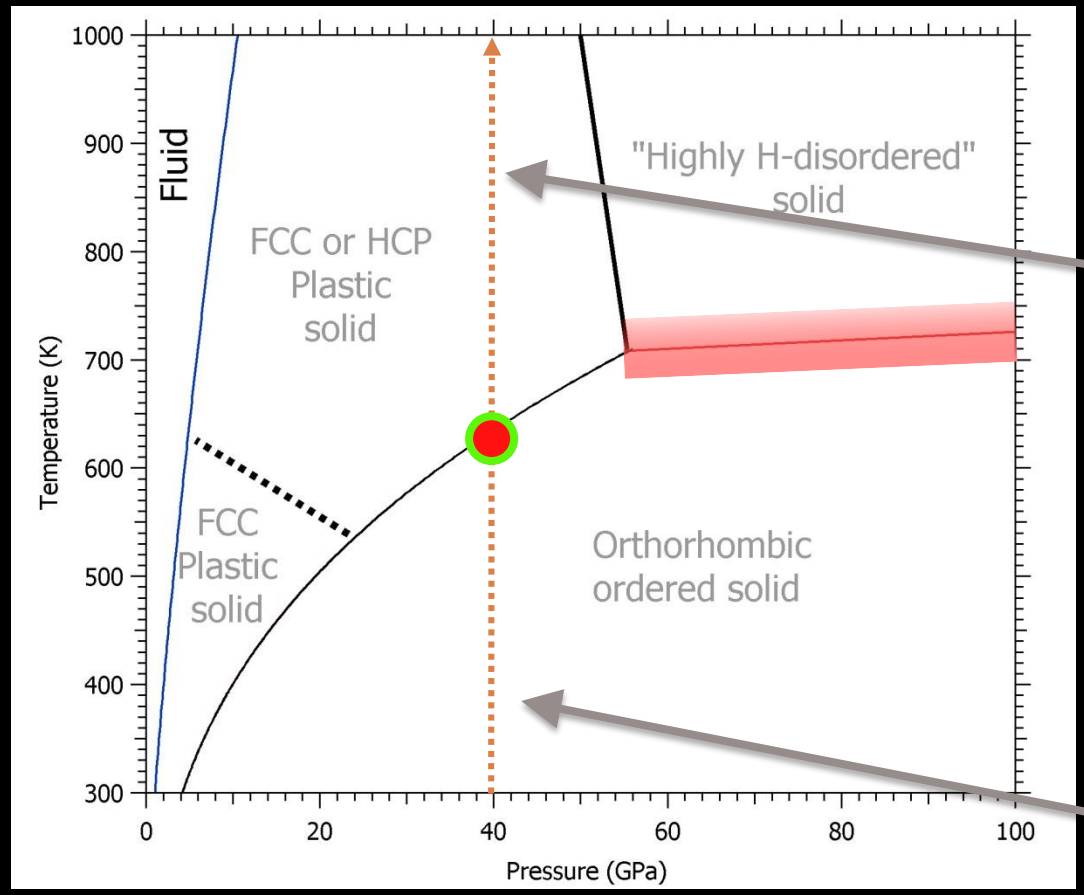

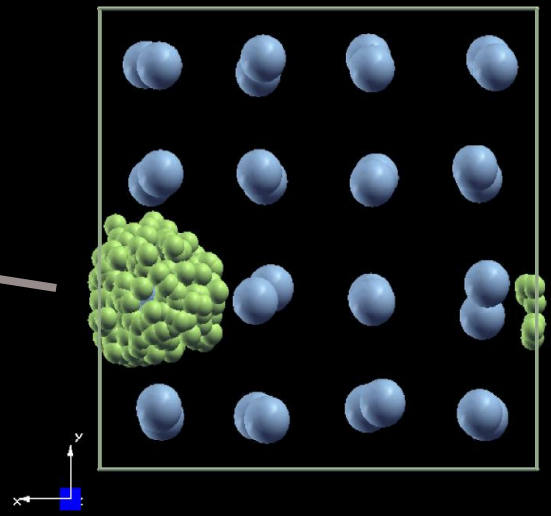

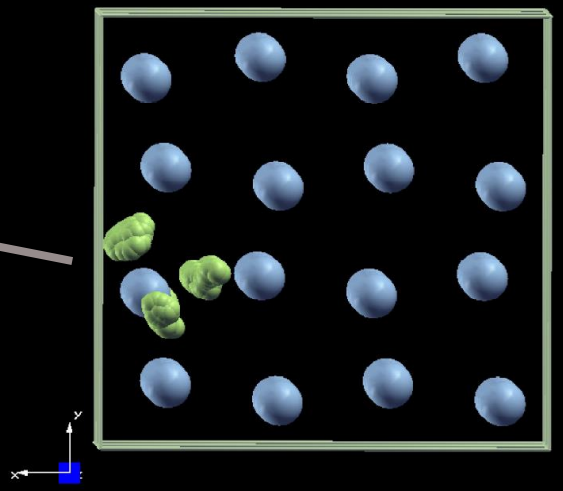

- Plasticity observed for T > 600 K
- No protonic diffusion up to 1200 K

Ab initio MD - Annealing at 70 GPa

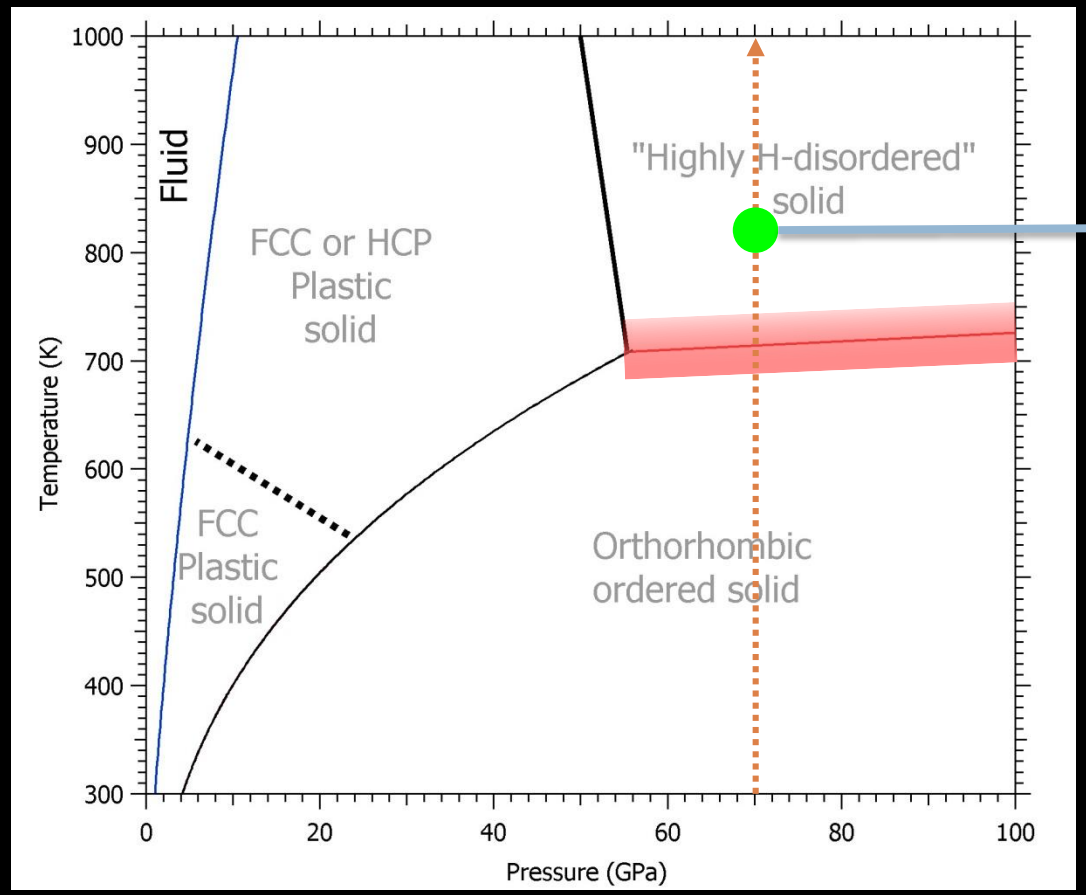

70 GPa, 850 K

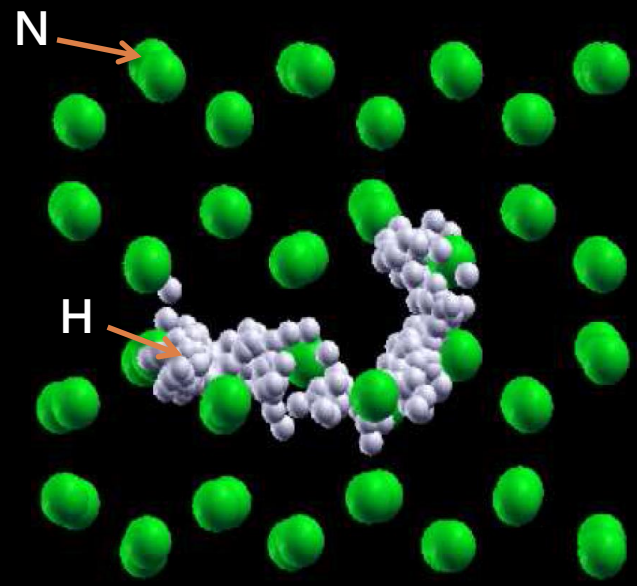

Positions of 1 H atom
over 4 ps

- H^+ can "jump" from one molecule to the other via H-bonds
- diffusion of H^+ through the nitrogen lattice sets in
- Large increase of entropy consistent with experiment

S. Ninet et al, PRL 2012

Perspective studies with EBS

Superionic ammonia

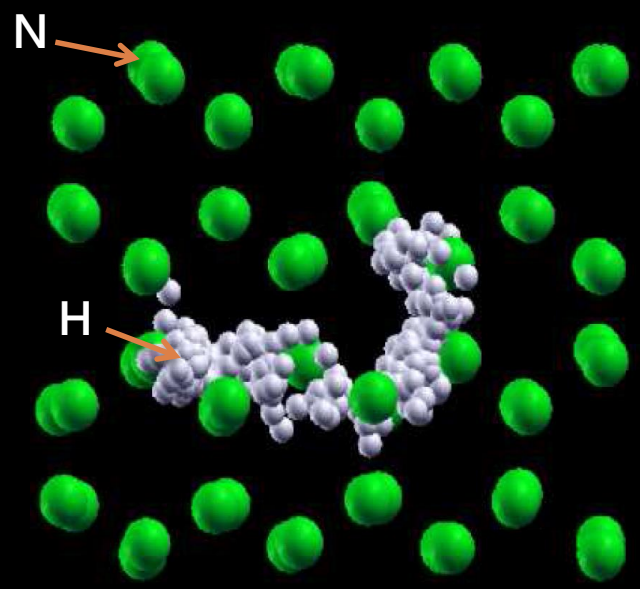

Ionic ammonia [S. Ninet, F. Datchi et al, PRB 89 (2014)]
P>150 GPa 300 K

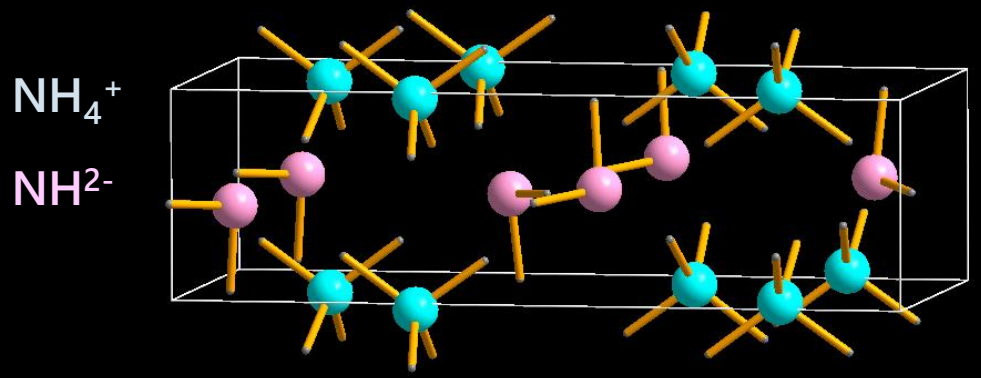

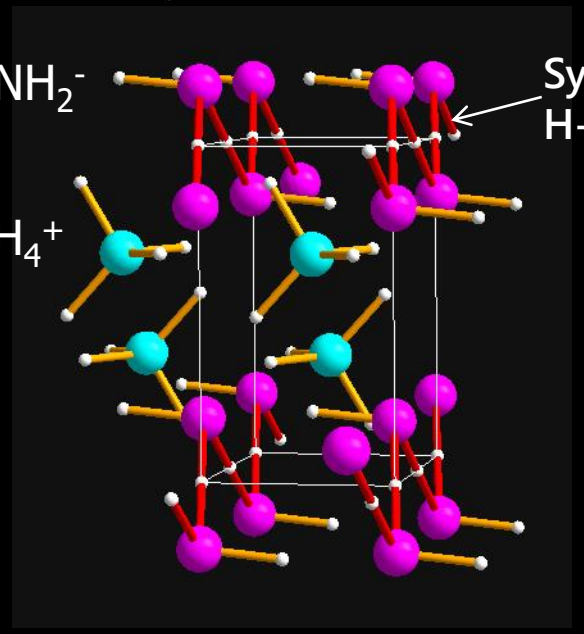

Symmetric and ionic NH_3 P>330 Gpa
[Pickard & Needs, 2008]

- Obtain a structural fingerprint of proton diffusion
- Discover new "exotic" phases

Stucture of light (low-Z) fluids at extreme conditions in the DAC

How to quantitatively measure the structure of low-Z fluids in the DAC ?

- Long-term project ESRF + ANR project MOFLEX
- New instrumental developments (Soller slits, vertical laser heating)

- First HP measurements of S(Q) on H_2 and CO_2
- Melting line and S(Q) of N_2 to Mbar pressures
- Melting line of NH_3 & H_2O
- Liquid-liquid transition in sulfur

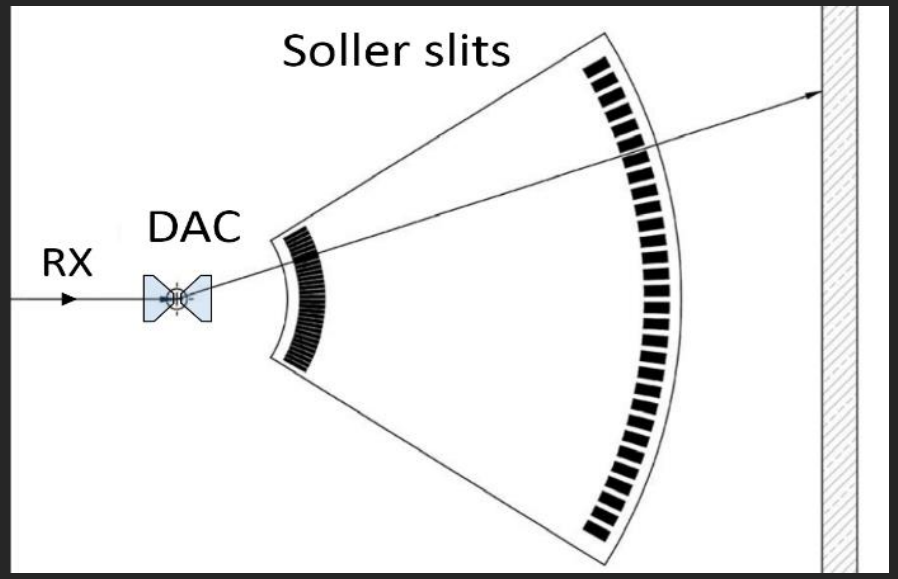

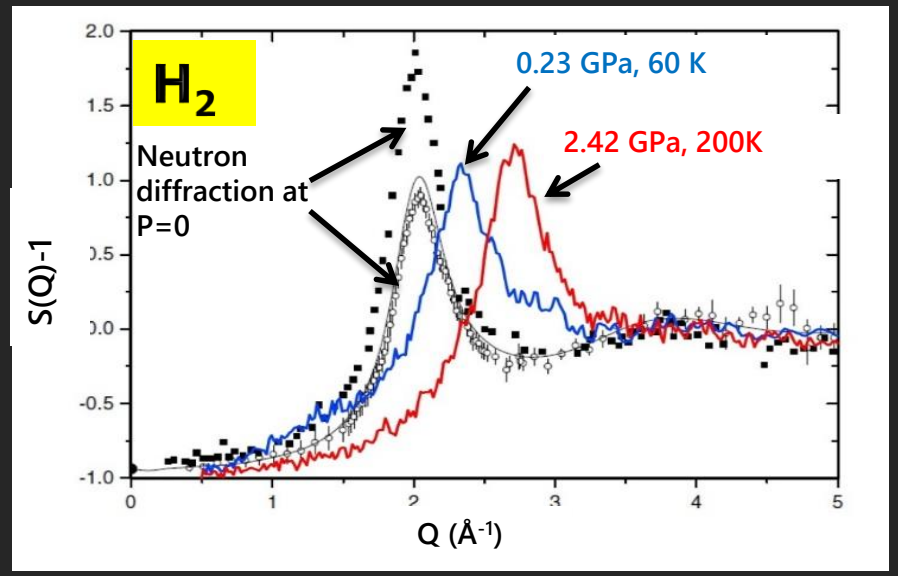

G. Weck et al, PRB (rapid) 91 (2015)

N_2 : is there a liquid-liquid transition ?

- Laser heating experiments to 120 GPa
- DFT predicts a L-L transition at ~90 GPa, 2000 K.
- No maximum on the melting line, nor evidence of L-L transition on S(Q)

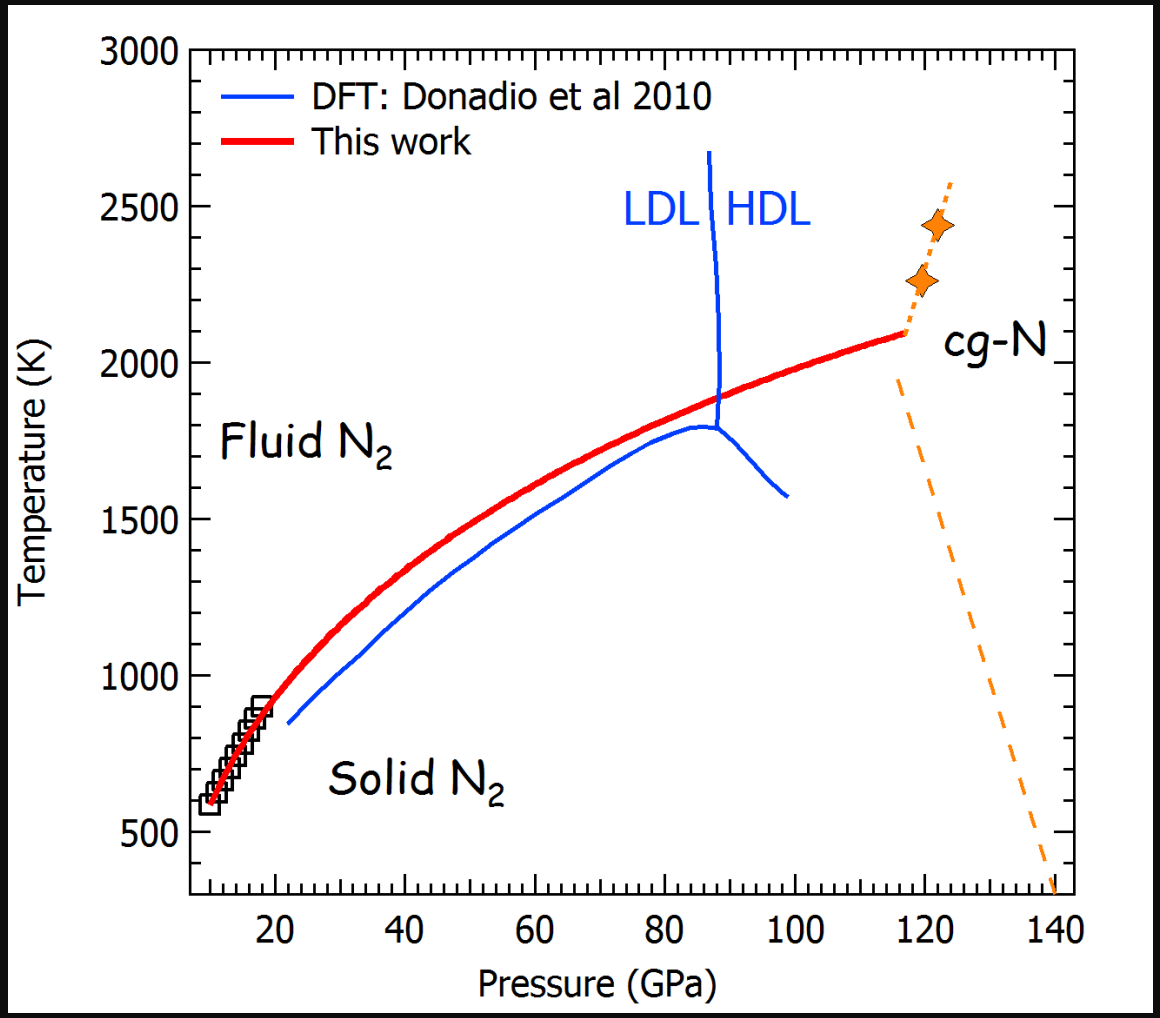

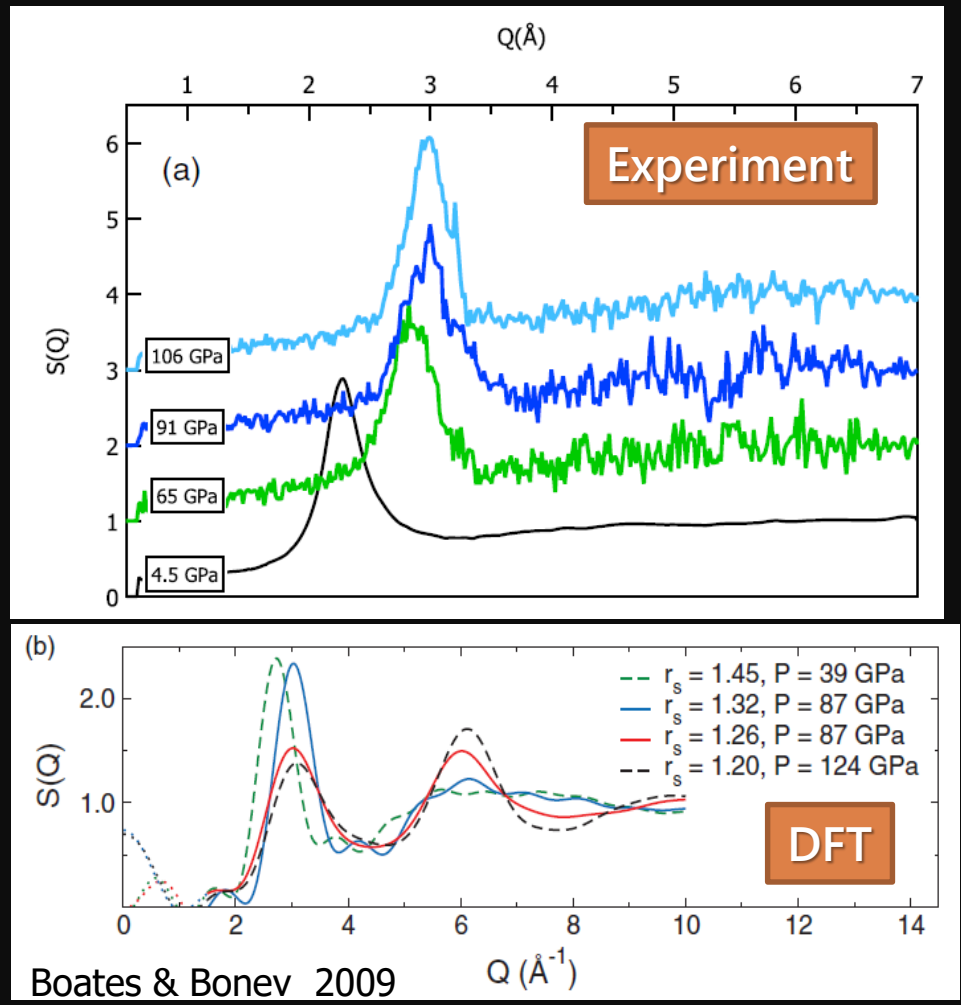

G Weck, et al, PRL 2017
ESRF highlight 2018

Perspectives with EBS

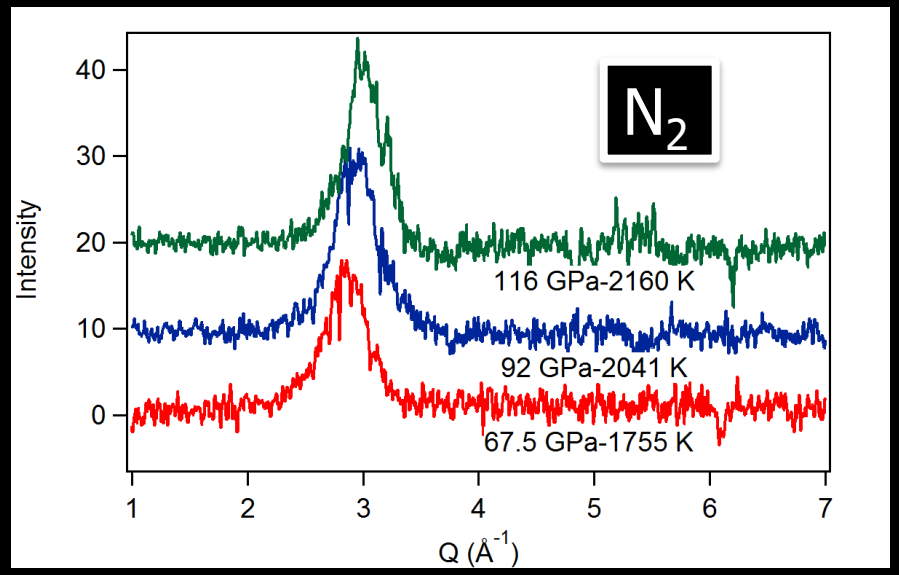

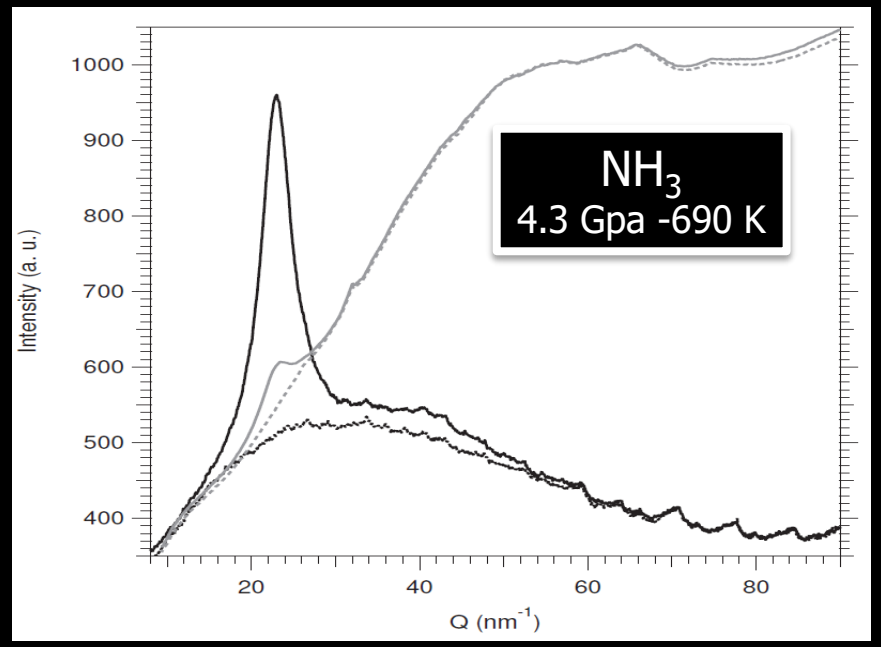

- Flux increase:
  - Better signal/noise, increased Q range
    → Better resolution
  - Shorter acquisition time
    → time-resolved studies
- Smaller beam:
  - Smaller sample, increased P-T range
  - Spatially resolved studies
- Larger coherence
  - Opens access to x-ray imaging